2008

Enantiomeric separations of natural compounds and metal complexes and the detection of anions using positive mode electrospray ionization mass spectrometry

Molly Warnke
Iowa State University

Enantiomeric separations of natural compounds and metal complexes and the detection of anions using positive mode electrospray ionization mass spectrometry

by

Molly Melissa Warnke

A dissertation submitted to the graduate faculty

in partial fulfillment of the requirements for the degree of

DOCTOR OF PHILOSOPHY

Major: Analytical Chemistry

Program of Study Committee:
Daniel W. Armstrong, Co-major professor
Robert S. Houk, Co-major professor
Jacob Petrich
Emily Smith
Hans Stauffer

Iowa State University

Ames, Iowa

2008

TABLE OF CONTENTS

ABSTRACT

This dissertation focuses on two different areas of analysis: liquid chromatography (LC) enantiomeric separations and the detection of anions using electrospray ionization mass spectrometry (ESI-MS) and LC-ESI-MS.

Enantiomeric separations of two distinct classes of chiral compounds were investigated. The first class is pterocarpans, which are isoflavanoids with *cis*-fused benzopyran benzofuranyl structures. In the reverse phase mode of operation, all pterocarpan enantiomers could be separated using cyclodextrin based chiral stationary phases (CSPs) with hydroxypropyl-β-cyclodextrin, acetyl-β-cyclodextrin, and γ-cyclodextrin showing the broadest enantioselectivity. Two macrocyclic glycopeptide CSPs, ristocetin A and vancomycin also proved useful in the reverse phase mode. Not as many separations were achieved in the normal phase mode for either set of CSPs.

Chiral extended metal atom chains (EMACs) were first synthesized by F.A. Cotton and co-workers as the smallest possible molecular wires. It was not possible to resolve these enantiomers by crystallization and derivatization was impossible. The vancomycin macrocyclic glycopeptide stationary phase proved to be the best approach for separating these unusual chiral entities. Partial or baseline separation of 5 helical EMAC racemates was achieved in the polar organic mode or normal phase mode chromatography. In chapter 4, vibrational circular dichroism (VCD) is used to assign the absolute configuration of $Ni_3(dipyridylamine)_4Cl_2$.

Negative mode ESI-MS of anions can be problematic due to spray stability and background noise issues. The use of a positively charged reagent which pairs with the anion allows for the detection of anions in positive mode ESI-MS. Singly charged anions can be

paired with dicationic reagents, while doubly charged anions can be paired with tricationic reagents to result in an overall +1 charged complex. In this dissertation, a variety of linear tricationic reagents were examined to determine which structural features are important for anion detection. The application of linear tricationic reagents and previously reported trigonal tricationic reagents were then applied to the detection of a larger variety of divalent anions (e.g. disulfonates, dicarboxylates) and bisphosphonates, which are a class of drug used to treat bone diseases. The use of MS-MS and LC-ESI-MS are also discussed.

CHAPTER 1

INTRODUCTION

1.1 THESIS ORGANIZATION

High performance liquid chromatography (HPLC) and electrospray ionization mass spectrometry (ESI-MS) are two very important methods used in analytical laboratories. This dissertation presents research in two areas: enantioselective HPLC separations/applications and the ESI-MS analysis of anions in the positive mode. This introduction presents a brief overview of both areas. It is followed by six chapters, each on a manuscript either published or submitted for publication. The final chapter presents the general conclusions from both research areas.

1.2 ENANTIOMERIC SEPARATIONS

The resolution of enantiomers is very important, especially in the pharmaceutical industry. Although enantiomers have identical chemical and physical properties in an achiral environment, they can have different pharmacological, toxicological, metabolic, and pharmacokinetic properties within the chiral environment of biological systems. In 1992, due to advances in enantiomeric LC separations, the Food and Drug Administration (FDA) issued guidelines for the development of sterioisomeric drugs. If a drug is to be developed as a racemate, the effects of each single enantiomer and the racemate must be determined [2]. Enantiomeric separations are also important for evaluating the products of asymmetric syntheses and the evaluation of the enantiomeric composition of naturally occurring molecules, which are of increasing interest as new drugs or new drug leads [3].

Analytical techniques such as gas chromatography (GC), HPLC, supercritical fluid chromatography (SFC), and capillary electrophoresis (CE) are routinely used for

enantiomeric separations [4]. HPLC is used most often in industry because it is robust and offers good reproducibility. HPLC and SFC are the favored techniques for preparative scale separations. There are over 100 chiral stationary phases (CSP) available commercially. The most important classes based on structure are macrocyclic, pi-pi association, and polymeric CSPs [5]. Macrocyclic CSPs will be discussed in the following section.

1.3 MACROCYCLIC CHIRAL STATIONARY PHASES

Macrocyclic CSPs include three groups of chiral selectors: chiral crown ethers, cyclodextrins, and macrocyclic glycopeptides. The cyclodextrin-based chiral selectors account for a vast majority of GC and CE enantioseparations. Cyclodextrins are also important HPLC CSPs, especially in reverse phase and polar organic modes. Cyclodextrins and macrocyclic glycopeptides stationary phases will be discussed in the sections below.

1.3.1 Cyclodextrin based CSPs

Native α, β, and γ cyclodextrins are macrocyclic compounds formed from 6, 7, or 8 α -1,4-linked D-glucose units respectively. The shape of a cyclodextrin is like a hollow, truncated cone (Fig. 1) [4]. This cavity size increases as the number of glucose units increases. The interior cavity of the cyclodextrin is hydrophobic while the exterior rims are hydrophilic. Inclusion complexes form in aqueous or hydro-organic solutions when nonpolar molecules or nonpolar moieties are attracted more strongly to the hydrophobic interior of the cyclodextrin than to the mobile phase [6,7].

The first successful cyclodextrin based CSP involved binding cyclodextrin to silica gel via an ether linkage and was introduced by Armstrong [7]. This CSP was the first that could be used in reverse phase mode and separated many compounds. Later studies led to a more thorough understanding of separation mechanisms [6,8]. A minimum of three points of

interaction are required for chiral recognition, with cyclodextrins and any other CSP. In the reverse phase mode, an inclusion complex must be formed between the analyte and the cavity. Also, the chiral center of the molecule should be positioned near the exterior rim of the cyclodextrin so that interactions between the analyte and the mouth of the cyclodextrin are possible. These interactions include hydrogen bonding, dipolar, and steric interactions. For chiral discrimination, at least one of these interactions needs to be different for each enantiomer.

Derivatized cyclodextrin based CSPs offer additional sites for interactions leading to chiral recognition. The hydroxypropyl-β-cyclodextrin (Cyclobond I 2000 RSP) has been shown to separate compounds not separated on the native β-cyclodextrin CSP [9]. Cyclodextrins derivatized with aromatic groups are effective for separations in the normal phase mode [10,11]. Nonpolar solvent molecules occupy the cyclodextrin cavity in the normal phase mode, therefore π-π interactions, dipole stacking, and hydrogen bonding interactions are important for chiral recognition [10]. Polar organic mode chromatography, where the mobile phase consists of mainly acetonitrile can also be used with cyclodextrin CSPs. In this mode, the solvent occupies the cyclodextrin cavity and the analyte resides on top of the chiral selector, so that hydrogen bonding is maximized [12].

1.3.2 Macrocyclic Glycopeptides

Macrocyclic glycopeptide based CSPs have also been shown to separate a wide variety of chiral compounds [13]. The commercially available CSPs are those based on the macrocyclic glycopeptide antibiotics vancomycin, ristocetin A, teicoplanin, and teicoplanin aglycone. All of these chiral selectors have similar peptide backbones, multiple stereogenic centers, and functionalities such as carboxylic acids, amines, sugar moieties, and aromatic

rings [14]. The teicoplanin aglycone is the only chiral selector without saccharide groups attached. Along with a variety of functional groups, these chiral selectors have a secondary structure in the form of a twisted “C” shaped basket that is relatively non-polar [15,16]. Interactions between an analyte molecule and the functional groups or hydrophobic cavity of the macrocyclic glycopeptide based CSP can lead to enantioselectivity.

The macrocyclic glycopeptide CSPs can be used in all mobile phase modes: reverse phase, normal phase, and polar organic [17]. In the reverse phase mode, electrostatic interactions and hydrophobic interactions are thought to be the most important for chiral recognition [13]. In the normal phase mode, the polar functional groups and aromatic rings of the CSP provide the interactions needed for both retention and chiral recognition. The dominant analyte-CSP interactions include hydrogen bonding, pi-pi interactions, dipole stacking, steric repulsion and sometimes electrostatic interactions. In the polar organic mode, the dominant interactions between the analyte and CSP are hydrogen bonding, electrostatic, dipolar, and steric interactions [18]. Due to the dominance of different types of interactions in these three chromatographic modes, chiral recognition can vary dramatically. Hence, very different types of chiral molecules can be separated in one mode vs. another. Method development with macrocyclic glycopeptides is often simplified by the fact that the stationary phases are complementary. If a partial separation is obtained on one stationary phase, it is likely the analyte can be baseline separated on a related glycopeptide CSP [17,19]. Chapters 2 and 3 focus on the use of macrocyclic glycopeptide and cyclodextrin based CSPs for the separation of natural product analogs and chiral metal complexes.

1.4 VIBRATIONAL CIRCULAR DICHROISM

Just as the separation of chiral molecules is necessary in many fields, structural characterization of enantiomers is also important. Absolute configuration and conformations of a chiral molecule are important factors in determining pharmaceutical activity [3]. Circular dichroism and optical rotation are two well known and highly used methods for absolute configuration determination [20,21], but they rely on the comparison of the measured rotation sign to related compounds of known absolute configuration. Incorrect assignments can be made, even with the number of useful correlations, rules, or procedures available [22]. X-ray crystallography can be used for the determination of absolute configuration. This method requires a single crystal of sufficient size and quality, which can be difficult to obtain. Vibrational circular dichroism (VCD) circumvents these problems by correlating an optical activity measurement to accurate quantum mechanical calculations, which leads to the direct determination of the absolute configuration of a molecule. For traditional CD, electronic transitions are probed in the visible spectral region. The same principles are applied in VCD, but in the mid-IR region with fundamental vibrational frequencies being probed [23].

VCD was discovered in the 1970s [24,25] and instrumentation has been commercially available since 1997 [22]. For assignation of absolute configuration by VCD, experimental VCD and IR spectra are measured using an instrumental configuration as shown in Figure 2. Next, the vibrational absorption and CD spectra must be predicted using quantum mechanical programs. A widely used theoretical level is the density functional method with the B3LYP functional and 6-31G* basis set [25]. For a molecule with a single conformation, the starting geometry can be obtained in a straight-forward manner through a molecule-building

program. Either of the two possible absolute configurations is arbitrarily chosen as a starting point and the geometry is further optimized to obtain the minimum energy geometry.

Vibrational absorption and CD intensities for all vibrational bands are then calculated for the chosen absolute configuration. A spectrum can be predicted based on the calculated band positions and intensities. If the predicted VCD band signs match the experimentally observed VCD band signs, then the absolute configuration of the experimentally investigated molecule is assigned the configuration of the enantiomer used in the calculations [25]. If the predicted signs and experimental signs are opposite, then the opposite absolute configuration is assigned. Figure 3 shows the comparison of the experimental VCD spectrum and the predicted spectrum for both enantiomers of (+)-3-chloro-1-butyne. It is clear that the VCD signs of the experimental spectrum match that of the (R)-enantiomer, hence (+)-3-chloro-butyne is (R)-3-chloro-butyne. The VCD spectrum of molecules that can exist as multiple-conformers is more complicated as the relative populations of conformers must be taken into account for the calculations. A population-weighted VCD spectrum is generated from individual conformer calculations and compared to the experimentally observed VCD spectrum to assign absolute configuration, as for single-conformer molecules [25]. Chapter 4 is a report of the use of VCD to assign the absolute configuration to the enantiomers of one of the metal complexes (Ni_3(dipyridylamine)$_4Cl_2$) separated in Chapter 3.

1.5 ANALYSIS OF ANIONS USING MASS SPECTROMETRY

Anion analysis is important in many areas of study, especially involving environmental samples, biological tissues and fluids, and foods and beverages. Separation techniques are often employed with such complex matrices to separate ions of interest from potential interferences in the matrix. Ion chromatography and capillary electrophoresis are

the most common separation methods used for ion analysis. Reverse phase mode chromatography can be used if the anion is sufficiently hydrophobic. Ion selective electrodes have also been used for anion detection. Most anions have little UV absorbance and unless derivatized, direct detection with a UV detector can be difficult.

Conductivity detection is used frequently for ion chromatography detection because it is a universal detector [26]. Analytes are detected when a difference in conductance between the ion and the background electrolyte is measured. Direct detection occurs when the conductance of the analyte is larger than that of the background, while when analyte conductance less than that of the background indirect detection must be used. Lower concentrations and conductivity of the background electrolyte lead to lower baseline noise, which improves detection sensitivity. Because of this, most conductivity detection is performed using background suppression. In this method the background electrolytes such as sodium hydroxide or sodium carbonate are converted to species of low conductance, like water or H_2CO_3, by cation exchange of the counterion for hydrogen ion. Suppression technology has been thoroughly reviewed [27,28]. Conductivity detection is a universal and useful method for anion detection, but it does not offer any structural information and lower limits of detection are required for some analyses.

Ion-selective electrodes have also been used for ion chromatography detection [29-31]. These electrodes detect selected analytes, even in complex matrices, however the use of ion-selective electrodes with ion chromatography is not very common. Because of the high selectivity of the ion-selective electrode, the information obtained in conjunction with a separation technique might be the same as that obtained by flow injection analysis [26]. In recent years, improvements in sensitivity and limits of detection have been made with ion-

selective electrodes [32], however they are most often used without a separation technique and in non-sample limited applications.

The use of mass spectrometry as a detection method for anion analysis is growing in popularity. The mass spectrometer can discriminate between anionic species and/or provide structural information about the analytes, providing a second dimension of analysis. Inductively coupled plasma (ICP) and atmospheric pressure ionization methods (API), most often ESI, are methods of major importance for detection in ion chromatography. ICP interfaces are compatible with traditional ion chromatography flow rates (1 mL/min) and can detect several elements with great sensitivity [33,34]. ICP-MS is a very popular method for detecting metallic and halogenated species [35-45]. While ICP is useful for elemental analysis, the high temperature used leads to the complete destruction of the analyte, ruling out any other structural information. Identification of unknown analytes is difficult using ICP, however API techniques, ESI and atmospheric pressure chemical ionization (APCI) can be used to elucidate structural and identity information of analytes from the resulting mass spectrum.

ESI is a useful ionization technique for many classes of analytes. Briefly, in electrospray ionization, liquid flow (effluent) is pumped through a capillary which has an applied voltage ($\pm$2-6 kV). This current flow creates charge separation at the surface of the liquid, thereby producing a “Taylor cone” protruding from the capillary tip. Droplets that contain an excess of charge (positive or negative depending on the polarity of the capillary voltage) will then detach from the end of the Taylor cone (Fig. 4). These droplets eventually yield “naked” ions for analysis by mass spectrometry via one of two generally accepted mechanisms [46, 47]: the charge residue model (CRM) and the ion evaporation model (IEM).

More detailed descriptions of the electrospray ionization process can be found elsewhere [46-48].

The inherent negative charge of anions would seem to make the use of negative mode ESI-MS detection an obvious choice. While negative mode ESI is the most straightforward method for detecting anions, there are some drawbacks. The negative ion mode is more prone to corona discharge than the positive ion mode. Corona discharge is an electrical discharge resulting from the ionization of a fluid surrounding a conductor. In ESI, corona discharge occurs when the high concentration of electrons on the capillary lead to ionization of molecules around the capillary. The large quantity of ionized molecules leads to significant background interferences and poor spray stability [48]. If corona discharge persists, it can lead to arcing, which not only leads to a reduction in spray current, but can also damage the electrical components of the instrument [48]. Yamashita and Fenn noticed that the onset of arcing occurred at lower applied potentials in negative ion mode than in positive ion mode [49].

Corona discharge can be reduced by the use of electron-scavenging gases [50,51] and/or halogenated solvents [52-54]. Halogenated solvents have a high relative electron affinity and can thus “capture” electrons, which reduces or eliminates corona discharge and increases spray stability. Butanol [51] and 2-propanol [48] have also been recommended for use as LC-MS solvents when negative mode is used. These solvents have higher proton affinities than traditional LC solvents like water and methanol. Electron scavenging gases, such as oxygen or SF_6, work in a similar manner. Commercial instruments today often use nitrogen from liquid N_2 dewars or generators which makes adding high electron affinity gases more difficult. Along with the difficulties of using electron scavenging gases, the

halogenated solvents and alcohol modifiers referred to above are not commonly used in reverse phase chromatography or ion chromatography. A sensitive, positive mode ESI-MS method to determine anions using common HPLC solvents would be very beneficial.

Recently, a method was developed to detect singly charged anions using positive mode ESI-MS by pairing the anion with a dicationic reagent to create a positively charged complex [55-58]. The use of tricationic reagents which pair with divalent anions for the detection of a +1 complex also has been reported recently [59]. Using positive mode ESI-MS avoids the spray stability problems of negative mode ESI-MS. Beyond this, pairing the anion with the dicationic or tricationic reagent has other benefits. For example, monitoring of the anion/cation pair moves the detected species to a higher mass region where there is lower background noise. Also, anions of low mass may be moved well above the low mass cutoff of quadrupole instruments (e.g., ion traps). In addition, the pairing reagents may be used to differentiate between the analyte of interest and an interference of the same m/z [57].

The final three chapters of this dissertation focus on the expansion of positively charged reagents for the detection of anions by positive mode ESI-MS. In chapter 5, a variety of linear tricationic reagents are evaluated with a small number of divalent anions to determine what types of charge groups and alkyl chain lengths make ideal linear pairing agents. Chapters 6 and 7 apply the superior linear trications from chapter 5 and the best rigid, trigonal trications from a previous study [59] to the detection of a wider range of divalent anions and bisphosphonate drugs. Also in these chapters, MS/MS was used to lower the background and therefore the limits of detection for many of the anions presented.

1.6 REFERENCES

[1] FDA, *Chirality*, **1992**, *4*, 338

[2] Thompson, R. *J. Liq. Chrom. Rel. Technol*., **2005**, *28*, 1215-1231.

[3] Stephens, P.J.; Devlin, F.J., Pan, J. *Chirality*, **2008**, *20*, 643-663.

[4] Liu, Y.; Lantz, A.W.; Armstrong, D.W. *J. Liq. Chromatogr. Rel. Technol*. **2004**, *27*, 1121.

[5] Armstrong, D.W.; Zhang, B. *Anal. Chem*. **2001**, *19*, 557A-561A.

[6] Armstrong, D.W.; Ward, T.J.; Armstrong, R.D.; Beesley, T.E.**,** *Science*, **1986,** *232*, 1132-1135.

[7] Armstrong, D.W.; DeMond, W.; *J. Chromatogr. Sci*., **1984,** *22*, 411-415.

[8] Armstrong, D.W.; DeMond, W.; Czech, B.P. *Anal. Chem*. **1985**, *57*, 481

[9] Stalcup, A.M.; Chang, S.; Armstrong, D.W.; Pitha, J. *J. Chromatogr*., **1990,** *513*, 181-194.

[10] Stalcup, A.M.; Chang, S.; Armstrong, D.W. *J. Chromatogr*., **1991,***540*, 113-128.

[11] Armstrong, D.W.; Stalcup, A.M.; Hilton, M.L.; Duncan, J.; Faulkner, J.R., Jr.; Chang, S. *Anal. Chem.*, **1990,** *62*, 1610-1615.

[12] Armstrong, D.W. *LC-GC, Supplemental Issue*, 1997, S20.

[13] Xiao, T.L.; Armstrong, D.A.. In *Methods in Molecular Biology*, Güblitz, G., Schmid, M.G., Eds.; Humana Press, Inc., Totowa, NJ, **2004**; Vol. *243*, 115, 149-159.

[14] Armstrong, D.W.; Tang, Y.; Chen, S.; Zhou, Y.; Bagwill, C.; Chen, J., *Anal. Chem*., **1994,** *66*, 1473-1484.

[15] Nair, U.B.; Chang, S.S.C.; Armstrong, D.W.; Rawjee, Y.Y.; Eggleston, D.S.; McArdle, J.V. *Chirality*, **1996,** *8*, 590-595.

[16] Gasper, M.P.; Berthod, A.; Nair, U.B.; Armstrong, D.W. *Anal. Chem*., **1996,** *68*, 2501-2514.

[17] Chirobiotic Handbook: A guide to Using Macrocyclic Glycopeptide Bonded Phases for Chiral LC Separations, 5th ed.; Advanced Separation Technologies Inc.: Whippany, NJ; **2004**.

[18] Hrobonoba, K.; Lehottay, J.; Cizmarikova, R.; Armstrong, D.W., *J. Liq. Chromatogr. Relat. Technol*. **2001**, *24*, 2225-2237.

[19] Chen, S.; Liu, Y.; Armstrong, D.W.; Borrell, J.I.; Martinez-Teipel, B.; Matallana, J.L. *J. Liq. Chromatogr*. **1995**, *18*, 1495.

[20] Salvadori, P.; Ciardelli, F. In: Optical rotatory dispersion and circular dichrosim. Ciardelli, F; Salvadori, P., editors. Heyden and Sons: London. **1973**, 3.

[21] Berova, N.; Nakanishi, K.; Woody, R.W. *Circular dichroism: principles and applications*, 2nd ed. Wiley-VCH: New York; **2000**

[22] Freedman, T.B.; Cao, X.; Dukor, R.K.; Nafie, L.A. *Chirality*, **2003**, *15*, 743

[23] Polavarapu, P.; He, J. *Anal. Chem*. **2004**, *76*, 61A.

[24] Holzworth, G.; Hsu, E.C.; Mosher, H.S.; Faulkner, T.R.; Moscowitz, A.; *J. Am. Chem. Soc*. **1974**, *96*, 251

[25] Nafie, L.A.; Cheng, J.C.; Stephens, V.J.; *J. Am. Chem. Soc*. **1975**, *97*, 3842.

[26] Buchberger, W. W. *J. Chromatogr.* , **2000**, *884*, 3-22.

[27] Buchberger, W. W.; Haddad, P. R. *J. Chromatogr. A* **1997**, *789*, 67-83

[28] Haddad, P. R. Jackson, P. E.; Shaw, M. J. *J. Chromatogr. A* **2003**, *1000*, 725-742.

[29] Isildak, I.; Asan, A. *Talanta* **1999**, *48*, 967-978.

[30] Isildak, I. *Chromatographia* **1999**, *49*, 338-342.

[31] Poels, I.; Nagels, L.J.; Verreyt, G.; Geise, H.J. *Anal. Chim. Acta* **1998**, *370*, 105.

[32] Pretsch, E. *Trends Anal. Chem.* **2007**, *26*, 46-51

[33] Sutton, K. L.; Caruso, J. A. *J. Chromatogr. A* **1999**, *856*, 243-258.

[34] Wang, T. *J. Liq. Chromatogr. & Rel. Technol.* **2007**, *30*, 807-831.

[35] Pantsar-Kallio, M.; Manninen, P. K. G. *Anal. Chim. Acta* **1996**, *318*, 335-343.

[36] Barnowski, C.; Jakubowski, N.; Stuewer,D.; Broekaert, J. A. C. *J. Anal. Atom. Spectrom.* **1997**, *12*, 1155-1161.

[37] Mandal, B. K., Ogra, Y., Suzuki, K. T. *Chem. Res. Toxicol.* **2001**, *14*, 371-378.

[38] Le, X. C., Lu, X., Li, X. *Anal. Chem.* **2004**, 27A-33A.

[39] Wuilloud, R. G., Altamirano, J. C., Smichowski, P. N., Heitkemper, D. T. *J. Anal. At. Spectrom.* **2006**, *21*, 1214-1223.

[40] Nischwitz, V., Pergantis, S. A. *J. Anal. At. Spectrom.* **2006**, *21*, 1277-1286.

[41] Salov, V. V., Yoashinaga, J., Shibata, Y., Morita, M. *Anal. Chem.* **1992**, *64*, 2425-2428.

[42] Yamanaka, M., Sakai, T., Kumagai, H., Inoue, Y. *J. Chromatogr. A.* **1997**, *789*, 259-265.

[43] Divjak, B., Novic, M., Goessler, W. *J. Chromatogr. A.* **1999**, *862*, 39-47.

[44] Dudoit, A., Pergantis, S. A. *J. Anal. At. Spectrom.* **2001**, *16*, 575-580.

[45] Guo, Z., Cai, Q., Yu, C., Yang, Z. *J. Anal. At. Spectrom.* **2003**, *18*, 1396-1399.

[46] Cole, R. B. *J. Mass Spectrom.* **2000**, *35*, 763-772.

[47] Kebarle, P.; Peschke, M. *Anal. Chim. Acta* **2000**, *406*, 11-35.

[48] Cech, N. B.; Enke, C. G. *Mass Spectrom. Rev.* **2001**, *20*, 362-287.

[49] Yamashita, M.; Fenn, J. B. *J. Phys. Chem.* **1994**, *88*, 4671-4675.

[50] Ikonomou, M. G.; Blades, A. T.; Kebarle, P. J. *J. Am. Soc. Mass Spectrom*. **1991**, *2*, 497-505.

[51] Straub, R. F., Voyksner, R. D. *J. Am. Soc. Mass Spectrom.* **1993**, *4*, 578-587.

[52] Cole, R. B.; Harrata, A. K. *J. Am. Soc. Mass Spectrom*. **1993**, *4*, 546-556.

[53] Apffel, A.; Chakel, J. A.; Fischer, S.; Lichtenwalter, K.; Hancock, W. S. *Anal. Chem.* **1997**, *69*, 1320-1325.

[54] Cole, R. B.; Zhu, J. *Rapid. Comm.Mass Spectrom*. **1999**, *13*, 607-611.

[55] Soukup-Hein, R.J.; Remsburg, J.W.; Dasgupta, P.K.; Armstrong, D.W. *Anal. Chem.*, **2007,** *79*, 7346.

[56] Remsburg, J.W.; Soukup-Hein, R.J.; Crank, J.A.; Breitbach, Z.S.; Payagala, T.; Armstrong, D.W. *J. Am. Soc. Mass Spectrom.*, **2008**, *19***,** 261.

[57] Martinelango, P.K.; Anderson, J.L.; Dasgupta, P.K.; Armstrong, D.W.; Al-Horr, R.S.; Slingsby, R.W. *Anal. Chem*., **2005**, *77*, 4829.

[58] Martinelango, P.K.; Tian, K.; Dasgupta, P.K. *Anal. Chim. Acta*, **2006**, *567*, 100.

[59] Soukup-Hein, R.J. Remsburg, J.W.; Soukup-Hein, R.J.; Breitbach, Z.S.; Sharma, P.S.; Payagala, T.; Wanigasekara, E.; Huang, J.; Armstrong, D.W. *Anal. Chem.*, **2008,** *80***,** 2612.

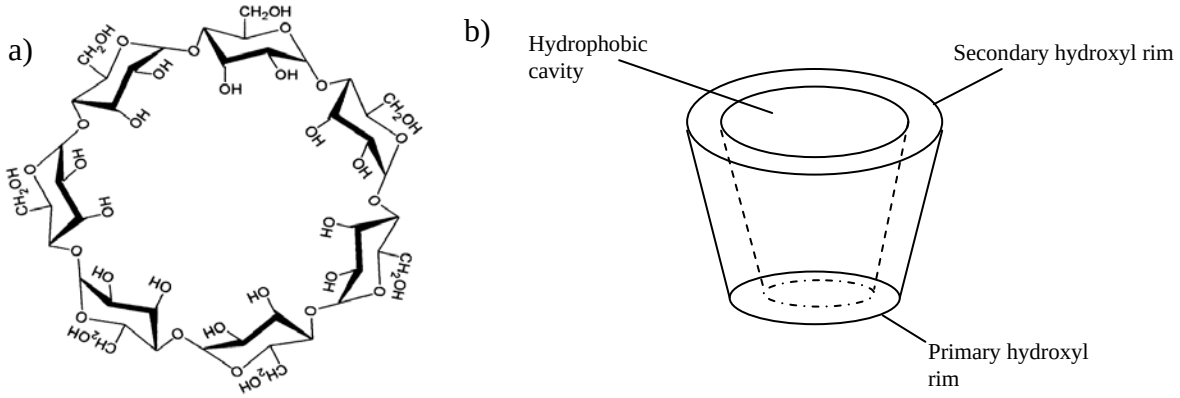

Figure 1. Structure of β-cyclodextrin (a) and the toroidal shape of a cyclodextrin molecule (b) (from Ref. [4]).

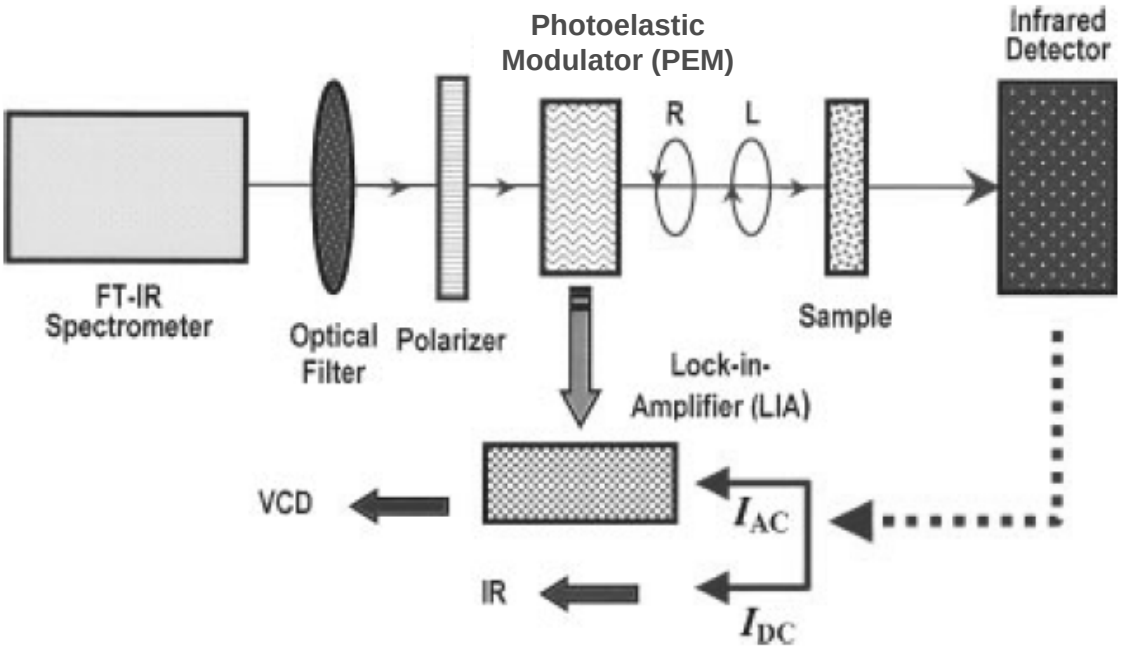

Figure 2. Block diagram of the optical-electronic layout of a Fourier transform vibrational circular dichrosim spectrometer (from Ref. [22]).

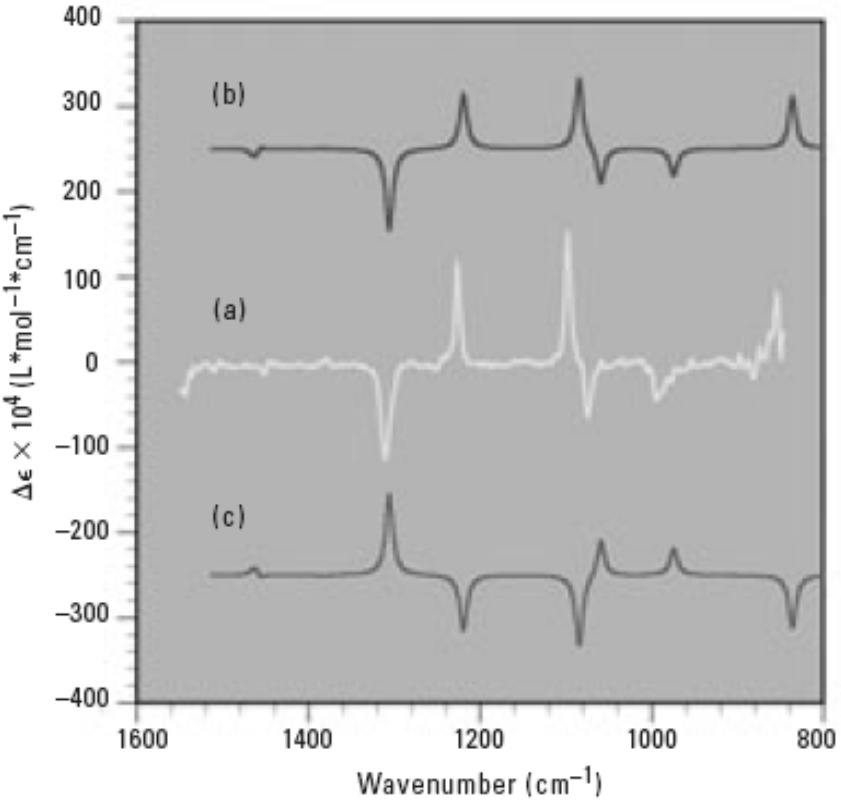

Figure 3. Comparison of (a) the experimental mid-IR VCD spectrum of (+)-3-chloro-1-butyne with the predicted spectra for the (b) (*R*)-and (c) (*S*)-enantiomers of 3-chloro-1-butyne (from Ref [23]).

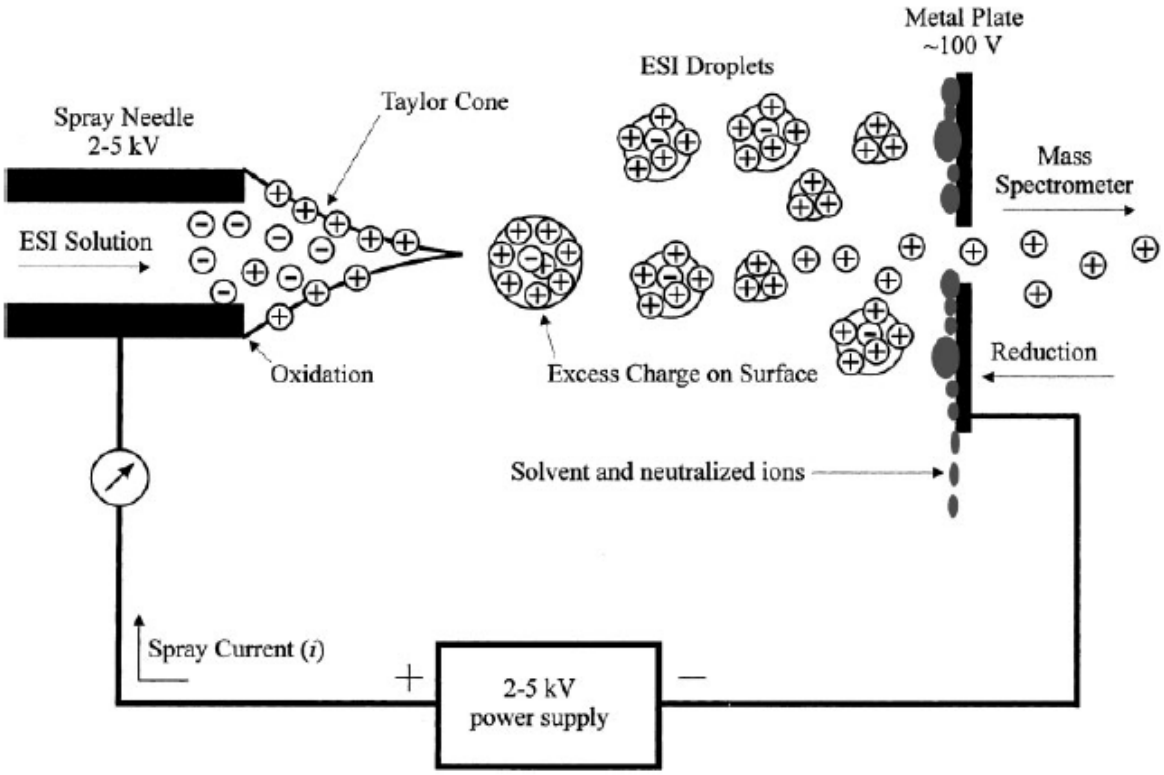

Figure 4. Schematic of the electrospray ionization process. The analyte solution is pumped through a needle to which a high voltage is applied. A Taylor cone with an excess of positive charge on its surface forms as a result of the electric field gradient between the ESI needle and the counter electrode. Charged droplets are formed from the tip of the Taylor cone, and these droplets evaporate as they move towards the entrance of the mass spectrometer to produce free, charged analyte molecules that can be analyzed for mass-to-charge ratio. From Ref. [48].

CHAPTER 2

USE OF NATIVE AND DERIVATIZED CYCLODEXTRIN BASED AND MACROCYCLIC GLYCOPEPTIDE BASED CHIRAL STATIONARY PHASES FOR THE ENANTIOSEPARATION OF PTEROCARPANS BY HIGH PERFORMANCE LIQUID CHROMATOGRAPHY

A paper published in *Journal of Liquid Chromatography and Related Technologies*[1]

M.M. Warnke, C.R. Mitchell, R.V. Rozhkov, D.E. Emrich,
R.C. Larock, and D.W. Armstrong

ABSTRACT

The enantioselectivity of native and derivatized cyclodextrin stationary phases and macrocyclic glycopeptides for chiral pterocarpans was evaluated using high performance liquid chromatography (HPLC). All enantiomers could be baseline resolved in the reverse phase mode on cyclodextrin based, Cyclobond, chiral stationary phases (CSPs). The hydroxypropyl-β-cyclodextrin, acetyl-β-cyclodextrin, and gamma-cyclodextrin CSPs show the broadest enantioselectivity in the reverse phase mode. Some compounds were baseline separated on the ristocetin A and vancomycin macrocyclic glycopeptide chiral stationary phases in the reverse phase mode. Separations on the ristocetin A columns produced the highest resolutions (up to ~7.1) in this study. The 3,5-dimethylphenyl carbamate derivatized cyclodextrin column showed the broadest enantioselectivity in normal phase LC. Of the macrocyclic glycopeptide CSPs, ristocetin A and teicoplanin aglycone (Chirobiotic R and

[1] Reproduced from Journal of Liquid Chromatography and Related Technologies, 2005, 28(6), 823-834.

TAG respectively) separated the most compounds in the normal phase mode. However, baseline separations were only achieved with the teicoplanin and teicoplanin aglycone.

2.1 INTRODUCTION

Pterocarpans are *cis*–fused benzopyran benzofuranyl structures and one of the largest groups of natural isoflavanoids, second only in prevalence to the isoflavones [1]. Isoflavanoids have been isolated mainly from fodder crops, beans, peas, and some shrubs. Many pterocarpans are phytoalexins, or antifungal compounds formed in a plant after it has been infected by fungal organisms [2,3]. Other pterocarpans have shown anti-microbial activity [4] and activity against snake and spider venom [5]. The structure and numbering system for pterocarpans is shown in Figure 2.1.

Although there are two stereogenic centers at carbons 6a and 11a, pterocarpans exist as only one set of enantiomers because of the *cis*-fused ring system. In most cases, the (-)-(6a*R*, 11a*R*)-isomer is the biologically produced pterocarpan enantiomer [3,4,5]. Synthetic pterocarpans are often produced as racemates [6,7,8]. Thus, enantioseparation is important in isolating the active enantiomer. Previously, enantiomeric separations have been achieved for both natural and synthetic pterocarpan compounds using both HPLC and capillary electrophoresis [9,10].

Native α, β, and γ cyclodextrins are macrocyclic compounds formed from 6, 7, or 8 gluco-pyranose units respectively. Chiral stationary phases (CSP) based on cyclodextrins are able to separate enantiomers by forming inclusion complexes in the reverse phase mode of operation [11,12]. The hydrophobic part of the analyte molecule complexes with the hydrophobic interior cavity of the cyclodextrin. Interactions with the hydroxyl groups or

derivative groups on the rim complete the necessary three points of interaction required to achieve enantioselective complexation [11]. The cavity size increases as the number of gluco-pyranose units increases. The native β-cyclodextrin CSP (Cyclobond I 2000) was shown to effectively separate enantiomers of polycyclic aromatic hydrocarbons [13,14].

Derivatized cyclodextrin based CSPs offer additional sites for interactions leading to chiral recognition. The hydroxypropyl-β-cyclodextrin (Cyclobond I 2000 RSP) has been shown to separate compounds not separated on the native β-cyclodextrin CSP [15]. Cyclodextrins derivatized with aromatic groups are effective for separations in the normal phase mode [16,17]. Nonpolar solvent molecules occupy the cyclodextrin cavity in the normal phase mode, therefore π-π interactions, dipole stacking, and hydrogen bonding interactions are important for chiral recognition [16].

Macrocyclic glycopeptide based CSPs have also been shown to separate a wide variety of chiral compounds [18]. The commercially available CSPs are those based on the macrocyclic glycopeptide antibiotics vancomycin, ristocetin A, teicoplanin, and teicoplanin aglycone. All of these chiral selectors have a similar peptide backbone, multiple stereogenic centers, and functionalities such as carboxylic acids, amines, sugar moieties, and aromatic rings [19]. The teicoplanin aglycone is the only chiral selector without saccharide groups attached. Along with a variety of functional groups, these chiral selectors have a secondary structure in the form of a twisted “C” shaped basket that is relatively non-polar [20,21]. Interactions between an analyte molecule and the functional groups or hydrophobic cavity of the macrocyclic glycopeptide based CSP can lead to enantioselectivity.

2.2 EXPERIMENTAL

2.2.1 Materials

The pterocarpan compounds studied are shown in Table 1. The compounds were synthesized by reacting 1 equivalent of a substituted 2-iodophenol and 2 equivalents of benzopyran or a substituted benzopyran with 5% palladium acetate catalyst, 1 equivalent of Na_2CO_3, and 15% *n*-Bu_4NCl in DMF at 100º C for 1 day [22].

The methanol (MeOH), acetonitrile (ACN), and heptane used in the mobile phases are all HPLC grade and were purchased from Fisher Scientific (Fair Lawn, New Jersey). The ethyl alcohol (EtOH) was purchased from Aaper Alcohols (Shelbyville, Kentucky) and is of punctilious grade. Water used in the separations was filtered and deionized using activated charcoal and a 5 μm filter. Mobile phases were degassed through ultrasonication and vacuum for 5 minutes.

2.2.2 Equipment

The cyclodextrin based chiral stationary phases used were Cyclobond I 2000, Cyclobond I 2000 DM (consisting of dimethylated β-cyclodextrin), Cyclobond I 2000 RSP (consisting of hydroxypropyl derivatized β-cyclodextrin), Cyclobond I 2000 AC (consisting of acetylated β-cyclodextrin), Cyclobond I 2000 DMP (consisting of 3,5-dimethylphenylcarbamate derivatized β-cyclodextrin), Cyclobond I 2000 RN (consisting of naphthylethyl carbamate derivatized β-cyclodextrin), Cyclobond II (γ-cyclodextrin), and Cyclobond III (α-cyclodextrin). The macrocyclic glycopeptide based chiral stationary phases used in this study were the Chirobiotic R (based on ristocetin A), Chirobiotic V (based on vancomycin), Chirobiotic T (based on teicoplanin), and Chirobiotic TAG (based on

teicoplanin aglycone). All stationary phases were obtained from Astec (Whippany, New Jersey, USA).

The chromatographic experiments were performed on an HP1050 HPLC, equipped with an autosampler, quaternary pump, and VWD UV detector. All experiments were performed at ambient temperature and a flow rate of 1.0 ml/min.

2.2.3 Calculations

The retention factor for the first enantiomeric peak, k_1, was calculated by the equation: t_{r1}-t_m/t_m, where t_{r1} is the retention time of the first peak and t_m is the retention time of the void volume. The selectivity, α, is determined as follows: k_2/k_1, where k_2 is the retention factor of the second enantiomeric peak. The resolution is calculated as follows $2(t_{r2}-t_{r1})/(w_1+w_2)$, where w_1 and w_2 are the widths at the peak's base.

2.3 RESULTS AND DISCUSSION

The β-cyclodextrin and γ-cyclodextrin CSPs were the most useful native cyclodextrin CSPs, separating all five compounds. The difference between the two cyclodextrins is one gluco-pyranose unit, which creates a larger cavity for the gamma cyclodextrin. Figure 2.2 shows separations on both the beta and gamma cyclodextrin CSPs. On the former column, there is a definite substituent effect on enantioselectivity. The unsubstituted pterocarpan (compound 1) has very low enantioselectivity, while the substituted pterocarpans (compounds 5 and 3) have much higher enantioselectivities and resolutions. The substituent can be on the benzofuran or benzopyran portion of the molecule, and either improves enantioseparation on the β-cyclodextrin column. Enantiomers of the unsubstituted pterocarpan (compound 1) are almost completely resolved on the γ-cyclodextrin CSP, which

is a vast improvement from the results on the β-cyclodextrin CSP. This can only be due to the difference in how well the analyte fits into the cyclodextrin cavity versus the larger γ-cyclodextrin cavity. However, it should be noted that the γ-cyclodextrin CSP was ineffective in separating pterocarpans with substituted benzopyran groups.

The nonaromatic derivatized cyclodextrin based CSPs produced the best separations of all the cyclodextrin based CSPs. All five pterocarpan compounds were baseline or near baseline separated on the Cyclobond I 2000 AC CSP. The Cyclobond I 2000 RSP CSP and Cyclobond I 2000 DM CSP each separated four of the five compounds. However, separations on the Cyclobond I 2000 RSP CSP had higher resolutions than those on the Cyclobond I 2000 DMP CSP (see Table 2.1).

Compound 1 had the highest resolution and enantioselectivity of all of the compounds on the Cyclobond I 2000 AC CSP. The enantioselectivity, resolution, and retention factors are similar for compounds 2, 3 and 4, which are pterocarpans with substituents on the benzene ring of the benzofuran moiety. Because of these similarities, it appears that the type of substituent plays only a minor role in the enantiomeric separation on the acetylated β-cyclodextrin CSP. Compound 5, with a methyl ether substituent on the aromatic ring of the benzopyran moiety, has a lower enantioselectivity and resolution and a higher retention factor than the other pterocarpans.

The Cyclobond I 2000 DM CSP showed similar trends to the AC CSP. On the DM CSP, pterocarpans without a substituent or with a substituent on the benzofuran moiety (compounds 1, 2, and 4) had similar resolutions and enantioselectivities. The benzopyran substituted compound 5 had lower resolution and enantioselectivity.

Conversely, compound 5 had higher enantioselectivity and resolution on the Cyclobond I 2000 RSP CSP (Fig 2.3A) than on the Cyclobond I 2000 DM CSP (Fig. 2.3B). On the other derivatized cyclodextrin CSPs, compounds 1-4 showed similar separations and were always better than those for compound 5. The enantioseparation of compound 5 was the best on the RSP CSP (highest α and Rs). The nature of the benzofuran substituent appears to affect the enantioseparation on the RSP CSP. Compound 2 with a methyl ketone substituent has a smaller resolution and enantioselectivity than compound 3 with its methyl ether substituent. The two enantiomers of the nitro-substituted pterocarpan, compound 4, were not separated.

The aromatic derivatized cyclodextrin CSPs, the Cyclobond I 2000 DMP and Cyclobond I 2000 RN, were not highly effective in the reverse phase mode, with no baseline separations despite long retention times. However, the normal phase mode was much more successful. The Cyclobond I 2000 DMP had higher resolutions and selectivities and lower retention factors. A comparison of the performance of the Cyclobond I 2000 DMP column in the reverse phase mode and the normal phase mode is shown in Figure 2.4. In the reverse phase mode, compound 2 shows a slight shoulder. In the normal phase mode, a much better separation of the two enantiomers is achieved.

The macrocyclic glycopeptide CSPs are also effective for the enantioseparation of these pterocarpans. From the data in Table 2.1, it is clear that only the pterocarpans with substituents on the benzofuran side can be separated on the Chirobiotic columns in either the reverse phase or normal phase mode. The location of the substituent on the pterocarpan along with interactions between the substituent and chiral selector appear to be necessary for chiral recognition with the glycopeptide chiral selectors.

The principle of complementary separations for the macrocyclic glycopeptide based CSPs states that if a compound partially separates on one of the Chirobiotic columns, it is likely it will baseline separate on one of the other columns using the same or similar mobile phase conditions [18]. Figure 2.5 illustrates this concept. Compound 2 separated with an α value of 1.10 and baseline resolution on the Chirobiotic V CSP. The separation on the Chirobiotic R CSP has an α value of 1.29 and over twice the resolution of the Chirobiotic V CSP. The difference in performance of the Chirobiotic V and R CSPs is much more dramatic for the separation of compound 3. In this case a non baseline resolved set of peaks with a selectivity of 1.06 on the Chirobiotic V column, improves to a selectivity of 1.65 and a resolution of 7.07 on the Chirobiotic R column.

In the normal phase mode separations with the macrocyclic glycopeptide columns, the Chirobiotic TAG and R columns separated the most enantiomers. Again, only the pterocarpans with benzofuranyl substituents separated. Compound 4 was baseline separated on the Chirobiotic R, T, and TAG columns in the normal phase mode. The electron-withdrawing nitro substituent makes the aromatic systems of the pterocarpan somewhat π electron deficient, so there can be stronger π-π interactions with the aromatic systems in the stationary phase.

2.4 CONCLUSIONS

The native cyclodextrin CSPs were effective in the enantioseparation of all five pterocarpan compounds in the reverse phase mode. The Cyclobond I 2000 RSP and Cyclobond I 2000 AC columns were the most effective of this class of CSPs. In the reverse phase mode, baseline separations were achieved for all compounds using these two CSPs.

The Chirobiotic R CSP separated the most compounds in the reverse phase mode and had the best resolution and enantioselectivities found in this study. In the normal phase mode, the Cyclobond I 2000 DMP was the only cyclodextrin based CSP to show enantioselectivity. Also in normal phase mode, some of the pterocarpans were partially separated on the Chirobiotic R and Chirobiotic V CSPs, and baseline separations were achieved for one compound on the Chirobiotic T and Chirobiotic TAG CSPs.

2.5 ACKNOWLEDGEMENTS

Support of this work by the National Institutes of Health, NIH RO1 GM53825-08 is gratefully acknowledged.

2.6 REFERENCES

[1] Dewick, P.M. Isoflavanoids, in *The Flavonoids: Advances in Research Since 1986*, Harborne, J.B., Ed.; Chapman and Hall: London, 1994; 166-180.

[2] Harborne, J.B.; Baxter, H., Eds. *The Handbook of Natural Flavonoids*, John Wiley & Sons: Chichester, England, 1999; xiv-xvi.

[3] Dewick, P.M.; Steele, M.J. Biosynthesis of the phytoalexin phaseollin in *phaseolus vulgaris*. **1992,** Phytochemistry, *21*(7), 1599-1603.

[4] Mitscher, L.A.; Gollapudi, S.R.; Gerlach, D.C.; Drake, S.D.; Veliz, E.A.; Ward, J.A. Erycristin, a new antimicrobial pterocarpan from *erythrina crista-galli*. **1988,** Phytochemistry, *27*(2), 381-385.

[5] Nakagawa, M.; Nakanishi, K. Structures of cabenegrins A-I and A-II, potent anti-snake venoms. **1982,** Tetrahedron Lett., *23*, 3855-3858.

[6] Horino, H.; Inoue, N. A new route to chromocoumarans. Synthesis of (±)-pterocarpin. **1976** J. Chem. Soc. Chem. Commun., 500-501

[7] Kiss, L; Antus, S.; A convenient synthesis of pterocarpans **2000,** Heterocycl. Commun. *6*: 309-314

[8] Lichtenfels, R.A.; Coelho, A.L.; Costa, P.R.R. Total synthesis of pteorcarpan: (+)-neorautenane. **1995,** J. Chem. Soc. Perkin Trans. I 949-950.

[9] Antus, S.; Bauer, R.; Gottsgen, A.; Wagner, H. Enantiomeric separation of racemic pterocarpans by high-performance liquid chromatography on (+)-poly(triphenylmethyl methacrylate)-coated silica gel. **1990**, J. Chromatogr., *508*, 212-216.

[10] Allen, D.J.; Gray, J.C.; Paiva, N.L.; Smith, J.T. An enantiomeric assay for the flavonoids medicarpin and vestitone using capillary electrophoresis. **2000,** Electrophoresis, *21,* 2051-2057.

[11] Armstrong, D.W.; Ward, T.J.; Armstrong, R.D.; Beesley, T.E. Separation of Drug Stereoisomers by the Formation of β-Cyclodextrin Inclusion Complexes. **1986,** Science, *232*, 1132-1135.

[12] Armstrong, D.W.; DeMond, W.; Cyclodextrin bonded phases for the liquid chromatographic separation of optical, geometrical, and structural isomers. **1984,** J. Chromatogr. Sci., *22*, 411-415.

[13] Armstrong, D.W.; Alak, A.; DeMond, W.; Hinze, W.L.; Riehl, T.E. Separation of mycotoxins, polycyclic aromatic hydrocarbons, quinines, and heterocyclic compounds on cyclodextrin bonded phases: an alternative LC packing. **1985,** J. Liq. Chromatogr. *8*(2), 261-269.

[14] Armstrong, D.W.; Demond, W.; Alak, A.; Hinze, W.L.; Riehl, T.E.; Bui, K.H. Liquid chromatographic separation of diastereomers and structural isomers on cyclodextrin-bonded phases. **1985,** Anal. Chem., *57*, 234-237.

[15] Stalcup, A.M.; Chang, S.; Armstrong, D.W.; Pitha, J. (*S*)-2-Hydroxypropyl-β-cyclodextrin, a new chiral stationary phase for reversed-phase liquid chromatography. **1990,** J. Chromatogr., *513*, 181-194.

[16] Stalcup, A.M.; Chang, S.; Armstrong, D.W Effect of the configuration of the substituents of derivatized β-cyclodextrin bonded phases on enantioselectivity in normal-phase liquid chromatography. **1991,** J. Chromatogr., *540*, 113-128.

[17] Armstrong, D.W.; Stalcup, A.M.; Hilton, M.L.; Duncan, J.; Faulkner, J.R., Jr.; Chang, S. Derivatized cyclodextrins for normal-phase liquid chromatographic separation of enantiomers **1990,** Anal. Chem., *62*, 1610-1615.

[18] Xiao, T.L.; Armstrong, D.A. Chiral Separations: Methods and Protocols. In *Methods in Molecular Biology*, Güblitz, G., Schmid, M.G., Eds.; Humana Press, Inc., Totowa, NJ, 2004; Vol. 243, 115, 149-159.

[19] Armstrong, D.W.; Tang, Y.; Chen, S.; Zhou, Y.; Bagwill, C.; Chen, J. Macrocyclic Antibiotics as a New Class of Chiral Selectors for Liquid Chromatography. **1994**, Anal. Chem., *66*, 1473-1484.

[20] Nair, U.B.; Chang, S.S.C.; Armstrong, D.W.; Rawjee, Y.Y.; Eggleston, D.S.; McArdle, J.V. Elucidation of vancomycin's enantioselective binding site using its copper complex. **1996,** Chirality, *8*, 590-595.

[21] Gasper, M.P.; Berthod, A.; Nair, U.B.; Armstrong, D.W. Comparison and Modeling Study of Vancomycin, Ristocetin A, and Teicoplanin for CE Enantioseparations. **1996,** Anal. Chem., *68*, 2501-2514.

[22] Richard C. Larock, Daniel Emrich and Roman Rozhkov, work in progress.

Table 2.1 Retention factor (k_1'), enantioselectivity (α) and enantioresolution (Rs) of pterocarpans on columns listed.

	1			2			3			4			5		
	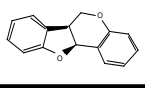			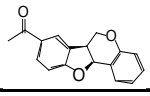			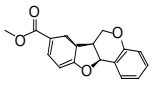			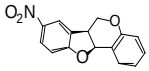			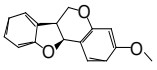		
Cyclodextrin Based Chiral Stationary Phases	k_1	∴	R_s	k_1	∴	R_s	k_1	∴	R_s	k_1	∴	R_s	k_1	∴	R_s
Reverse Phase Mode															
Cyclobond I 2000 (a)	7.12	1.01	0.32	7.78	–	--	10.01	1.11	1.96	8.40	--	--	8.52	1.06	1.21
Cyclobond II(b)	3.23	1.08	1.33	3.43	1.08	1.39	4.26	1.13	1.03	2.68	1.06	0.86	3.98	--	--
Cyclobond III (c)	3.48	–	–	4.25	–	--	7.96	--	--	5.99	--	--	5.84	--	--
Cyclobond I 2000 RSP(d)	4.33	1.12	1.93	3.29	1.07	1.17	4.56	1.11	1.75	3.30	--	--	5.73	1.13	2.09
Cyclobond I 2000 AC(e)	8.01	1.22	2.78	8.23	1.15	1.69	10.00	1.18	2.27	8.33	1.17	2.00	11.90	1.11	1.44
Cyclobond I 2000 DM(f)	6.92	1.09	0.73	6.15	1.06	0.76	8.82	--	--	5.99	1.08	0.89	7.55	1.03	0.56
Cyclobond I 2000 DMP(d)	7.76	–	–	11.98	1.05	0.68	14.02	--	--	9.88	--	--	15.39	1.04	0.60
Cyclobond I 2000 RN(g)	15.31	–	–	14.00	1.03	0.63	20.40	1.05	1.11	8.96	--	--	17.40	1.06	1.33
Normal Phase Mode															
Cyclobond I 2000 DMP (h)	0.22	–	–	2.85	1.10	1.40	1.09	1.06	1.21	3.17	1.12	2.03	0.58	--	--
Cyclobond I 2000 RN (h)	0.15	–	–	2.31	–	--	0.90	--	--	2.13	--	--	0.37	--	--

Macrocyclic Glycopeptide Based Chiral Stationary Phases	k_1'	∴	R_s	k_1'	∴	R_s	k_1'	∴	R_s	k_1'	∴	R_s	k_1'	∴	R_s
Reverse Phase Mode															
Chirobiotic R(e)	1.82	–	–	2.52	1.29	4.19	3.52	1.65	7.07	4.36	1.25	3.75	2.47	--	--
Chirobiotic V (g)	4.04	–	–	6.10	1.10	1.71	12.20	1.06	1.12	6.61	--	--	5.69	--	--
Chirobiotic TAG(i)	20.12	–	–	23.80	–	--	30.00	--	--	10.72	--	--	22.62	--	--
Chirobiotic T(g)	9.06	–	–	17.89	1.03	0.54	19.25	--	--	10.13	--	--	12.20	--	--
Normal Phase Mode															
Chirobiotic R(j)	0.28	–	–	2.35	1.02	0.65	0.85	1.04	0.90	2.19	1.08	1.38	0.30	--	--
Chirobiotic V(j)	0.21	–	–	2.46	1.05	1.26	0.85	--	--	1.89	--	--	0.27	--	--
Chirobiotic TAG(h)	0.29	–	–	6.00	1.07	0.98	2.19	1.02	0.44	4.65	1.36	3.24	0.51	--	--
Chirobiotic T(j)	0.15	–	–	2.14	–	--	0.66	--	--	1.79	1.20	3.39	0.48	--	--

Mobile Phase Conditions

(a) 80/20 water/acetonitrile
(b) 90/10 water/acetonitrile
(c) 80/20 water/methanol
(d) 60/40 methanol/water
(e) 60/40 water/methanol
(f) 80/20 water/acetonitrile
(g) 70/30 water/methanol
(h) 95/5 heptane/ethanol
(i) 75/25 water/acetonitrile
(j) 90/10 heptane/ethanol

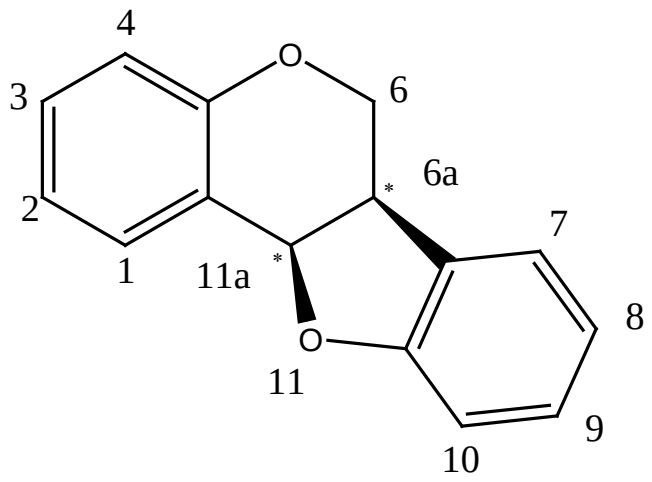

Figure 2.1. Numbering system of an unsubstituted pterocarpan. The stereocenters are denoted with asterisks.

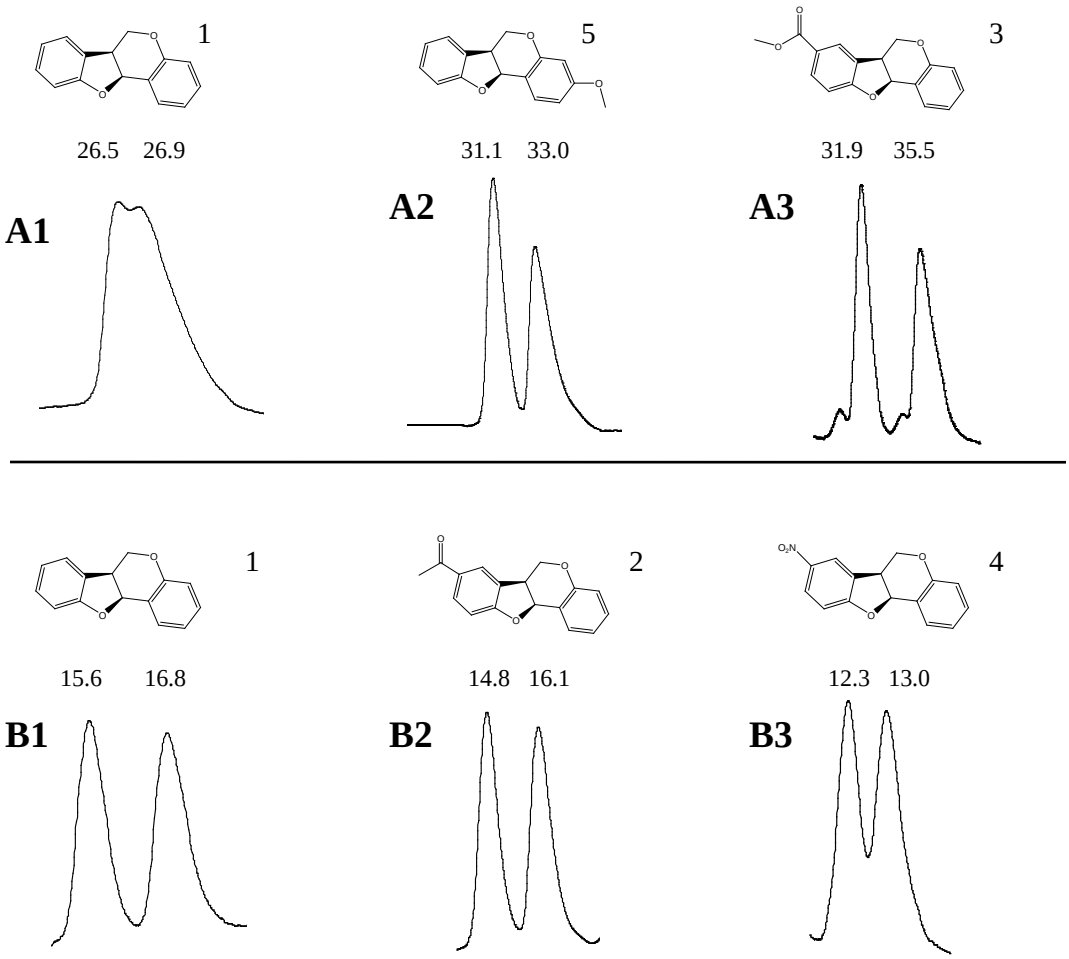

Figure 2.2. Comparison of separations on beta and gamma cyclodextrin based CSPs. A1, A2, and A3 are the enantioseparations of compounds 1, 5, and 3 respectively on the beta cyclodextrin. A1-A3 mobile phase conditions are 20/80 ACN/ H_2O. B1, B2, and B3 are the enantioseparations of compounds 1, 2, and 4 respectively on the gamma cyclodextrin. B1-B3 mobile phase conditions are 10/90 ACN/H_20.

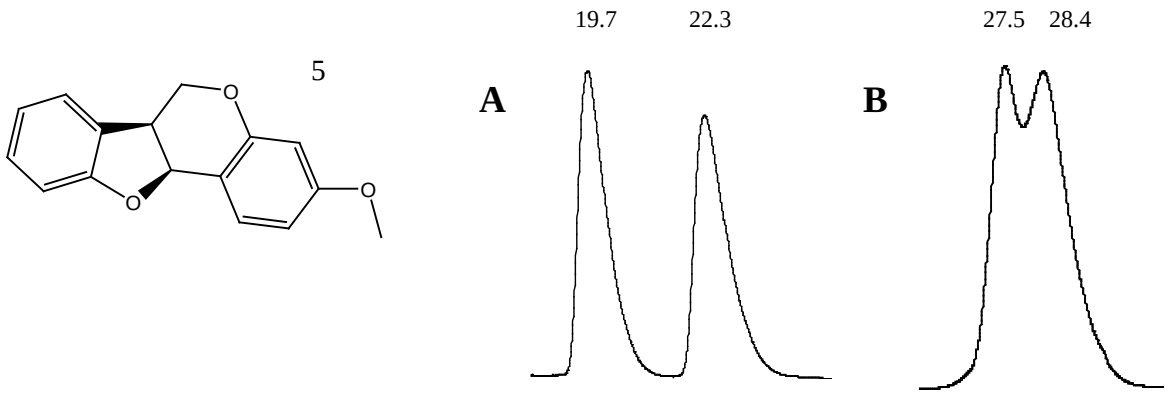

Figure 2.3. Enantioseparation of methyl ether substituted pterocarpan (compound 5). A) Separation on Cyclobond I 2000 RSP using 40/60 MeOH/H_20. B) Separation on Cyclobond I 2000 DM using 20/80 ACN/ H_20.

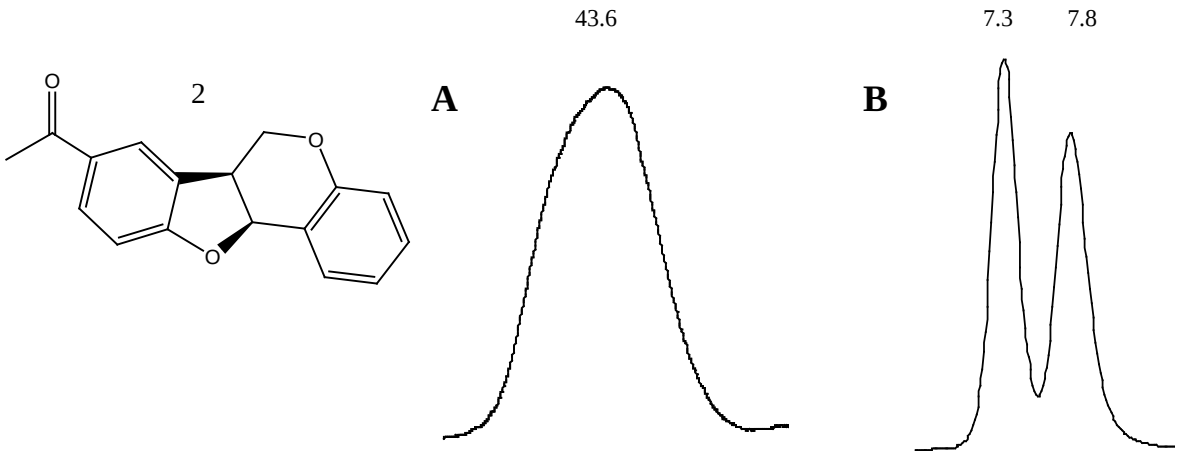

Figure 2.4. Comparison of separations in normal and reverse phase modes. Compound 2 was separated on the Cyclobond I 2000 DMP column using the following mobile phase conditions: A) 40/60 MeOH/H_20 and B) 95/5 Heptane/EtOH.

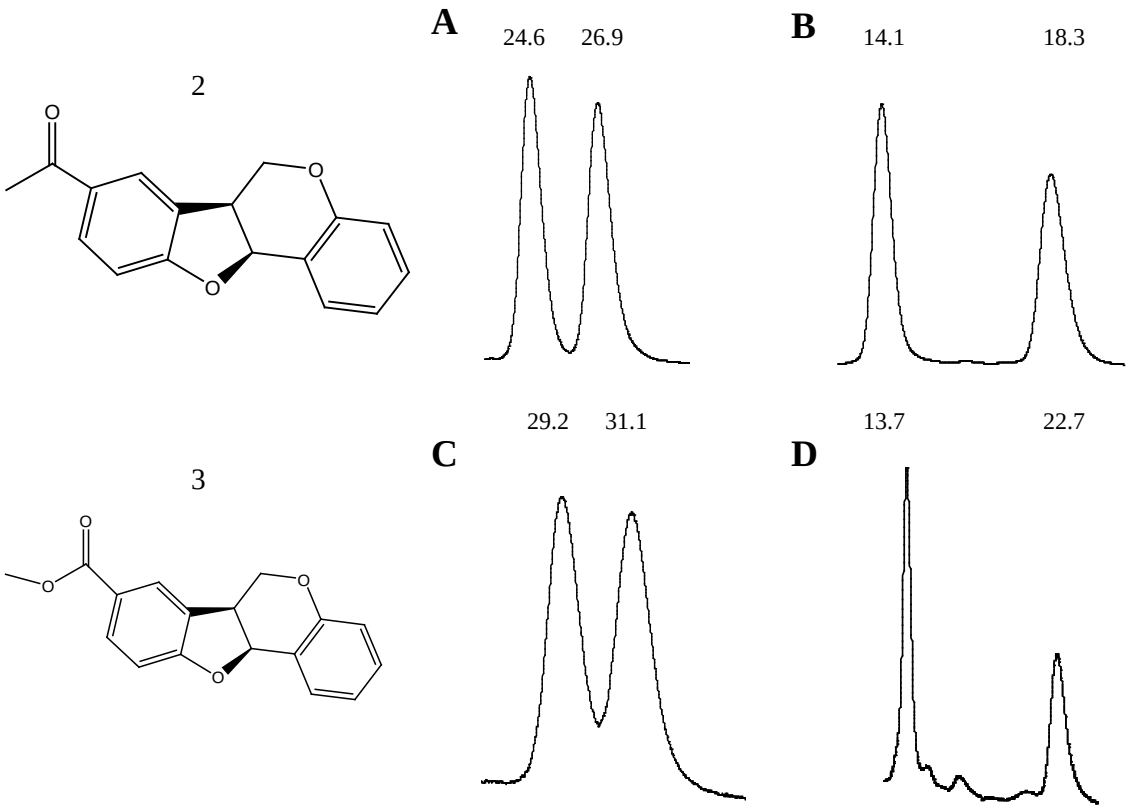

Figure 2.5. Enantioseparations on macrocyclic glycopeptide CSP. The methyl ketone substituted pterocarpan (compound 2) was separated on A) Chirobiotic V at 30/70 MeOH/H_2O and B) Chirobiotic R at 40/60 MeOH/ H_2O. The methyl ester substituted pterocarpan (compound 3) was separated on C) Chirobiotic V at 30/70 MeOH/ H_2O and D) Chirobiotic R at 40/60 MeOH/ H_2O.

CHAPTER 3

ENANTIOSEPARATION OF EXTENDED METAL ATOM CHAIN COMPLEXES: UNIQUE COMPOUNDS OF EXTRAORDINARILY HIGH SPECIFIC ROTATION

A paper published in *Chirality*[2]

Molly M. Warnke, F. Albert Cotton, Daniel W. Armstrong

ABSTRACT

Extended metal atom chains (EMACs) contain a linear metal chain wrapped by various ligands. Most complexes are of the form $M_3(dpa)_4X_2$, where M=metal, dpa=2,2'-dipyridylamide, and X=various anions. The ligands form helical coils about the metal chain, which results in chiral EMAC complexes. The EMACs containing the metals Co and Cu were partially separated in polar organic mode using a vancomycin based chiral stationary phase. Under similar conditions, two EMACs with Ni metal and varying anions could be baseline separated. The polar organic mode was used because of the instability of the compounds in aqueous mobile phases. Also, these conditions are more conducive to preparative separations. Polarimetric measurements on the resolved enantiomers of $Ni_3(dpa)_4Cl_2$ indicate that they have extraordinarily high specific rotations (on the order of 5000 deg·cc/g·dm).

3.1 INTRODUCTION

Some extended metal atom chains (EMACs), consisting of at least three metal atoms wrapped by various ligands, have shown promise as molecular wires [1-4]. The simplest examples of EMACs are a class of trimetal dipyridylamido complexes of the form

[2] Reproduced from Chirality, 2007, 19, 179-183. Copyright © 2007 with permission from Elsevier.

$M_3(dpa)_4X_2$, where M=metal, dpa=2,2'-dipyridylamide, and X=various anions. These complexes have interesting magnetic and electrochemical properties, but also contain an axis of chirality.

The general structure of the $M_3(dpa)_4X_2$ complexes and the structural abbreviation for the dpa ligand are shown in Figure 3.1a and 3.1b respectively. The axis of chirality runs along the trimetal chain. Chirality arises because steric hindrance of the pyridyl rings forces the dpa ligand from a planar configuration into a helical configuration [5]. Helical enantiomers are designated P for plus if following the helix describes a clockwise direction and M for minus if the direction is counterclockwise [6].

Thus far there have been no reports of successful asymmetric syntheses of EMAC enantiomers. There have been no reports of enantiomeric separations of these compounds via crystallization, chromatography, or capillary electrophoresis. Furthermore, EMACs are not good biological substrates and thus do not lend themselves to biological/enzymatic resolutions/enrichments. Previously, amylose and cellulose based chiral stationary phases (CSPs) have been used to separate racemic complexes containing one or two metals atoms or four atoms in a tetrahedrane-type cluster by high performance liquid chromatography (HPLC) [7-9]. Cyclodextrin CSPs have been used to separate metallocene enantiomers [10,11]. Teicoplanin, one of the macrocyclic glycopeptide CSPs, successfully separated ruthenium complexes containing one or two Ru atoms [12].

Macrocyclic glycopeptides have separated many classes of chiral compounds [13]. The available CSPs are based on the antibiotics vancomycin, ristocetin-A, teicoplanin, and teicoplanin-aglycone [13-15]. All of these chiral selectors are similar in that they have a peptide backbone and multiple functional groups such as carboxylic acids, amines, and

aromatic moieties [15]. Another feature of the macrocyclic glycopeptides is a twisted "C-shaped" basket that is relatively non-polar [16,17]. Enantioselectivity arises from interactions with the analyte and functional groups or the hydrophobic basket. Macrocyclic glycopeptide CSPs can be operated under reverse phase, normal phase, and polar organic modes [13]. This study reports the first enantiomeric separation of Ni, Co, Cu, and Cr EMACs with various ligands and counterions.

3.2 MATERIALS AND METHODS

The formulas of the EMACs used in this study are shown in Table 1. The basic mechanism for forming the $M_3(dpa)_4Cl_2$ is: 3MCl2+4Lidpa → $M_3(dpa)_4Cl_2$ + 4LiCl [5, 18-20]. The synthesis for the other compounds in this study can be found in reference 3.

Mobile phases and sample solutions were prepared using HPLC grade methanol (MeOH), acetonitrile (ACN), tetrahydrofuran (THF) and heptane along with reagent grade 1-propanol purchased from Fisher Scientific (Fair Lawn, New Jersey). Additionally, HPLC grade methylene chloride was purchased from VWR (West Chester, PA). Ammonium trifluoroacetate (NH_4TFA) and sodium sulfate were purchased from Aldrich (Deerfield, IL). The ammonium nitrate (NH_4NO_3) was purchased from Fisher Scientific. Water used in the extraction steps was filtered and deionized using a Millipore water system. Mobile phases were degassed with helium for 5 minutes.

The macrocyclic glycopeptide based chiral stationary phases used in this study was the Chirobiotic V (based on vancomycin) and the Chirobiotic T (based on teicoplanin). The stationary phase was obtained from Astec (Whippany, New Jersey, USA).

The chromatographic experiments were performed on an HP1050 HPLC, equipped with an autosampler, quaternary pump, and VWD UV detector. All experiments were performed at ambient temperature, with flow rates as designated in figure captions, and with UV detection at 270 nm. Samples were dissolved in either acetonitrile for polar-organic mode separations or tetrahydrofuran for normal phase mode separations.

Chiral detection was performed with a Jasco CD-2095 (Easton, Maryland) circular dichroism detector. The chiral detector was in line with an HPLC system consisting of a pump (LC-6A, Shimadzu, Kyoto, Japan), a system controller (SCL-6A), Chromatopac (CR 601, Shimadzu), UV detector (SPD-6A, Shimadzu) and a 200-µl injector valve (Rheodyne, Cotati, CA, USA). The wavelength of detection was 270 nm.

For the preparative separation and polarimetry experiments, a semi-preparative (250x21.2 mm) Chirobiotic V macrocyclic glycopeptide based chiral stationary phase was used. The stationary phase was obtained from Astec (Whippany, New Jersey, USA). The mobile phase consisted of 95/5/0.25 ACN/MeOH/ NH_4TFA. The trinickel dipyridylamido complex was dissolved in 60/40 ACN/MeOH before injecting 200 µl.

An HPLC system consisting of a pump (LC-6A, Shimadzu, Kyoto, Japan), a system controller (SCL-6A), Chromatopac (CR 601, Shimadzu), UV detector (SPD-6A, Shimadzu) and a 200-µl injector valve (Rheodyne, Cotati, CA, USA) was used. Peaks were collected at 270 nm.

After collection, the enantiomers were evaporated to dryness, then dissolved with dichloromethane. Each enantiomer was washed with deionized water to remove the salt from the mobile phase. Sodium sulfate was added to the enantiomer/dichloromethane solution and it was then allowed to sit for several hours to remove any excess water. The sodium sulfate

was removed and the dichloromethane was evaporated. Each enantiomer was prepared in methylene chloride to the concentration shown in Table 2, then analyzed at ambient temperature using a Jasco P-1010 polarimeter at a wavelength of 589 nm. The cell pathlength is 1 dm.

The retention factor for the first eluted enantiomer, k_1, was calculated using the equation: tr_1-tr_m/ tr_m, where tr_1 is the retention time of the first enantiomer peak and tr_m is the retention time of the void volume. The selectivity factor, α, was calculated as follows: k_2/ k_1, where k_2 is the retention factor for the second eluted enantiomer. Resolution is calculated as: $2(tr_2- tr_1)/(w_1+ w_2)$ where w_1 and w_2 are the widths at the peak's base.

Specific rotation, $[\alpha]^{589}_{22}$, is calculated using the equation: α/lc, where α is the observed optical rotation, l is the pathlength of the cell in dm, and c is the concentration of analyte in g/cc. Note that this use of α should not be confused with that previously defined for chromatographic selectivity.

3.3 RESULTS AND DISCUSSION

The Chirobiotic T and Chirobiotic V were the only macrocyclic glycopeptide stationary phases to show enantioselectivity for the trimetal dipyridylamido complexes. Separations on the vancomycin-based stationary phase had higher efficiencies and better resolutions than on the teicoplanin CSP at similar mobile phase conditions. Consequently, this study focuses on separations obtained on the Chirobiotic V stationary phase. Separations were peformed in either the polar-organic mode or normal-phase mode because the dpa anion is a very strong base and the complexes decomposed under aqueous conditions. Also, the organic solvents used in the polar organic mode better facilitate preparative separations due to the ease of mobile phase removal after separation.

The complexes of the form $M_3(dpa)_4X_2$ could all be separated on the Chirobiotic V stationary phase with the exception of $Cr_3(dpa)_4Cl_2$. The chromium trimetal complex was unstable under all conditions used in this study. Table 3.1 gives the formulas, chromatographic data, and optimized separation conditions used for each complex investigated.

Ammonium nitrate and ammonium trifluoroacetate were useful mobile phase additives for enantioseparation. For most separations, increasing the salt content decreased retention time and lowered the selectivity factor, but improved peak shape. This behavior is illustrated in Figure 3.2, where chromatograms of the separation of $Ni_3(dpa)_4Cl_2$ (complex 3) appear at different additive concentrations.

The copper and cobalt complexes, 1 and 2 respectively, were nearly baseline separated using the Chirobiotic V column. The enantiomeric separations were confirmed by using a chiral detector in-line with UV detection. The retention factors were similar for complexes 1-3 (Table 3.1), but the resolution and selectivity varied for each metal complex. The Co and Cu complexes appear to decompose to varying degrees in the mobile phase. The chromatographic evidence for this was the appearance of a peak for the dissociated dpa ligand (data not shown).

The nickel complexes with the dpa ligand (3 and 4) were much more stable in solution and on the chromatographic column. Complex 3 was baseline separated (Fig. 3.3) as was complex 4. Even with different axial groups, at optimized separation conditions, the selectivity is the same for both complexes.

The last EMAC complex investigated, complex 5, consisted of a tri-nickel chain wrapped by two septadentate ligands (Fig. 3.1c). This complex showed no enantiomeric

separation in the polar-organic mode, but could be separated in the normal-phase mode. This complex contrasts with the others (1-4) which were also soluble in many organic solvents used in normal-phase mode chromatography, but could not be separated in that mode.

Polarimetry results showed high specific rotation for each enantiomer of the $Ni_3(dpa)_4Cl_2$ complex (Table 3.2). The first and second eluted enantiomers are -5000$\pm$192 deg·cc/g·dm and +5205$\pm$182 deg·cc/g·dm respectively. Two rotations of equal and opposite signs confirmed the enantiomeric separation. The $Ni_3(dpa)_4Cl_2$ specific rotations are higher than those reported for some other compounds containing an axis of chirality [21-24]. For example, hexahelicene, an asymmetric molecule due to steric hindrance, has a reported specific rotation of -3640 deg·cc/g·dm [21]. Optically active polymers often have high optical rotations as well. Triphenylmethyl methacrylate was polymerized using (-)-sparteine-*n*-Bu-Li complex as a chiral catalyst. The polymer contained no asymmetry, but had a helical axis and a reported specific rotation of +490 deg·cc/g·dm [23]. A specific rotation of +1355 deg·cc/g·dm was reported for the polymerization of phenyl[bis(2-pyridyl)] methyl methacrylate with an (S)-(+)-1-(2-pyrrolidinylmethyl) pyrrolidine – *N*,*N*-diphenylethylenediamine monolithium amide [24]. This polymer also has a one-handed helical structure. To our knowledge, the largest reported specific rotation (19,852 deg·cc/g·dm) is for that of the chiral C_{76} fullerene [25].

3.4 CONCLUSION

Five EMAC complexes with varying ligands and metals could be partially or baseline separated using the Chirobiotic V chiral stationary phase. Due to the instability of the complexes in water, the polar organic mode or the normal phase mode of chromatography was utilized. Mobile phase additives were determined to be necessary for enantioseparations

in the polar organic mode. These additives enhanced enantioselectivity but also improved resolution by increasing efficiency. Polarimetry experiments confirmed the enantiomeric separation and also determined that the nickel complex enantiomers have very high specific rotation values.

3.5 ACKNOWLEDGEMENTS

MMW and DWA gratefully acknowledge the support of the NIH (5 ROI GM053825-11) and the Robert A. Welch Foundation. FAC gratefully acknowledges the support of the Robert A. Welch Foundation and Texas A&M University.

3.6 REFERENCES

1. Berry JF, Cotton FA, Murillo CA, Roberts BK. An efficient synthesis of acetylide/trimetal/acetylide molecular wires. Inorg Chem 2004;43:2277-2283.
2. Berry JF, Cotton FA, Daniels LM, Murillo CA. A trinickel dipyridylamido complex with metal-metal bonding interactions: prelude to polynickel molecular wires and devices? J Am Chem Soc 2002;124:3212-3213.
3. Berry JF, Cotton FA, Lu T, Murillo CA, Wang X. Enhancing the stability of trinickel molecular wires and switches: Ni_3^{6+}/Ni_3^{7+}. Inorg Chem 2003a;42:3959-3601.
4. Berry JF. Extended Metal Atom Chains. In: Cotton FA, Murillo CA, Walton RA Eds. Multiple Bonds Between Metal Atoms, 3rd Ed. New York: Springer;2005. p 669.
5. Cotton FA, Daniels LM, Jordan IV GT, Murillo CA. Symmetrical and Unsymmetrical Compounds having a linear Co_3^{6+} chain ligated by a spiral set of dipyridyl anions. J Am Chem Soc 1997;119:10377-10381.

6. Nasipuri D. Stereoisomerism: Axial chirality, planar chirality, and helicity. In: Stereochemistry of Organic Compounds: Principles and Applications. New York: John Wiley and Sons;1991. p 94-95.
7. Werner A, Michels M, Zander L, Lex J, Vogel E. “Figure eight” cyclooctapyrroles: enantiomeric separation and determination of the absolute configuration of a binuclear metal complex. Angew Chem Int Ed. 1999;38:3650-3653.
8. Ramsden JA, Garner CM, Gladysz JA. Facile Separations of enantiomers of chiral organometallic compounds with a bakerbond chiralcel hplc column. Organometallics 1991;10:1631-1633.
9. Wang X, Li W, Zhao Q, Li Y, Chen L. Normal-phase hplc enantioseparation of novel chiral metal tetrahedrane-type clusters on an amylose-based chiral stationary phase. Anal Sci 2005;21:125-128.
10. Armstrong DW, DeMond W, Czech BP. Separation of metallocene enantiomers by liquid chromatography: chiral recognition via cyclodextrin bonded phases. Anal Chem 1985;57:481-484.
11. Snegur LV, Boev VI, Nekrasov YS, Ilyin MM, Davankov VA, Starikova ZA, Yanovsky AI, Kolomiets AF, Babin VN. Synthesis and structure of biologically active ferrocenylalkyl polyfluoro benzimidazoles. J Organometallic Chem 580;1999:26-35.
12. Gasparrini F, D’Acquaria I, Vos JG, O’Connor CM, Villani C. Efficient enantiorecognition of ruthenium(II) complexes by silica-bound teicoplanin. Tetrahedron: Asymm 2000;11:3535-3541.

13. Xiao TL, Armstrong DW. Chiral Separations: Methods and Protocols. In: Gublitz F, Schmid MG, editors. Methods in molecular biology. Totona, NJ: Humana Press, Inc; 2004;Vol 243 p 149-159.

14. Armstrong DW, Liu Y, Ekborg-Ott KH. A covalently bonded teicoplanin chiral stationary phase for HPLC enantioseparations. Chirality 1995;7:474-497.

15. Armstrong DW, Tang Y, Chen S, Zhou Y, Bagwill C, Chen J. Macrocyclic antibiotics as a new class of chiral selectors for liquid chromatography. Anal Chem 1994;66:1473-1484.

16. Nair UB, Chang SSC, Armstrong DW, Rawjee YY, Eggleston DS, McArdle JV. Elucidation of vancomycin's enantioselective binding site using its copper complex. Chirality 1996;8:590-595.

17. Gasper MP, Berthod A, Nair UB, Armstrong DW. Comparison and modeling study of vancomycin, ristocetin a, and teicoplanin for CE enantioseparations. Anal Chem 1996;68:2501-2514.

18. Berry JF, Cotton FA, Lei P, Murillo CA. Further structural and magnetic studies of tricopper dipyridylamido complexes. Inorg Chem 2003b;42:377-382.

19. Cotton FA, Daniels LM, Murillo CA, Pascual I. Compounds with linear, bonded trichromium chains, J Am Chem Soc 1997;119:10223-10224.

20. Clerac R, Cotton FA, Dunbar KR, Murillo CA, Pascual I, Wang X. Further study of the linear trinickel (II) complex of dipyridylamide. Inorg Chem 1999;38:2655-2657.

21. Newman MS, Lednicer D. The synthesis and resolution of hexahelicene. J Am Chem Soc 1956;78:4765-4770.

22. Schlogl K, Werner A, Widhalm M. Biphenyl tricarbonylchromium complexes. Part 8. Optical resolutions, chiroptical properties, kinetics, and absolute chiralities of mono-tricarbonylchromium complexes of o,o'-bridged biphenyls. J Chem Soc Perkin Trans I 1993;8:1731-1735.

23. Budge JR, Ellis Jr PE, Jones RD, Linard JE, Szymanski T, Basolo F, Baldwin JE, Dyer RL. Optically active poly(triphenylmethyl methacrylate) with one-handed helical conformation. J Am Chem Soc 1979;101:4763-4765.

24. Ren C, Chen C, Fu X, Nakano T, Okamato Y. Helix-sense-selective polymerization of phenyl[bis(2-pyridyl)]methyl methacrylate and chiral recognition ability of the polymer. J Polym Sci, Part A: Polym Chem 1993;31:2721-8.

25. Polavarapu PL, He J, Crassous J, Ruud K. Absolute configuration of C_{76} from optical rotatory dispersion. Chem Phys Chem 2005;6:2535-2540.

Table 3.1. Retention factor (k), selectivity, (α) and resolution (Rs) for metal complexes along with optimized separation conditions.

#	Formula	k	α*	Rs	Separation Condition
1	$Cu_3(dpa)_4Cl_2$	2.02	1.35	1.35	80/20 ACN/MeOH with 0.3% NH_4TFA at 1 mL/min
2	$Co_3(dpa)_4Cl_2$	2.44	1.08	1.10	90/10 ACN/MeOH with 0.3% NH_4NO_3 at 0.4 mL/min
3	$Ni_3(dpa)_4Cl_2$	2.06	1.20	1.55	90/10 ACN/MeOH with 0.4% NH_4NO_3 and 0.2% NH_4TFA at 0.4 mL/min
4	$Ni_3(dpa)_4\ (NCCH_3)_2(PF_6)_2$	3.50	1.20	1.50	97/3 ACN/MeOH with 0.15% NH_4TFA at 0.4 mL/min
5	$Ni_3(epapda)_2(Ph_4B)_2$	10.10	1.06	1.35	97/3 Heptane/1-propanol at 1.0 mL/min

* Note that this α refers to the chromatographic selectivity factor (as defined in the materials and methods section) and it should not be confused with the specific rotations (given in Table 2.2.)

Table 3.2. Polarimetric data for $Ni_3(dpa)_4Cl_2$ specific rotation determination, where $\alpha^{589}{}_{22}$ is the observed rotation, c is the concentration of the complex, $[\alpha]^{589}{}_{22}$ is the specific rotation. All experiments were performed in methylene chloride and with a 1 dm cell.

	$\alpha^{589}{}_{22}$	c	$[\alpha]^{589}{}_{22}$
First eluted enantiomer	-0.0156 deg·cc/g·dm	3.12×10^{-6} g/cc	-5000° $\pm$192
Second eluted enantiomer	+0.0228 deg·cc/g·dm	4.38×10^{-6} g/cc	+5205° $\pm$182

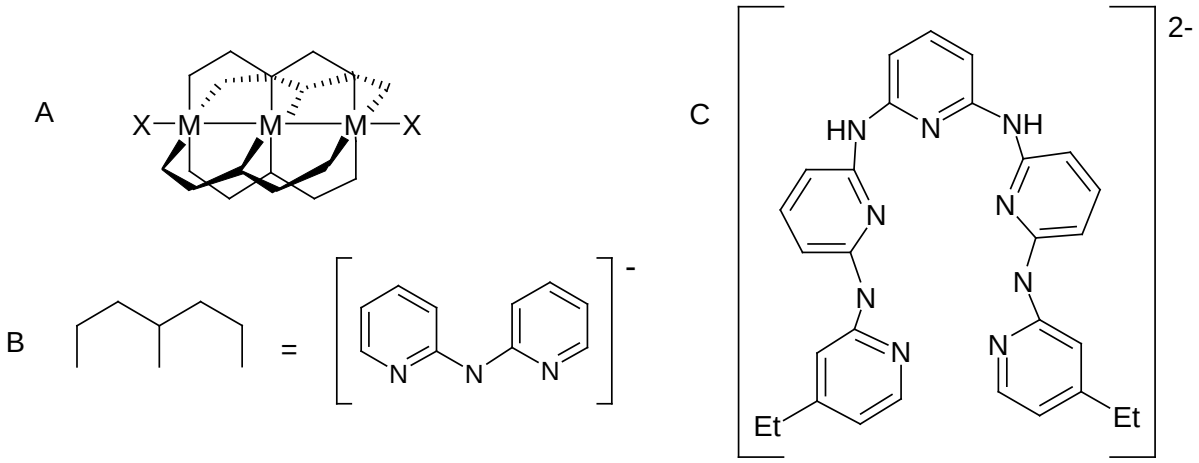

Figure 3.1. Representation of $M_3(dpa)_4X_2$ structure and various ligands. In 1A, M=Ni, Co, Cu, or Cr and X=Cl or ACN. In 1B, the dipyridylamido ligand (dpa^-) is shown as well as the stick figure used in 1A. The $epadpa^{2-}$ ligand (*N*-*N*'-bis(4-ethylpyridyl amido pyridyl)-2,6-diaminopyridine) is shown in 1C.

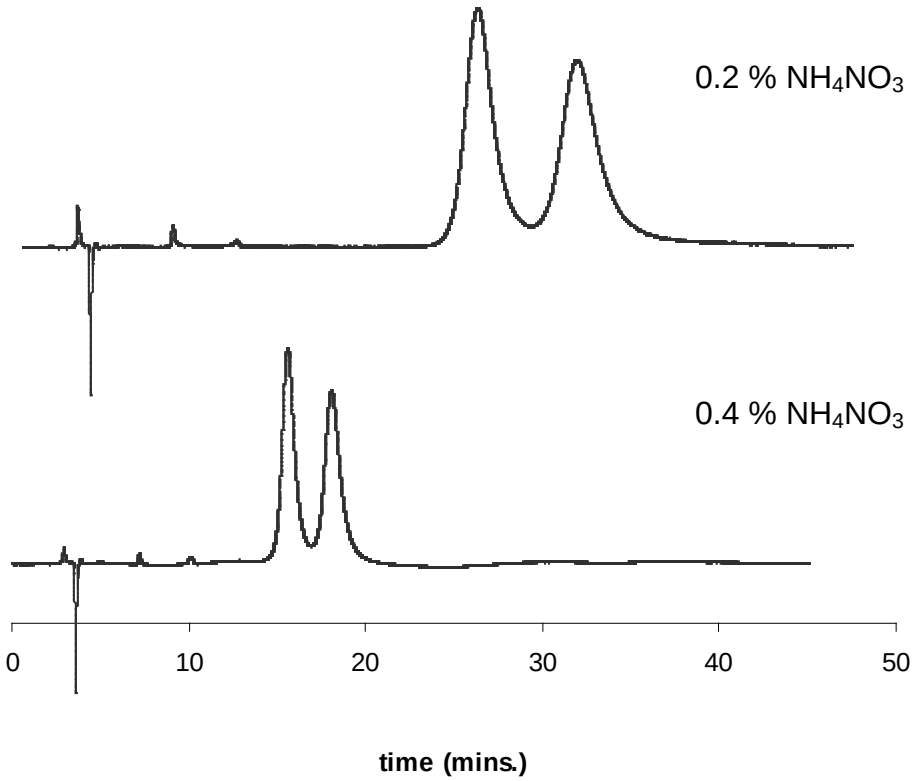

Figure 3.2. Chromatograms showing the additive effect on the enantioseparation of $Ni_3(dpa)_4Cl_2$. The complex was separated on the Chirobiotic V with a mobile phase consisting of 90/10 ACN/MeOH with the percentage of NH_4NO_3 as shown on the chromatogram. The flow rate was 1 mL/min and detection was at 270 nm.

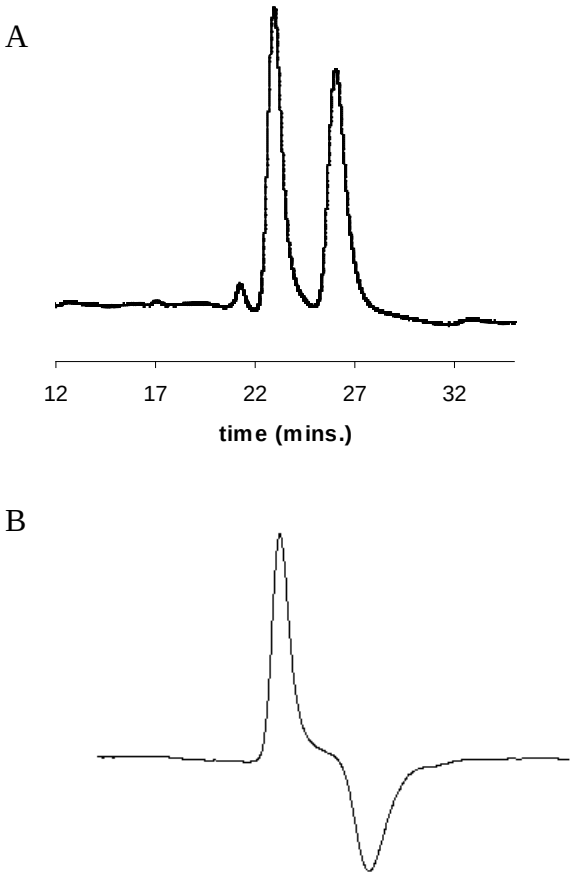

Figure 3.3. Enantioseparation of the trinickel dipyridylamido complex on the Chirobiotic V stationary phase. The mobile phase consisted of 90/10 ACN/MeOH with 0.4% w/v NH_4NO_3 and 0.2% w/v NH_4TFA and the flow rate was 0.4 mL/min. Chromatogram A shows the enantiomeric separation when using UV detection (270 nm). Chromatogram B (below) is the same separation shown when using a circular dichroism detector (270 nm).

CHAPTER 4

RESOLUTION OF ENANTIOMERS IN SOLUTION AND DETERMINATION OF THE CHIRALITY OF EXTENDED METAL ATOM CHAINS

A paper published in *Inorganic Chemistry*[3]

Daniel W. Armstrong, F. Albert Cotton, Ana G. Petrovic,
Prasad L. Polavarapu, Molly M. Warnke

ABSTRACT

The resolution of enantiomers of extended metal atom chains of the type $Ni_3[(C_5H_5N)_2N]_4Cl_2$ has been accomplished by chromatographic methods in solution, and the chirality was determined using vibrational circular dichroism, electronic circular dichroism, optical rotatory dispersion, and density functional theory calculations.

4.1 COMMUNICATION

Among the multifarious approaches[1,2] to making molecular wires is one that aims to take the image of a real-life wire and scale it down to the greatest possible extent, as shown in Figure 4.1. Most efforts to follow this particular approach have entailed the use of poly(pyridylamide) ligands (Chart 4.1). In this way, the metals Cr (n = 0-2), Co (n = 0-2), Ni (n = 0-3), Cu (n = 0), Ru (n = 0), and Rh (n = 0) have been incorporated into molecules of the type shown in Figure 4.2 for the case of n = 0, and some of their properties (especially) for n = 0 have been studied in detail.[2] For n = 0, the anion, dpa, is derived from dipyridylamine. One of the intrinsic properties of the chirality of extended metal atom chains (EMACs) is that

[3] Reproduced with permission from Inorganic Chemistry, 2007, 46, 1535-1537. Copyright © 2007 American Chemical Society

they have a helical winding of the four insulating polypyridyl ligands around the central metal *wire*, but these species are typically isolated as racemic crystals. In one case where chiral crystals are formed, $[Co_3(dpa)_4(CH_3CN)_2](PF_6)_2$,[3] the enantiomorphous crystals had to be separated by hand. To determine whether the conformation was *P* or *M*[4] (Chart 4.2), each crystal had to be examined by X-ray crystallography. A general, simple approach for resolving chiral EMAC-type molecular wires, and establishing their chirality, is presented here for the first time.

The results given here are for $Ni_3(dpa)_4XCl$ molecules, where X represents Cl (**1a**) or OH (**1b**). Extensive efforts to obtain single crystals of the individual enantiomers were unsuccessful, but a few racemic crystals that appeared because of incomplete separation revealed that there was a roughly 1:1 mixture of Cl^- and OH^- axial anions. The replacement of Cl by OH evidently occurs in the course of the chromatographic separation. The separation of the *P* and *M* isomers was achieved by use of a preparative chromatographic procedure using a macrocyclic glycopeptide-based chiral stationary phase.[5,6]

After collection of each enantiomer as it eluted from the column, the solvent from each enantiomeric mixture was evaporated to dryness. The samples were then dissolved in dichloromethane and washed with deionized water to remove the salt that was left from the mobile phase. The desiccant sodium sulfate was added to each of the enantiomer/dichloromethane mixtures and then allowed to stand for several hours to remove excess water. The sodium sulfate was then removed, and the dichloromethane was evaporated, leaving the resolved EMAC enantiomers.

To determine the absolute configuration of each enantiomer, chiroptical spectroscopic techniques were utilized. These included[7] vibrational circular dichroism (VCD), electronic circular dichroism (ECD), and optical rotatory dispersion (ORD). The final interpretation was assisted by density functional theory (DFT) calculations. In this report, the labels $(+)_{589nm}$ and $(-)_{589nm}$ are employed to designate the signs of optical rotation (OR) of the enantiomers at 589 nm.

The vibrational absorbance (VA) and VCD spectra of $(+)_{589nm}$-**1** and $(-)_{589nm}$-**1** were recorded in the mid-IR spectral region, from 2000 to 900 cm^{-1}, with a 1 h data collection time, at 8 cm^{-1} resolution.[8] In the absorption and VCD spectra, shown in Figure 4.3, the solvent spectra were subtracted to establish the zero baseline. Additionally, a small frequency region between ~1238 and 1196 cm^{-1} has been excluded because the presence of a strong solvent absorption band in this region makes the solvent subtraction difficult.

OR as a function of the concentration was measured on an Autopol IV polarimeter, using a 1.0 dm cell. Solutions of $(+)_{589nm}$- and $(-)_{589nm}$-**1** in a $CHCl_3$ solvent were prepared by successive dilutions from a parent stock solution. OR measurements were made at all wavelengths accessible by the polarimeter: 633, 589, 546, 436, 405, and 365 nm. These concentration-dependent studies have resulted in data points ranging in concentration from ~0.00013 to 0.000013 g/mL for the $(-)_{589nm}$ enantiomer and from ~0.000181 to 0.0000181 g/mL for the $(+)_{589nm}$ enantiomer. The intrinsic rotation, which represents specific rotation at infinite dilution, was extracted from the ORs at different concentrations.

The calculations of vibrational frequencies, IR absorptions, VCD, and ECD were performed with the *Gaussian 03* program.[9] Geometry optimization was first carried out with the B3LYP functional. The same functional was also used for the VA and VCD calculations. On the basis of previous experience,[10] the BHLYP functional, which uses an increased admixture of Hartree-Fock exchange in time-dependent DFT calculations, was also employed. The LANL2DZ basis set[11] was used for all computations. A Kramers-Kronig transform of the calculated ECD intensities provided the ORD spectrum.[12] The theoretical absorption and VCD spectra were simulated with Lorentzian band shapes and a 5 cm^{-1} half-width at half-peak height. The calculated vibrational frequencies have been scaled by a factor of 0.9612. The theoretical ECD spectrum was simulated from the first 50 singlet→singlet electronic transitions using Gaussian band shapes and a 20 nm half-width at 1/*e* of peak height.

Panel A in Figure 4.3 shows the observed VA spectrum from 1100 to 1750 cm^{-1} and the calculated spectrum for the *P* enantiomer. The absorption bands are labeled, and a key to the assignments is provided as Supporting Information. The computation was done for **1a**, and no account was taken of the fact that some axial OH groups were present in the experimental sample. This is why the Ni-O-H bending mode at ca. 1700 cm^{-1} is not in the computed spectrum. The ~1190-1240 cm^{-1} gap corresponds to strong absorption interference from the $CHCl_3$ solvent. Panel B of Figure 4.3 shows the mirror-image VCD spectra of the $(+)_{589nm}$ and $(-)_{589nm}$ enantiomers. In panel C, the VCD spectrum of the $(-)_{589nm}$ enantiomer is compared with the VCD spectrum calculated for the *P* enantiomer.

The mirror-image ECD spectra[13] of the $(+)_{589nm}$ and $(-)_{589nm}$ enantiomers of **1b** and their comparison to the predicted ECD spectrum for the *P* enantiomers are shown in Figure 4.3. It is clear that the $(-)_{589nm}$ enantiomer has *P* helicity, in agreement with the conclusion from the VCD results. The experimental ORD spectrum in the 400-650 nm region for the $(-)_{589nm}$ enantiomer shown in Figure 5 exhibits a negative-positive-negative feature, which is reproduced by the ORD predicted for the *P*-helical structure. As for the ECD, the predicted positive ORD maximum at 533 nm and zero crossing positions at 458 and 573 nm are shifted from the corresponding positions (436, 414, and 500 nm, respectively) in the experimental ORD. These shifts are not unusual because it is well-known[14] that DFT calculations do not yield accurate wavelengths for the electronic transitions.

The agreement between the theoretical and experimental chiroptical spectra (VCD, ECD, and ORD) leads to the conclusion that the $(-)_{589nm}$ enantiomer of **1** has the *P*-helical configuration and, conversely, the $(+)_{589nm}$ enantiomer of **1** has the *M*-helical configuration.

4.2 ACKNOWLEDGEMENT

We thank Dr. John F. Berry for supplying the racemic nickel compound. Support from the NSF, the Robert A. Welch Foundation (to D.W.A. and F.A.C.), and the Texas A&M University (to F.A.C.) is gratefully acknowledged. A grant from the National Computational Science Alliance (to P.L.P.; Grant CHE040009N) supported the computational work utilizing the IBM P690 at the University of Illinois. A teaching assistantship (to A.G.P.) from Vanderbilt University is gratefully acknowledged. D.W.A. and M.M.W. also acknowledge the support of the National Institutes of Health (NIH R01 GM53825-11).

[1] In *Extended Linear Chain Compounds*; Miller, J. S., Ed.; Plenum Press: New York, 1982.

[2] (a) Cotton, F. A.; Murillo, C. A. *Eur. J. Inorg. Chem.* **2006**, *21*, 4209. (b) Berry, J. F. Extended Metal Atom Chains. In *Multiple Bonds Between Metal Atoms*; Cotton, F. A., Murillo, C. A., Walton, R. A., Eds.; Springer Science and Business Media, Inc.: New York, 2005; pp 669-706. (c) Chae, D.-H.; Berry, J. F.; Jung, S.; Cotton, F. A.; Murillo, C. A.; Yao, Z. *Nano Lett.* **2006**, *6*, 165. (d) Berry, J. F.; Cotton, F. A.; Lu, T.; Murillo, C. A.; Wang, X. *Inorg. Chem.* **2003**, *42*, 3595.

[3] Clerac, R.; Cotton, F. A.; Dunbar, K. R.; Lu, T.; Murillo, C. A.; Wang, X. *Inorg. Chem.* **2000**, *39*, 3065.

[4] In a helical system, *P* and *M* stand for positive or negative as they relate to the torsion angles along the axis of the helix. For example, see: (a) Nasipuri, D. *Stereochemistry of Organic Compounds*; Wiley Eastern Ltd.: New Delhi, India, 1991. (b) Cahn, R. S.; Ingold, C.; Prelog, V. *Angew. Chem., Int. Ed. Engl.* **1966**, *5*, 385. (c) Taber, D. F.; Malcolm. S. C.; Bieger, K.; Lahuerta, P.; Sanau, M.; Stiriba, S.-E.; Perez-Prieto, J.; Monge, M. A. *J. Am. Chem. Soc.* **1999**, *121*, 860.

[5] A semipreparative (250 × 21.2 mm) Chirobiotic V macrocyclic glycopeptide-based chiral stationary phase was used. The stationary phase was obtained from Advanced Separation Technologies (Whippany, NJ). The mobile phase consisted of 95/5/0.15 ACN/MeOH/NH_4TFA pumped at a flow rate of 8 mL/min. The trinickel dipyridylamido complex was dissolved in 60/40 ACN/MeOH before injection. A high-performance liquid chromatography (HPLC) system consisting of a pump (LC-6A; Shimadzu, Kyoto, Japan), a

system controller (SCL-6A), Chromatopac (CR 601; Shimadzu), a UV detector (SPD-6A; Shimadzu), and a 200 μL injector valve (Rheodyne, Cotati, CA) was used. The wavelength of detection was 270 nm. Chiral detection was performed with a Jasco CD-2095 (Easton, MD) circular dichroism detector. See: Warnke, M. M.; Cotton, F. A.; Armstrong, D. W. *Chirality* **2007**, *19*, 179.

[6] For the chromatographic procedure, the methanol (MeOH) and acetonitrile (ACN) used in the mobile phases are HPLC grade and were purchased from VWR (West Chester, PA) as well as the dichloromethane used in extraction. Ammonium trifluoroacetate (NH_4TFA) was purchased from Aldrich (Deerfield, IL) and sodium sulfate was purchased from Fisher (Fair Lawn, NJ). HPLC-grade water from an in-house Milli-Q system was used for extractions. Mobile phases were degassed with helium for 5 min.

[7] For recent reviews in VCD, ECD, and ORD, see: (a) Polavarapu, P. L.; He, J. *Anal. Chem.* **2004**, *76*, 61A. Freedman, T. B.; Cao, X.; Dukor, R. K.; Nafie, L. A. *Chirality* **2003**, *15*, 743. Stephens, P. J.; Devlin, F. J. *Chirality* **2000**, *12*, 172. (b) Pecul, M.; Ruud, K.; Helgaker, T. *Chem. Phys. Lett.* **2004**, *388*, 110. Diedrich, C.; Grimme, S. *J. Phys. Chem. A* **2003**, *107*, 2524. (c) Polavarapu, P. L. *Chirality* **2006**, *18*, 348. Crawford, T. D. *Theor. Chem. Acc.* **2006**, *115*, 227.

[8] Spectra were measured in a demountable cell containing CaF_2 windows and a 200 μm path length spacer and at a concentration of ~0.0126 M in a $CHCl_3$ solvent environment using a commercial Fourier transform VCD spectrometer, Chiralir.

[9] *Gaussian 03*; Gaussian Inc.: Wallingford, CT.

[10] Polavarapu, P. L.; He, J.; Crassous, J.; Ruud, K. *ChemPhysChem* **2005**, *6*, 2535.

[11] Hay, P. J.; Wadt, W. R. *J. Chem. Phys.* **1985**, *82*, 270.

[12] Polavarapu, P. L. *J. Phys. Chem. A* **2005**, *109*, 7013.

[13] The ECD spectra were recorded on a Jasco J720 spectrometer in the 200-800 nm region, using a 0.01 cm path length cell. The concentration was ~0.00129 M in a $CHCl_3$ solvent.

[14] Bauernschmitt, R.; Ahlrichs, R. *Chem. Phys. Lett.* **1996**, *256*, 454.

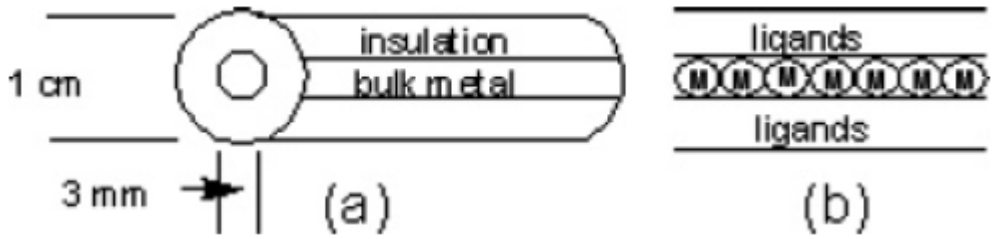

Figure 4.1. How a normal wire (a) may be reduced to the smallest possible molecular wire (b).

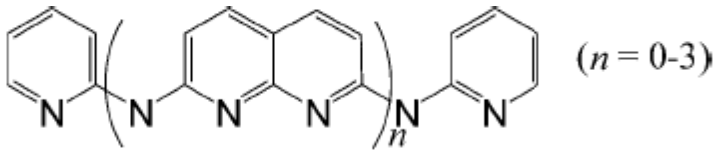

Chart 4.1 Poly(pyridylamide) Ligands

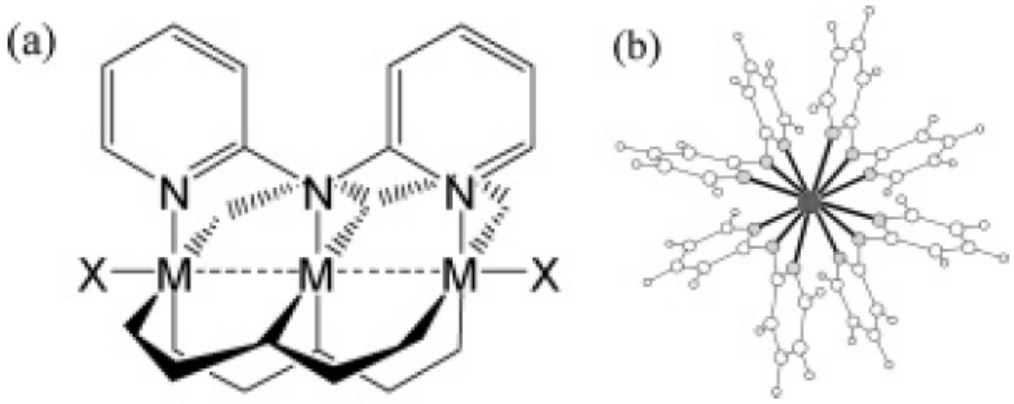

Figure 4.2 (a) Schematic drawing of an $M_3(dpa)_4X_2$ EMAC. (b) End view showing the helicity (*P* in this case).

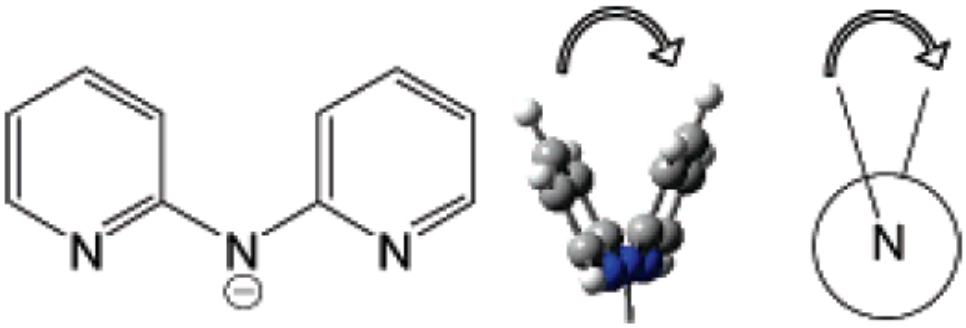

Chart 4.2 Representation of the *P* helicity of Dipyridyl ligands.

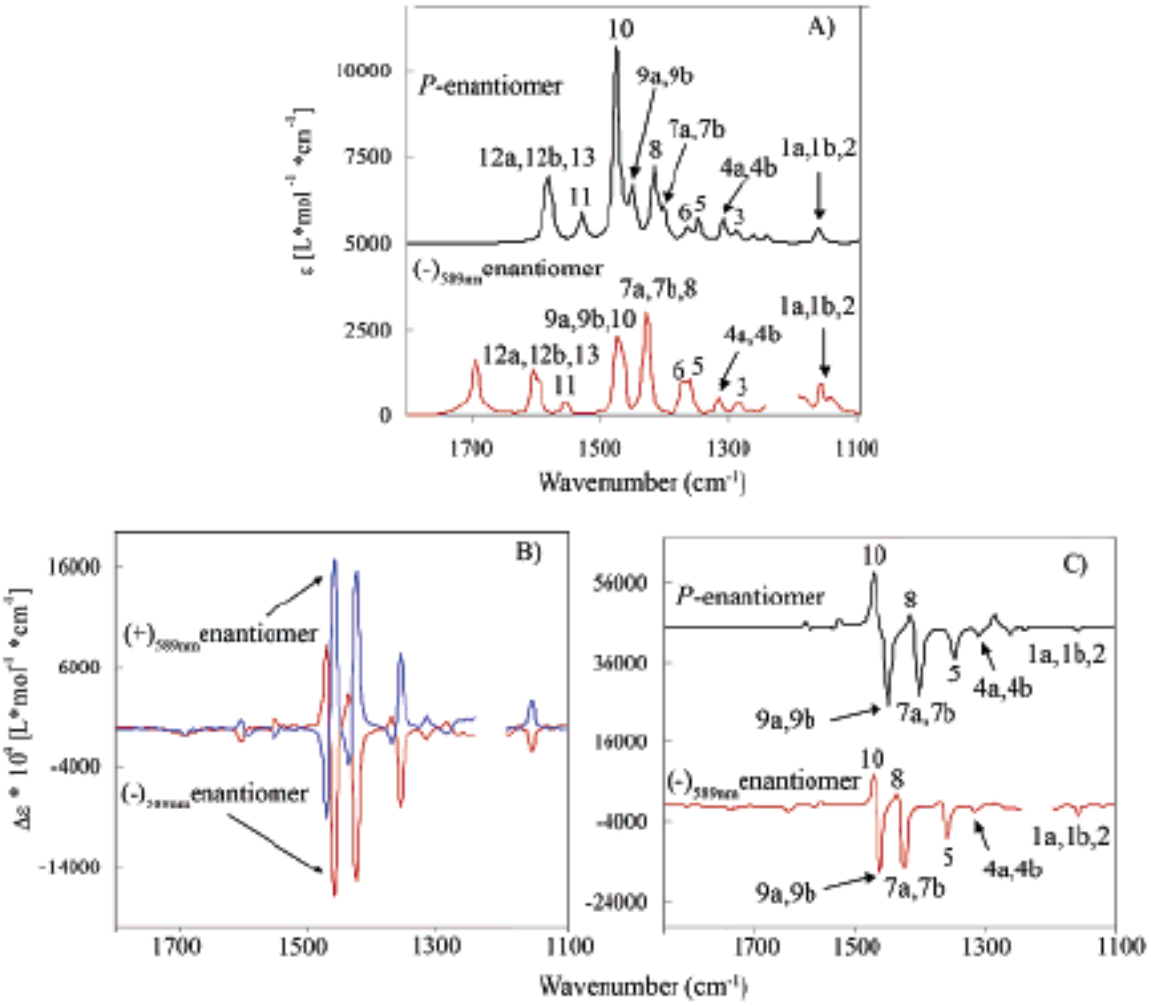

Figure 4.3 VA (panel A) and VCD spectra of **1**. The experimental VCD spectra are shown for both enantiomers in panel B. Calculated spectra for *P*-**1a** (topmost trace in panels A and C) were obtained with B3LYP/LANL2DZ. Calculated spectra in panels A and C have been shifted up for clarity.

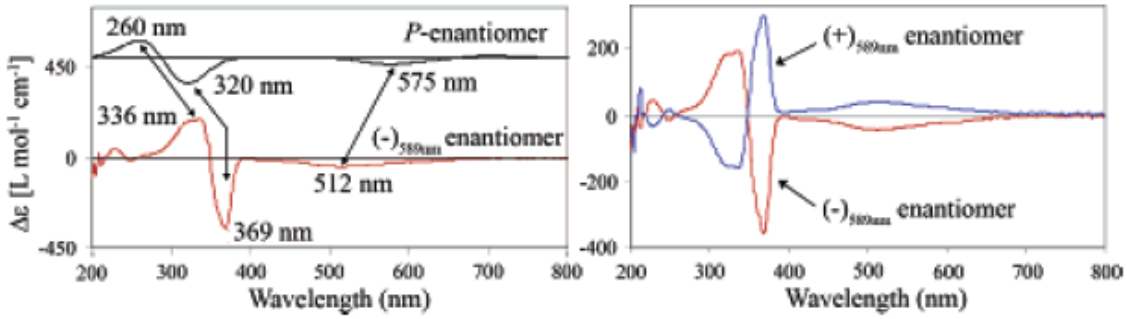

Figure 4.4. Electronic CD spectra of **1**. Experimental ECD spectra are shown for both enantiomers in the right panel. The predicted spectra for *P*-**1a** (topmost trace in the left panel) was obtained with time-dependent BHLYP/LANL2DZ and shifted up for clarity.

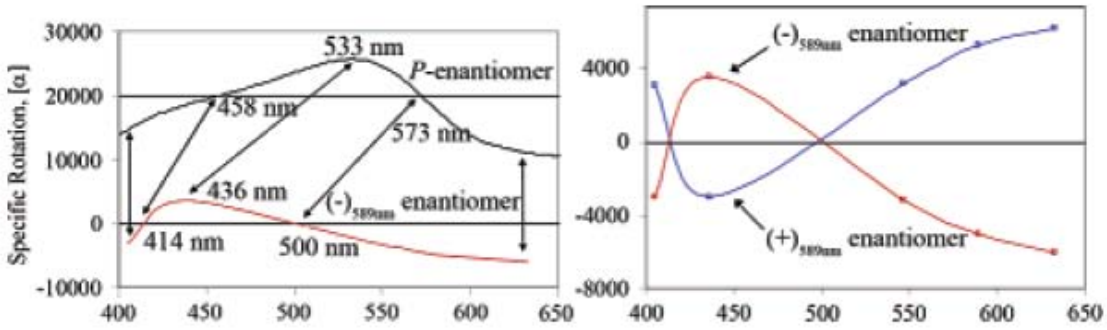

Figure 4.5. ORD spectra of **1**. The right panel shows experimental spectra for the two enantiomers, while the left panel shows a comparison between the predicted ORD for the P enantiomer of **1** and the experimental spectrum for the $(-)_{589nm}$ enantiomer of **1**.

CHAPTER 5

EVALUATION OF FLEXIBLE LINEAR TRICATIONIC SALTS AS GAS-PHASE ION-PAIRING REAGENTS FOR THE DETECTION OF DIVALENT ANIONS IN POSITIVE MODE ESI-MS

A paper accepted by *Analytical Chemistry*[4]

Zachary S. Breitbach, Molly M. Warnke, Eranda Wanigasekara,
Xiaotong Zhang, Daniel W. Armstrong

ABSTRACT

Anion analysis is of great importance to many scientific areas of interest. Problems with the negative mode ESI-MS prevent researchers from achieving sensitive detection for anions. Recently, we have shown that cationic reagents can be paired with anions, such that detection can be done in the positive mode, allowing for low limits of detections for anions using ESI-MS. In this analysis, we present the use of 16 newly synthesized flexible linear tricationic ion-paring reagents for the detection of 11 divalent anions. These reagents greatly differ in structure from previously reported trigonal tricationic ion-pairing agents, such that they are far more flexible. Here we present the structural features of these linear trications that make for good ion-pairing agents, as well as, show the advantage of using these more flexible ion-pairing reagents. In fact, the limit of detection for sulfate using the best linear trication was found to be 25 times lower than when the best rigid trication was used. Also, MS/MS experiments were performed on the trication/di-anion complex to significantly reduce the

[4] Reproduced with permission from Analytical Chemistry, in press.

detection limit for many di-anions. Limits of detection in this analysis were as low as 50 femtograms.

5.1 INTRODUCTION

Anion analysis is of great importance to environmental researchers, biochemists, food and drug researchers, and the pharmaceutical industry; all of which are continually in need of facile, sensitive analytical techniques that can be used to both detect and quantitate trace anions.[1-22] Often, the anions of interest exist in complex matrices such as blood, water, and urine.[2,6,9,12,14-17] For this reason, separation techniques are routinely coupled with anion detection. Currently, some of these techniques utilize flow injection analysis or ion chromatography,[20-25] with detection frequently obtained through the use of ion selective electrodes, conductivity, or spectroscopic techniques.[26-30] Yet, these detection methodologies lack either universality or specificity.[30]

For many analytes, ESI-MS has provided broad specificity and lower detection limits. Given the anion's inherent charge, it is not surprising that negative ion electrospray ionization mass spectrometry (ESI-MS) has come to the forefront as a general analytical approach that can be directly coupled with liquid chromatography (LC) if desired. Unfortunately, for most types of analytes, the negative ion mode often results in poorer limits of detection (LOD) than the preferred positive ion mode.[31-34] Due to high negative voltages, the negative ion mode is more prone to corona discharge than the positive mode.[34-35] This causes the negative mode to have an increased chance for arcing events and ultimately more noise resulting in unsatisfactory LODs.[31] Corona discharge in the negative mode can be controlled by using halogenated solvents and substituting more alkylated alcohols (i.e., butanol or IPA) for methanol.[32,35-36] Ideally, LC-ESI-MS methodologies would use more

common solvents, such as methanol, water, and acetonitrile. Furthermore, it would be more practical to do all ion detection in the more stable and sensitive positive ion mode.

Recently, we have developed a method for the detection of singly charged anions in positive mode ESI-MS using only water/methanol solvents.[37] This technique involves the addition of a low concentration of a dicationic ion pairing reagent to the mobile phase. The dication pairs with the singly charged anion, resulting in a complex possessing an overall plus one charge, which can be detected in the positive ion mode. Benefits of this technique include: (a) the use of more practical solvents, (b) substantial increases in the sensitivity, (c) ease of use, (d) the ability to detect anions that fall below a trapping mass spectrometer's low mass cutoff region, and (e) detection of the complex at a much higher mass-to-charge region were there is far less chemical noise. To fully take advantage of factor (e) alone, it is best to choose a relatively high molecular weight pairing agent that will result in a complex of a single positive charge.

Subsequently, the dicationic ion-pairing agent was used to determine the LODs for over 30 singly charged anions.[37] Also in this work, it was shown for the first time that MS/MS can often be used to further lower the LODs of these anions. Overall, this analysis showed the true ultra-sensitivity of ion-pairing by producing the lowest reported LODs for several anions by any known technique.[37] The effectiveness of over 20 dicationic ion-pairing agents was evaluated in order to determine the structural properties that allow for low LODs.[38] A major finding in this study was that flexibility of the dication seemed essential for good sensitivity. Therefore, the best dicationic ion-pairing reagents cited were those which possessed a flexible alkyl chain that linked the two cationic moieties. Recently, the ion-paring technique was extended to the use of tri-cationic reagents for the detection of

divalent anions.[39] The essential tricationic reagents were found to bind divalent anions, and monitoring the complex in the positive ion mode was a more sensitive detection method than monitoring the naked doubly charged anions in the negative mode. However, the tricationic reagents used had a somewhat rigid trigonal structure (for a representative structure see the bottom of Fig. 5.1), which may be an undesirable feature of an ion-pairing agent from a sensitivity standpoint.

Recently, we devised a synthetic method to produce linear trications, which may be more flexible than their trigonal counterparts. In this work, we present the use of 16 newly synthesized linear tricationic ion-pairing reagents to determine the LOD for 11 divalent anions. Herein, we describe the differences and advantages of using the more flexible linear trications versus the more rigid trigonal trications. Also, we show that MS/MS experiments can be performed on the linear trication/di-anion complex, and that by monitoring a fragment of the complex, the LOD often can be dramatically lowered. This is the first ever report of using this type of an MS/MS experiment to detect doubly charged anions in the positive ion mode with any tricationic ion-pairing agent.

5.2 EXPERIMENTAL

Materials and the synthetic procedure for the tricationic ionic liquids are described in the supporting information, along with the ESI conditions. Throughout this study, a Finnigan LXQ (Thermo Fisher Scientific, San Jose, CA, USA) ESI-MS was used for all of the analyses. The MS was equipped with a six port injector (5 μL loop) and was coupled with a Finnigan Surveyor MS Pump. Between the injector and the ionization source, a Y-type mixing tee allowed for the addition of flow from a Shimadzu LC-6A pump. It was from this

pump that the tricationic ion-pairing agent was introduced to the solvent flow. Overall, the total flow to the ESI was 400 μL/min. The MS pump accounted for 300 μL/min (67% MeOH : 33% H_2O), while the LC pump applied the 40 μM trication solution in water at a rate of 100 μL/min. All the anions were dissolved in HPLC grade water, such that their initial concentration was 1 mg/mL. Serial dilutions were made from the stock solutions and the anions were directly injected using the six port injector. New stock solutions were prepared weekly and the injector was expected to be the largest cause for possible experimental error ($\pm$ 5%). The limits of detection were determined to be when an injection at a given concentration resulted in peaks giving a signal-to-noise ratio of three.

5.3 DISCUSSION

In previous reports, we have shown that dicationic ion-pairing reagents can be used to pair with singly charged anions, such that, the positively charged complex can be monitored in the positive mode, resulting in extremely low LODs.[37-38] More recently, we demonstrated that tricationic reagents could also be used to complex doubly charged anions, leading to much lower LODs for those divalent anions when detecting the complex in the positive mode.[39] Since the trications used previously had relatively rigid structures, a series of flexible ion-pairing agents were synthesized and tested to see if they offer greater sensitivity for the detection of anions in positive mode ESI. In addition, MS/MS of the paired ions was examined in hopes of further lowering the LOD in many cases.

Figure 5.1 shows the structures of the 16 linear trications used in this analysis (A1-4, B1-4, C1-4, and D1-4). All of the 16 linear trications have the same imidazolium core. They differ in the length of the alkyl chain (C_3, C_6, C_{10}, and C_{12}) that tethers the terminal charged

moieties to the central imidazolium, as well as, in the nature of the terminal charged moieties (methylimidazolium, butylimidazolium, benzylimidazolium, and tripropylphosphonium). By examining this series of linear trications, we were able to observe possible advantages of varying the chain length (i.e., flexibility) and determine which cationic moieties produce the lowest LOD for the sample anions. Also shown in Figure 5.1, are the structures of two previously reported rigid trications.[39] Of these, the E1 trication was shown to be a moderately successful pairing agent, while trication E2 was found to be the best known trigonal tricationic ion-pairing agent.[39] The results of these two rigid trications allows for a definitive comparison to the new flexible trications developed for this study.

Table 5.1 lists the LODs for the 11 doubly charged anions, when paired with the 16 linear trications and monitored in the positive mode. Overall, the LODs for the divalent anions ranged from the nanogram (ng) to the picogram (pg) level. In order to evaluate the effect of the chain length in the linear tricationic ion-pairing reagent, one can compare the trications of the same letter. For example, trications D1-4 differ only in the length of the hydrocarbon chain connecting the charged moieties (Fig. 5.1). In general, it appears that the common trend is that linear trications with hexyl or decyl linkage chains gave the lowest LODs, whereas, trications with propyl or dodecyl linkages resulted in higher LODs. This trend can be easily seen by comparing the LOD for thiosulfate when using the "D" series of linear trications. In this comparison, the order from best to worst ion-pairing agent was found to be D3, D2, D4, and D1. A likely explanation for this observation is that when the alkyl linkage chain is too short, the linear trication is less flexible and not as likely to "bend" around the anion. This finding supports our hypothesis that flexibility is a key feature in a good tricationic ion-pairing reagent. In contrast, when the alkyl chain gets too long, the

cationic moieties are too far from each other and can not work as a single unit when binding the anion. However, the effect of the linkage chain being too short is far more unfavorable than if it is too long. An example of this can be seen in Table 5.1, were trication A1 with the shortest linkage chain was found to be one of the three worst ion-pairing agents for all anions. Clearly, the results (Table 5.1 and Fig. 5.1) suggest that when using linear tricationic ion-pairing reagents, the alkyl linkage chain should be between six and ten carbons in length.

By evaluating the data for a series of trications that all have the same linkage chain, but different cationic moieties, the best terminal charged groups can be determined. Typically, the linear trications possessing the benzylimidazolium (the "C" moiety) and the tripropylphosphonium (the "D" moiety) terminal charged groups resulted in lower LODs than the methylimidazolium (the "A" moiety) or butylimidazolium (the "B" moiety) cationic groups. This observation is shown by the LODs for oxalate when paired with the linear tricationic "2" series. The order from best to worst ion-pairing agents was found to be C2, D2, A2, and B2. Another example of this can be seen in the LODs for both nitroprusside and dichromate, where (from best to worst) the order was C2, D2, B2, and A2. These results, along with the previously noted optimum linkage chain lengths, allow for the determination that trications C2 and D3 were the overall best tricationic ion-pairing agents. Trication C2 has hexyl linkage chains and benzylimidazolium terminal charged groups, and trication D3 has decyl linkage chains and tripropylphosphonium cationic moieties. Interestingly, in the three comprehensive studies we have done on ion-pairing agent structures, the tripropylphosphonium cationic moiety is the only one that has always resulted in a recommended ion-pairing agent.[38-39]

The other important comparison to be made with the data in Table 5.1 is the LODs resulting from using the flexible linear trication versus the more rigid trigonal trications (E1 and E2). As can be seen, the best linear trications, C2 and D3, rank very near the top for most of the anions tested. However, the best trigonal trication, E2, also ranks very near the top for many of the tested anions. From this observation, it was determined that the best linear trications and the best trigonal trication both work well when monitoring the same divalent anions. Interestingly, the linear and trigonal ion-pairing reagents seem to be complimentary to one another. Overall, the best linear trication was not found to be a greatly superior ion-pairing agent when compared to the best trigonal trication. Yet, some very useful and somewhat complimentary tricationic ion-pairing reagents were added to our repertoire. However, if the trigonal trication E1 (the moderately successful trigonal trication) is compared to the flexible linear trications, it can be seen that trication E1 ranks near the bottom for all the anions tested. It was determined that in general, the more flexible trications are better ion-pairing agents then the rigid trications. Obviously, there are other factors that play a part in finding the optimum ion-pairing agent, which allow trication E2 to work as well as the linear trications. Perhaps the most important factor is that it contains the highly favorable terminal tripropylphosphonium moiety.

Figure 5.2 illustrates the benefits of using a linear trication versus a trigonal trication for the detection of sulfate in the positive mode. In both detection scenarios, the same concentration of sulfate was injected (500 pg). In the upper panel (I), the ion-pairing agent was the best linear trication D3, and in the lower panel (II) the best trigonal trication E2 was used. It is apparent that the linear trication resulted in superior detection of sulfate, with a signal-to-noise seven times greater that that for the trigonal trication. It should be noted that

sulfate itself has a mass-to-charge ratio of -48, thus falling below the low mass cutoff of our MS instrument and rendering itself undetectable in the negative mode.

Another facet of this study was to show that selective reaction monitoring (SRM) experiments could be performed on the trication/anion complex, and that by monitoring a positively charged fragment of the complex, lower LODs for the divalent anions could be achieved. The key part of this type of experiment is to find the proper fragment to monitor. In many cases the monitored fragment for a given tricationic reagent was the same, but not always. Figure 5.3 shows a proposed fragmentation pattern for the more commonly observed dissociation of a trication D3/di-anion complex. As is shown by Figure 5.3, collision induced dissociation (CID) typically resulted in a singly charged alkyl linked phosphonium imidazole, which had a mass-to-charge ratio of 367.4. Monitoring this fragment can lead to a decrease in the LOD for the anion that was part of the parent complex.

Table 5.2 lists the results for the SRM experiments that were performed in this analysis. Trications D3 and C2 were paired with 11 divalent anions and tested for their LOD using the SRM method. For comparison, the SIM results are listed next to the SRM results. As can be seen, the SRM mode often resulted in lower LODs than the SIM mode. There were two analytes (D3/bromosuccinate and C2/oxalate) that showed no improvement, but in general there was nearly an order of magnitude improvement when using the SRM mode. In three cases, the SRM mode resulted in a two order of magnitude decrease in the LOD. One of these cases was the detection of nitroprusside using trication C2 as the ion-pairing agent and employing the SRM mode. For this system, the LOD for nitroprusside was determined to be 50 femtograms (fg), which is the lowest LOD for any mono- or divalent anion that has been tested to date. Clearly this is a very facile and sensitive method.

Also, listed in Table 5.2 are the SRM fragment masses that were monitored. As noted previously, many complexes produce the same fragment; 367.4 for trication D3 and 309.2 for trication C2. However, it was observed that there are some trication/di-anions that follow different disassociation pathways. For example, the trication D3/hexachloroplatinate complex produced a fragment of m/z 1003.5. This fragment corresponds to the loss of chloride from the hexachloroplatinate, while the overall cation-anion complex remained intact. A similar effect was seen with the SRM detection for nitroprusside. Here, nitroprusside loses a nitro group and still stays complexed with the trication. For these cases, it is interesting to see that the non-covalent trication/di-anion complex remains intact, while covalent bonds have been broken. One more example of this type of fragmentation was for bromine containing anions. Here the central imidazolium loses its acidic proton (in the 2 position of the imidazolium ring) and becomes a dication. This dication then complexes with a bromide anion that was lost from the di-anion. This means that for any bromine containing di-anions, the same fragment could be monitored (m/z 745/747 for D3 and m/z 629/631 for C2).

It should be noted that although the LODs for the 11 divalent anions in SIM and SRM are already quite low, they could be lowered further by completely optimizing the conditions for a particular complex. In this analysis, one general set of conditions were used for the entire study. Previously, we have shown that the LODs can be further decreased by a factor of three to ten with individual optimization of ESI condtions.[37-39] Finally, the use of some other types of MS systems (triple quad, etc.) with this technique can further reduce detection limits.

5.4 CONCLUSIONS

Sixteen newly synthesized linear tricationic ion-pairing agents were evaluated for their ability to detect doubly charged anions in positive mode ESI-MS. It was found that for linear trications, the optimum alkyl chain lengths coupling the cationic moieties should be between six and ten carbons in length. It was determined that the best cationic moieties were tripropylphosphonium and benzylimidazolium. In comparison to previously reported rigid tricationic ion-pairing agents, the flexible linear trications presented here generally make better MS ion-pairing agents. It was shown that when the same amount of sulfate was injected, the signal-to-noise ratio when using the best linear trication was seven times greater than when using the best trigonal trication. However, it was found that trigonal trication E2 remained useful as it was often complimentary to the linear trications. Lastly, one to three orders of magnitude decreases in the LODs were found when using SRM.

5.5 REFERENCES

(1) Hebert, G.N.; Odom, M.A.; Craig, P.S.; Dick, D.L.; Strauss, S.H. *J. Environ. Monit.* **2002**, 4, 90-95.

(2) Magnuson, M.L.; Urbansky, E.T.; Ketly, C.A. *Talanta* **2000**, 52, 285-291.

(3) Hansen, K.J.; Johnson, H.O.; Eldridge, J.S.; Butenhoff, J.L.; Dick, L.A. *Environ. Sci. Technol.* **2002**, 36, 1681-1685.

(4) Cahill, T.M.; Benesch, J.A.; Gustin, M.S.; Zimmerman, E.J.; Seiber, J.N. *Anal. Chem.* **1999**, 71, 4465-4471.

(5) Ghanem, A.; Bados, P.; Kerhoas, L.; Dubroca, J.; Einhron, J. *Anal. Chem.* **2007**, 79, 3794-3801.

(6) Wujcik, C.E.; Cahill, T.M.; Seiber, J.N. *Anal. Chem.* **1998**, 70, 4074-4080.

(7) Li, X.C.; Lu, X.; Li, X. *Anal. Chem.* **2004**, 26A-33A.

(8) Martinelango, P.K.; Anderson, J.L.; Dasgupta, P.K.; Armstrong, D.W.; Al-Horr, R.S.; Slingsby, R.S. *Anal. Chem.* **2005**, 77, 4829-4835.

(9) Martinelango, P.K.; Guemues, G.; Dasgupta, P.K. *Anal. Chim. Acta.* **2006**, 567, 79-86.

(10) Martinelango, P.K.; Tian, K.; Dasgupta, P.K. *Anal. Chim. Acta.* **2006**, 567, 100-107.

(11) Barron, L.; Paull, B. *Talanta* **2006**, 69, 621-630.

(12) Yamashita, N.; Kannan, K.; Taniyasu, S.; Horii, Y.; Okazawa, T.; Petrick, G.; Gamo, T. *Environ. Sci. Technol.* **2004**, 38, 5522-5528.

(13) Wuilloud, R.G.; Altamirano, J.C.; Smichowski, P.N.; Heitkemper, D.T. *J. Anal. At. Spectrom.* **2006**, 21, 1214-1223.

(14) Mandal, B.K.; Ogra, Y.; Suzuki, K.T. *Chem. Res. Toxicol.* **2006**, 14, 371-378.

(15) Tsikas, D. *Clin. Chem.* **2004**, 50, 1259-1261.

(16) Blount, B.C.; Valentin-Blasini, L. *Anal. Chim. Acta.* **2006**, 567, 87-93.

(17) Olsen, G.W.; Hansen, K.J.; Stevenson, L.A.; Burris, J.M.; Mandel, J.H. *Environ. Sci. Technol.* **2003**, 37, 888-891.

(18) Dyke, J.V.; Kirk, A.B.; Martinelango, P.K.; Dasgupta, P.K. *Anal. Chim. Acta.* **2006**, 567, 73-78.

(19) Elkins, E.R.; Hoeser, J.R. *J. AOAC Int.* **1994**, 77, 411-415.

(20) El Aribi, H.; Le Blanc, Y.J.C.; Antonsen, S.; Sakuma, T. *Anal. Chim. Acta.* **2006**, 567, 39-47.

(21) Guo, Z.; Cai, Q.; Yu, C.; Yang, Z. *J. Anal. At. Spectrom.* **2003**, 18, 1396-1399.

(21) Dudoit, A.; Pergantis, S.A. *J. Anal. At. Spectrom.* 2001, 16, 575-580.

(22) van Staden, J.F.; Tlowana, S.I. *Fresenius J. Anal. Chem.* **2001**, 371, 396-399.

(23) Salov, V.V.; Yoashinaga, J.; Shibata, Y.; Morita, M. *Anal. Chem.* **1992**, 64, 2425-2428.

(24) Ahrer, W.; Buchberger, W. *J. Chromatogr., A* **1999**, 854, 275-287.

(25) Nischwitz, V.; Pergantis, S.A. *J. Anal. At. Spectrom.* **2006**, 21, 1277-1286.

(26) Kappes, T.; Schnierle, P.; Hauser, P.C. *Anal. Chim. Acta.* **1997**, 350, 141-147.

(27) Isildak, I.; Asan, A. *Talanta* **1999**, 48, 967-978.

(28) Isildak, I.; *Chromatographia* **1999**, 49, 338-342.

(29) Chakraborty, D.; Das, A.K. *Talanta* **1989**, 36, 669-671.

(30) Buchberger, W.W. *J. Chromatogr., A* **2000**, 884, 3-22.

(31) Cech, N.B.; Enke, C.G. *Mass Spectrom. Rev.* **2001**, 20, 362-387.

(32) Voyksner, R.D. Combining Liquid Chromatography with Electrospray Mass Spectrometry. In *Electrospray Ionization Mass Spectrometry;* Cole, R.B., Ed; Wiley: New York, 1997; pp 139-158.

(33) Henriksen, T.; Juhler, R.K.; Svensmark, B.; Cech, N.B. *J. Am. Soc. Mass Spectrom.* **2005**, 16, 446-455.

(34) Kebarle, P.; Yeunghaw, H. On the Mechanism of Electrospray Mass Spectrometry. In *Electrospray Ionization Mass Spectrometry;* Cole, R.B., Ed; Wiley: New York, 1997; p 14.

(35) Straub, R.F.; Voyksner, R.D. *J. Am. Soc. Mass Spectrom.* **1993**, 4, 578-587.

(36) Cole, R.B.; Zhu, J.H. *Rapid Cummun. Mass Spectrom.* **1999**, 13, 607-611.

(37) Soukup-Hein, R.J.; Remsburg, J.W.; Dasgupta, P.K.; Armstrong, D.W. *Anal. Chem.* **2007**, 79, 7346-7352.

(38) Remsburg, J.W.; Soukup-Hein, R.J.; Crank, J.A.; Breitbach, Z.S.; Payagala, T.; Armstrong, D.W. *J. Am. Soc. Mass Spectrom.* **2008**, 19, 261-269.

(39) Soukup-Hein, R.J.; Remsburg, J.W.; Breitbach, Z.S.; Sharma, P.S.; Payagala, T.; Wanigasekara, E.; Armstrong, D.W. *Anal. Chem.* **2008**, 80, 2612-2616.

Table 5.1-Limits of Detection for Divalent Anions with Linear Tricationic Reagents*

Sulfate		Thiosulfate		Oxalate		Fluorophosphate	
Trication	LOD (pg)	Trication	LOD (pg)	Trication	LOD (pg)	Trication	LOD (pg)
D3	2.00×10^{1}	**D3**	6.25×10^{1}	**C2**	1.20×10^{1}	D4	2.50×10^{1}
D4	7.50×10^{1}	**C2**	6.25×10^{1}	D2	3.50×10^{1}	**D3**	2.63×10^{1}
D2	1.25×10^{2}	B3	6.25×10^{1}	A2	8.10×10^{1}	*E2*	3.75×10^{1}
B3	2.00×10^{2}	B2	6.25×10^{1}	D4	1.25×10^{2}	D2	4.25×10^{1}
B4	2.60×10^{2}	D2	7.50×10^{1}	B4	1.25×10^{2}	B3	9.00×10^{1}
C1	3.00×10^{2}	B4	7.50×10^{1}	**D3**	2.50×10^{2}	C3	1.50×10^{2}
B2	3.25×10^{2}	C1	8.75×10^{1}	*E2*	2.50×10^{2}	A3	2.00×10^{2}
C4	3.50×10^{2}	D4	9.00×10^{1}	A3	3.00×10^{2}	A2	2.00×10^{2}
C3	3.75×10^{2}	D1	1.00×10^{2}	B1	3.00×10^{2}	D1	2.00×10^{2}
C2	4.50×10^{2}	C4	1.00×10^{2}	B2	3.25×10^{2}	C4	2.10×10^{2}
B1	5.00×10^{2}	A3	1.00×10^{2}	C4	4.00×10^{2}	**C2**	2.25×10^{2}
E2	5.00×10^{2}	A4	1.00×10^{2}	C3	4.40×10^{2}	B2	2.75×10^{2}
A2	5.50×10^{2}	A2	1.25×10^{2}	C1	5.00×10^{2}	A4	4.50×10^{2}
A4	5.75×10^{2}	B1	1.25×10^{2}	*E1*	5.00×10^{2}	B4	5.00×10^{2}
A3	6.00×10^{2}	*E2*	1.25×10^{2}	A4	5.50×10^{2}	B1	8.75×10^{2}
D1	6.25×10^{2}	C3	1.75×10^{2}	A1	6.50×10^{2}	C1	1.50×10^{3}
E1	6.25×10^{2}	A1	5.00×10^{2}	D1	8.25×10^{2}	A1	4.50×10^{3}
A1	1.75×10^{3}	*E1*	7.50×10^{2}	B3	2.08×10^{3}	*E1*	5.00×10^{4}

Dibromosuccinate		Hexachloroplatinate		Nitroprusside		Dichromate	
Trication	LOD (pg)	Trication	LOD (pg)	Trication	LOD (pg)	Trication	LOD (pg)
D3	1.25×10^{2}	D2	3.50×10^{1}	**C2**	7.00	C4	3.50×10^{3}
E2	1.79×10^{2}	B2	3.50×10^{1}	D1	7.50	B4	3.75×10^{3}
D1	2.00×10^{2}	D1	3.75×10^{1}	*E2*	7.50	C3	3.88×10^{3}
C1	2.75×10^{2}	**D3**	4.00×10^{1}	C1	1.00×10^{1}	B3	4.25×10^{3}
B4	3.25×10^{2}	**C2**	5.00×10^{1}	D2	1.25×10^{1}	A3	5.00×10^{3}
B1	3.50×10^{2}	B1	7.00×10^{1}	B1	1.25×10^{1}	D4	5.50×10^{3}
B3	3.75×10^{2}	B3	7.50×10^{1}	**D3**	2.00×10^{1}	**D3**	6.25×10^{3}
A3	4.50×10^{2}	B4	7.50×10^{1}	B2	2.00×10^{1}	A4	6.25×10^{3}
C3	5.00×10^{2}	C1	7.50×10^{1}	C3	2.25×10^{1}	B1	6.25×10^{3}
D4	5.00×10^{2}	A2	7.50×10^{1}	B3	2.50×10^{1}	**C2**	6.38×10^{3}
A4	5.00×10^{2}	*E2*	7.50×10^{1}	A2	2.50×10^{1}	C1	6.50×10^{3}
D2	6.25×10^{2}	C4	8.50×10^{1}	A3	3.00×10^{1}	D2	7.50×10^{3}
C2	7.50×10^{2}	D4	1.00×10^{2}	B4	3.25×10^{1}	B2	7.50×10^{3}
B2	7.50×10^{2}	C3	1.25×10^{2}	D4	3.75×10^{1}	A2	7.50×10^{3}
A2	2.50×10^{3}	A3	1.25×10^{2}	C4	3.75×10^{1}	D1	8.75×10^{3}
A1	3.00×10^{3}	A4	1.75×10^{2}	A1	3.75×10^{1}	*E2*	1.00×10^{4}
E1	5.00×10^{3}	A1	5.00×10^{2}	*E1*	4.86×10^{1}	*E1*	1.25×10^{4}
C4	5.00×10^{4}	*E1*	1.58×10^{3}	A4	5.00×10^{1}	A1	1.50×10^{4}

Selenate		o-Benzenedisulfonate		Bromosuccinate	
Trication	LOD (pg)	Trication	LOD (pg)	Trication	LOD (pg)
E2	7.50×10^{1}	*E2*	1.50×10^{1}	*E2*	7.50×10^{1}
B3	2.50×10^{2}	D1	1.63×10^{1}	C4	6.25×10^{2}
C4	2.75×10^{2}	C1	1.75×10^{1}	**D3**	7.50×10^{2}
D3	3.75×10^{2}	B1	2.00×10^{1}	D1	7.50×10^{2}
B1	4.00×10^{2}	**C2**	3.20×10^{1}	A4	8.00×10^{2}
C2	4.25×10^{2}	B4	4.00×10^{1}	**C2**	1.00×10^{3}
C3	4.40×10^{2}	B2	4.00×10^{1}	B4	1.00×10^{3}
D4	5.00×10^{2}	D2	4.75×10^{1}	C3	1.50×10^{3}
D2	5.00×10^{2}	**D3**	6.50×10^{1}	D4	2.00×10^{3}
C1	5.00×10^{2}	A4	6.50×10^{1}	D2	2.25×10^{3}
B2	5.00×10^{2}	C3	7.50×10^{1}	A3	3.75×10^{3}
B4	5.25×10^{2}	*E1*	7.50×10^{1}	B3	4.00×10^{3}
A4	5.50×10^{2}	D4	1.00×10^{2}	*E1*	4.99×10^{3}
A3	7.00×10^{2}	B3	1.00×10^{2}	C1	5.00×10^{3}
D1	7.50×10^{2}	A3	1.00×10^{2}	A2	5.00×10^{3}
A2	7.50×10^{2}	A2	1.25×10^{2}	B2	5.50×10^{3}
E1	1.13×10^{3}	A1	3.75×10^{2}	B1	7.50×10^{3}
A1	3.38×10^{3}	C4	8.75×10^{3}	A1	1.25×10^{4}

*The limit of detection was determined to be the amount of analyte that resulted in S/N = 3. Also, the data for E1 and E2 was extracted from reference 39.

Table 5.2-Comparison of LODs in the SIM positive and SRM positive modes

	Trication D3			Trication C2		
	SIM LOD (pg)	SRM LOD (pg)	SRM Mass	SIM LOD (pg)	SRM LOD (pg)	SRM Mass
Sulfate	2.00×10^{1}	1.50×10^{1}	367.4	4.50×10^{2}	3.00×10^{2}	309.2
Thiosulfate	6.25×10^{1}	5.00×10^{-1}	367.4	6.25×10^{1}	3.50×10^{1}	309.2
Oxalate	2.50×10^{2}	1.00×10^{2}	367.4	1.20×10^{1}	7.50×10^{1}	549.2
Fluorophosphate	2.63×10^{1}	2.05×10^{1}	367.4	2.25×10^{2}	1.00×10^{2}	309.2
Dibromosuccinate	1.25×10^{2}	1.25×10^{1}	745/747	7.50×10^{2}	2.00×10^{1}	629/631
Hexachloroplatinate	4.00×10^{1}	4.50	1003.5	5.00×10^{1}	2.00×10^{1}	889.4
Nitroprusside	2.00×10^{1}	3.50	853.5	7.00	5.00×10^{-2}	737.4
Dichromate	6.25×10^{3}	5.75×10^{2}	367.4	6.38×10^{3}	3.00×10^{3}	643.4
Selenate	3.75×10^{2}	2.00	367.4	4.25×10^{2}	6.00×10^{1}	309.2
o-Benzenedisulfonate	6.50×10^{1}	1.00×10^{1}	367.4	3.20×10^{1}	3.75×10^{1}	309.2
Bromosuccinate	7.50×10^{2}	1.00×10^{3}	745/747	1.00×10^{3}	1.00×10^{3}	629/631

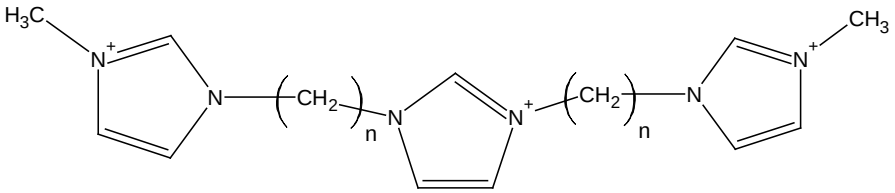

A1 = n = 3
A2 = n = 6
A3 = n = 10
A4 = n = 12

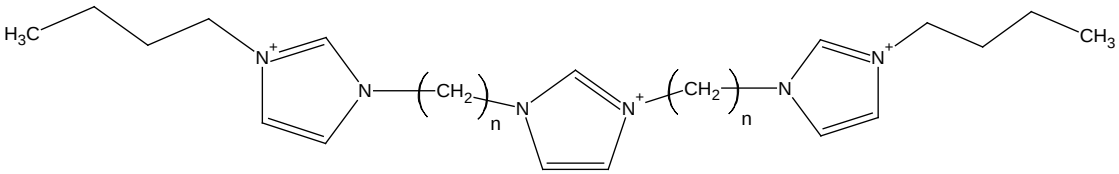

B1 = n = 3
B2 = n = 6
B3 = n = 10
B4 = n = 12

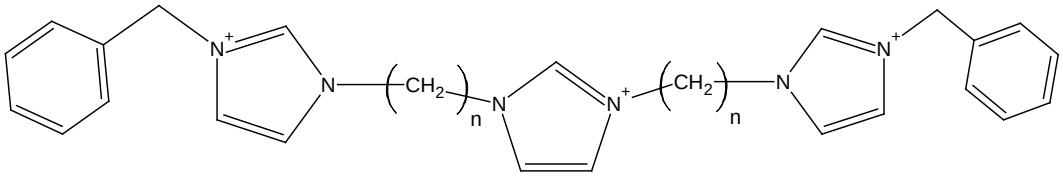

C1 = n = 3
C2 = n = 6
C3 = n = 10
C4 = n = 12

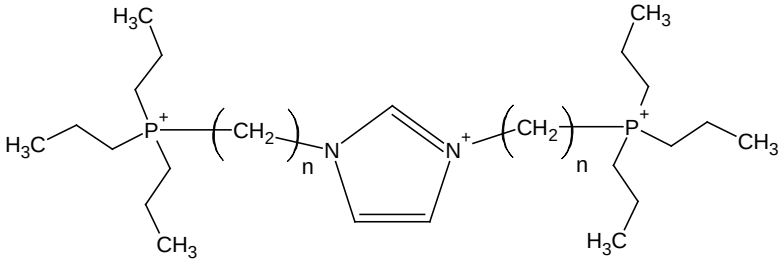

D1 = n = 3
D2 = n = 6
D3 = n = 10
D4 = n = 12

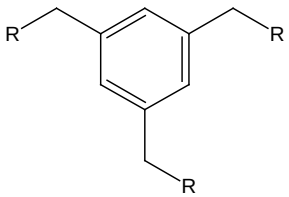

E1 = R = methylimidazolium
E2 = R= tripropylphosphonium

Figure 5.1. Structures of the tricationic ion-pairing reagents used in this analysis.

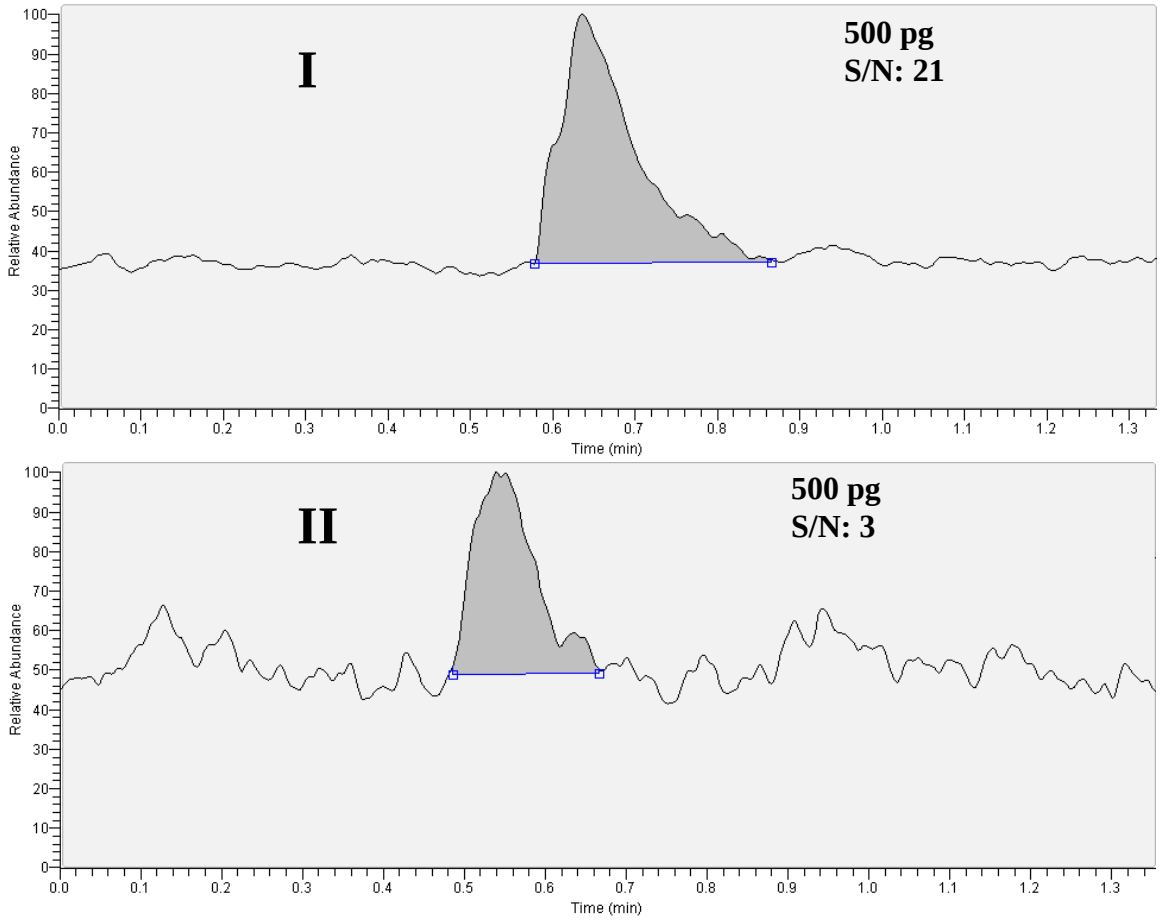

Figure 5.2. Comparison of the detection of sulfate in the positive mode using tricationic ion-paring reagents D3 (I) and E2 (II).

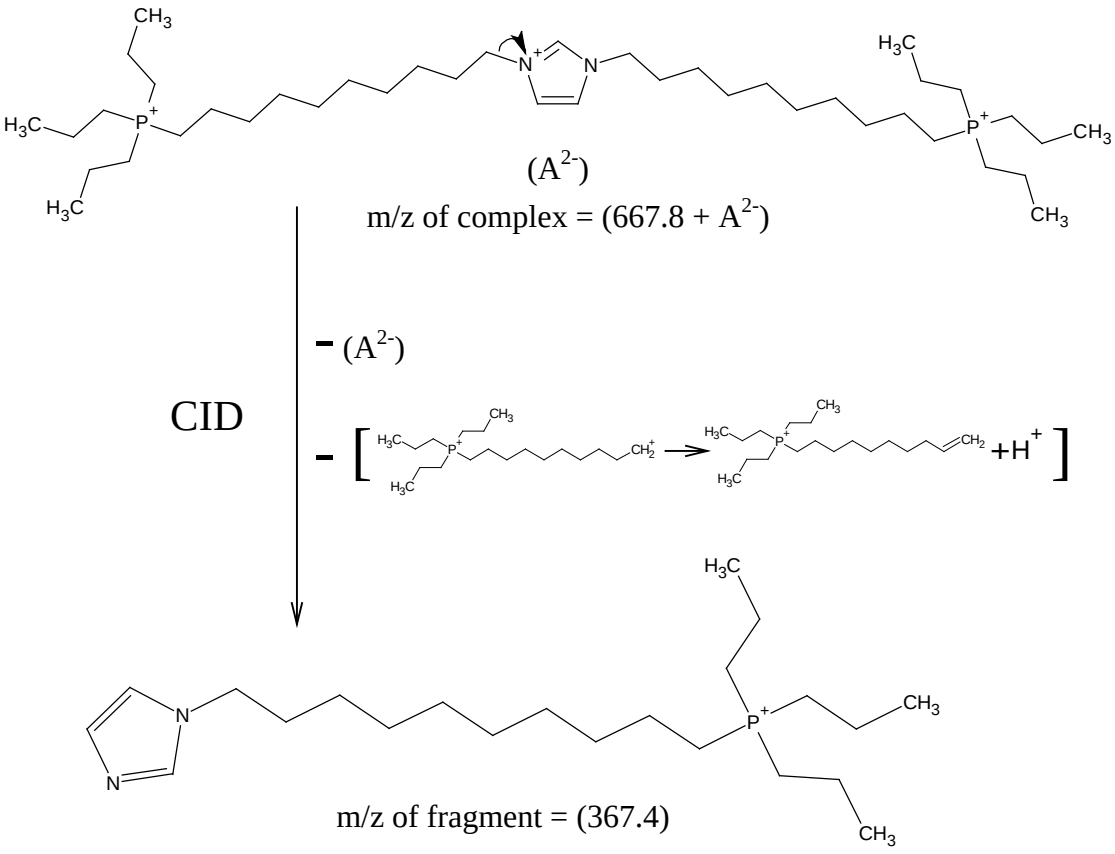

Figure 5.3. Proposed fragmentation pattern for a typical SRM experiment using trication D3.

CHAPTER 6

THE EVALUATION AND COMPARISON OF TRIGONAL AND LINEAR TRICATIONIC ION-PAIRING REAGENTS FOR THE DETECTION OF ANIONS IN POSITIVE MODE ESI-MS

A paper submitted to *Journal of the American Society of Mass Spectrometry*

Molly M. Warnke, Zachary S. Breitbach, Edra Dodbiba, Eranda Wanigasekara, Xiaotong Zhang, Pritesh Sharma, Daniel W. Armstrong

ABSTRACT

A general and sensitive method for detecting divalent anions by ESI-MS and LC-ESI-MS as positive ions has been developed. The anions are paired with tricationic reagents to form positively charged complexes. In this study, four tricationic reagents, 2 trigonal and 2 linear, were used to study a wide variety of anions, such as disulfonates, dicarboxylates, and inorganic anions. The limits of detection for many of the anions studied were often improved by tandem mass spectrometry. Tricationic pairing agents can also be used with chromatography to enhance the detection of anions. The tricationic reagents were also used to detect monovalent anions by monitoring the doubly charged positive complex. The limits of detection for some of the divalent anions by this method are substantially lower than by other current analytical techniques.

6.1 INTRODUCTION

The analysis of anions is of great necessity and interest in many fields of science. Low levels of organic acids have been determined in a variety of samples such as food, environmental, and biological matrices [1-9]. Some dicarboxylic acids, such as glutaric, fumaric, and adipic acids are marker compounds for certain metabolic disorders and have been determined in urine samples [10]. Aromatic sulfonates are used in many industrial processes and consumer products, such as laundry detergents. Many of these sulfonates end up in wastewater and municipal water supplies and have been determined by various methods [3, 11]. Because of the ramifications of low levels of anions in the environment, fast and effective trace methods of analysis are very important.

Complex environmental sample matrices often require a separation technique to isolate the analyte. Common separation methods include ion chromatography, [1, 12-15] ion pair chromatography, [3, 11, 16] reverse-phase mode chromatography, [17-19] and capillary electrophoresis (CE) [4, 5, 20]. To enhance the spectroscopic detection of anions that do not contain a UV chromophore, some CE and high performance liquid chromatography (HPLC) methods utilize sample derivatization [21, 22] or indirect UV or fluorescence detection methods [23-25]. Ions have also been detected by ion selective electrodes and conductivity [26-31]. Mass spectrometry (MS) is a universal detector for anions and is being used more and more, either alone [13, 32] or paired with a separation technique [3, 6, 18, 33].

Electrospray ionization (ESI)-MS is a logical choice for ion detection because of the inherent charge state of the analyte. Negative mode ESI-MS is the most common way of detecting anions. Problematically, negative ion mode operation with standard chromatographic solvents, such as methanol and water, can lead to poor spray stability,

corona discharge, and arcing, which ultimately lead to poor detection limits [34, 35]. Halogenated solvents [35-38] or electron scavenging gases [39] can be used to suppress these effects.

Operating in positive mode ESI would help to avoid the stability problems of negative mode ESI-MS and the use of unconventional solvents. A method was developed to detect singly charged anions using positive mode ESI-MS by pairing the anion with a dicationic reagent to create a positively charged complex [14, 15, 40-43]. There are multiple advantages to this method beyond the use of positive mode ESI-MS. One benefit of monitoring the anion/dication pair is moving the anion to a higher mass region where there is lower background noise. Additonally, anions of low mass are moved well above the low mass cutoff when ion trap instruments are used. Also, the pairing reagents may be used to differentiate between the analyte of interest and an interference of the same m/z [40].

Most recently, tricationic reagents were paired with divalent anions, which again could be detected as a singly charged complex [44, 45]. The first group of tricationic reagents used as pairing agents were classified as trigonal trications [44]. These trications have fairly rigid structures and provided detection sensitivity enhancement for many of the anions tested. Past results have indicated that rigid dicationic pairing agents did not work as well as more flexible dications [43], so a second class of tricationic reagents was developed. The second group of tricationic reagents are linear and more flexible [46]. The limit of detection (LOD) for some of the divalent anions tested was lower for the linear trications than the trigonal cations [45]. In the present study, the best two trigonal and two linear tricationic reagents from these previous studies will be used to determine detection sensitivity for a wide variety of divalent anions. LOD trends for a given tricationic reagent or class and

analyte type (e.g. dicarboxylate, disulfonate) would aid in future method development. The use of tricationic reagents in MS-MS and possible dissociation mechanisms are discussed as well. Additionally, these tricationic reagents can be used for the detection of monovalent anions as a doubly charged complex, which has not been previously studied with tricationic reagents. This leads to the possibility of detecting both singly and doubly charged anions using a singular tricationic reagent.

6.2 EXPERIMENTAL

The water and methanol used in these experiments were of HPLC grade and obtained from Burdick and Jackson (Morristown, NJ). Reagent grade sodium hydroxide and sodium fluoride were from Fisher Scientific (Pittsburgh, PA). The anions listed in Tables 6.1 and 6.3 were purchased as either the sodium or potassium salt or in the acid form from Sigma-Aldrich, with the exception of butanedisulfonic acid and 1,5-naphthalenedisulfonic acid which were purchased from TCI America (Portland, OR). Stock solutions (1 mg/mL) were made weekly and diluted serially for analysis.

The tricationic reagents evaluated in this study, as shown in Figure 1, were synthesized according to previous reports [44-47]. Before analysis, each trication was anion exchanged to the fluoride form as previously reported [44].

For direct injection analysis, a 40 μM trication-fluoride solution was pumped into a Y-type mixing tee at 100μL/min using a Shimadzu LC-6A pump (Shimadzu, Columbia, MD). Also directed into the mixing tee was a 2:1 mixture of methanol:water at a flow rate of 300 μL/min using the Surveyor MS pump (Thermo Fisher Scientific, San Jose, CA). This set up leads to an overall solvent composition of 50/50 water/methanol with 10μM tricationic

reagent and a total flow rate of 400 μL/min. The six-port injection valve on the mass spectrometer (5 μL loop) was used for sample introduction.

A Finnigan LXQ (Thermo Fisher Scientific) ESI-MS was used for the analysis of anions in this study. The ESI-MS conditions used were: spray voltage 3kV; sheath gas flow, 37 arbitrary units (AU); auxiliary gas flow rate, 6 AU; capillary voltage, 11 V; capillary temperature, 350° C; tube lens voltage, 105 V. The trication-anion complex was monitored in SIM mode with a width of 5 m/z units. This range was chosen to include isotope peaks, and LOD determinations were made from extracted ion chromatograms of the cation-anion complex m/z. For SRM experiments, the isolation width was 1-5 units with a normalized collision energy of 30 and an activation time of 30 ms. Data were analyzed using the Xcalibur and Tune Plus software. The limits of detection were determined when multiple injections of a given concentration resulted in a signal-to-noise ratio of three.

For the chromatography experiments, sample introduction was made by a Thermo Fisher Surveyor autosampler (5 μL injections). The stationary phase used was a Cyclobond 1 (25cm x 2.1 mm) obtained from Advanced Separation Technology (Whippany, NJ). The flow rate was 300 μL/min, and the column was equilibrated with 100% methanol and a step gradient to 100% water was applied at 5 minutes. The tricationic reagent (40μM) was added to the column effluent at 100 μL/min via the mixing tee. The MS was operated in SIM mode, monitoring the mass of each di-anion/trication complex throughout the chromatographic run.

6.3 RESULTS AND DISCUSSION

The tricationic reagents used in this study were chosen to represent the best performing trigonal and linear trications used in previous studies [44, 45]. These four

tricationic reagents offer a variety of functional groups as well as differences in rigidity. The linear trications contain an imidazolium core with different chain lengths and terminal charged groups. Linear trication 1 (LTC 1, Fig 6.1) has C_{10} linkages between the central imidazolium and tripropylphosphonium (TPP) terminal charged groups. Linear trication 2 (LTC 2, Fig 6.1) has benzylimidazolium terminal charge groups with a C_6 linkage chain. Trigonal trication 1 (TTC 1, Fig 6.1) has a benzene core with three TPP charged groups. Trigonal trication 2 (TTC 2, Fig 6.1) consists of a mesitylene core with three n-butylimidazolium groups in the 2,4,6 positions.

A variety of divalent anions were chosen to evaluate the ion-pairing performance of the tricationic reagents. The anions can be divided into categories based on their functional groups. The groups are: disulfonates, dicarboxylates, metal containing compounds, sulfur-oxo compounds, and miscellaneous compounds. Within the disulfonate and dicarboxylate categories, an effort was made to include compounds with varying chain lengths and functional groups to investigate any effect these might have on limits of detection.

Table 6.1 shows the 34 divalent anions used in this study and their limits of detection using each of the 4 tricationic reagents. They are arranged into the anion categories with the lower limits of detection at the top of each category. An examination of the LODs with the bold type-face, which indicate the lowest LOD for each anion, in Table 6.1 indicates that about 2/3 of the lowest LODs are for the linear tricationic reagents. Additionally, LTC 1 and TTC 1, which are the phosphonium containing reagents, (Fig. 6.1), account for 26 (of 34) of the lowest LODs. The exceptional overall performance of the TPP reagents for this set of divalent anions is in agreement with previous studies [45].

Generally, the disulfonates have lower limits of detection than dicarboxylates. The lowest LODs for the disulfonates are for dihydroxynaphthalenedisulfonate and *m*-benzenedisulfonate using TTC 1. The disulfonates with aromatic groups (dihydroxynaphthalenedisulfonate, *m*-benzenedisulfonate, 4-formyl-*m*-benzenedisulfonate, anthraquinone-2,6-disulfonate) usually had lower LODs than the straight chain disulfonates. Methane, ethane, propane, and butane disulfonic acids were evaluated with each tricationic reagent. There does not appear to be a trend in the detection limit based on the increasing chain length for the disulfonic acids except when using TTC 1, where methane disulfonic acid had a higher LOD than for the longer chain disulfonates. For the disulfonate category as a whole, the trigonal trication reagents performed better than the linear ones.

Two of the other sulfur containing compounds, besides the disulfonates, also showed low LODs. In fact, the LOD for tetrathionate, using LTC 1, is the lowest of all the anions tested when operating in SIM mode (50 femtograms). Tetrathionate and peroxidisulfate were very near the lowest LODs for both LTC 1 and 2, but had LODs higher than most of the disulfonates for TTC 1 and 2. There appears to be excellent complexation for these sulfur-oxo compounds with the linear trications.

Among the dicarboxylates studied, dipivaloyl-tartrate has the best LOD when pairing with all of the trications studied and for LTC 1 has a lower LOD than all of the disulfonates. For the tricationic reagents with benzene/mesitylene cores or charged groups (LTC 2, TTC 1, and TTC 2), the dicarboxylates with non-halogen chain substitutions (dipivaloyl-tartrate, phenylsuccinate, methylsuccinate, and malate) have lower limits of detection than the straight chain dicarboxylates (Table 6.1). The halogenated dicarboxylates (chlorosuccinate and dibromomaleate) had lower LODs using the trigonal trications (Table 6.1). For the

straight chain dicarboxylates studied, glutarate, (C_5), had the lowest limit of detection, followed by pimelate, (C_7), and then adipate, (C_6). With LTC 1, the LOD for adipate is about 7 times higher than for glutarate, though they only differ by one carbon in chain length. For the dicarboxylate category in general, the linear trications outperformed the trigonal ones.

The inorganic compounds studied generally had higher LODs than the organic acids and disulfonates. $ReCl_6^{2-}$ showed the best results of the inorganic compounds studied and had a limit of detection in the top five for LTC 1, LTC 2, and TTC 2. Two phosphorus containing compounds were also studied. Phenyl phosphate had lower LODs than hydrogen phosphite. This result is in general agreement with earlier work that used dicationic reagents and singly charged anions, which found that more oxidized species had better LODs [42].

The additional application of the tricationic reagent to enhance detection for chromatography is shown in Figure 6.2. Three dianions (camphorate, phenylsuccinate, and naphthalene-1,5-disulfonate) are separated using a beta-cyclodextrin stationary phase. The trication is added post-column. The better peak shape for the late eluting naphthalene-1,5-disulfonate peak is likely due to the step gradient employed. The first two peaks are broadened before the mobile phase is changed, while the third peak is eluted by the strong solvent. Chromatographic retention and separation of dianions could be very useful in cases of complex sample matrixes.

The limits of detection for most of the divalent anions could be reduced by using selected-reaction monitoring (SRM). Some advantages of SRM are to improve specificity in analysis, to lower noise in the region being analyzed, and/or to eliminate interference by a background ion in the mass spectrometer. In SRM, the dianion-trication complex is trapped,

excited, and the transition to a resultant fragment is monitored. SRM analysis was peformed for each dianion and the results are shown in Table 6.2.

For LTC 1, most SRM transitions were to a fragment of the trication. Most of the dianion/trication complexes fragmented to either m/z 665.5 $[LTC1\text{-}2H]^{+1}$ or m/z 367.4 corresponding to the C_{10}TPPImidazole (shown in Fig. 6.3a). The inorganic anions, tetrathionate, peroxidisulfate, fumarate, phenylphosphate, and phenyl succinate did not fragment to m/z 665 or 367.4. For these -2 anions, a portion of the dianion was lost and the +1 complex between a trication fragment and the remainder of the dianion was monitored. An example is tetrathionate where the complex fragment monitored (m/z 811.6) corresponds to the loss of SO_3. The most common fragments for LTC 2, were either the loss of 1 hydrogen each from 2 of the imidazolium rings (m/z 551.3) or the loss of the benzylimidazolium group (Fig 6.3b). For the complexes that lost the benzylimidazolium group, the dianion stayed complexed with the remainder of the trication. Unconventional fragmentation occurred with LTC 2 for the inorganic anions, peroxidisulfate, tetrathionate, rhodizonate, phenylphosphate, and dihydroxynaphthalenedisulfonate.

The predominant fragment monitored for TTC 1 is the loss of two hydrogens from the methylene carbons between the phosphorus and benzene ring. Only manganate, peroxidisulfate, tetrathionate, hexachlororhenate, and chromate underwent alternate fragmentation. The major fragmentation pathway for TTC 2 is the loss of the butylimidazolium group from the overall complex, so the dianion remains with the rest of the trication. Arsenate, peroxidisulfate, tetrathionate, rhodizonate, hexachlororhenate, glutaraldehyde bisulfate, dihydroxynaphthalenedisulfonic acid, adipate, pimelate,

succinaldehyde bisulfite, and camphorate followed alternate fragmentation patterns with TTC 2.

The group of compounds that had the largest improvements in LOD between SIM and SRM were the disulfonates. With one or more of the trications studied, each disulfonate had its LOD improved by at least an order of magnitude. The disulfonates were the only analytes to follow fragmentation for LTC 1 and LTC 2 as shown in Figure 6.3a and 6.3b, respectively. While the largest change in LOD was seen for the linear trications, the trigonal trications had the lowest LOD for 5 of the 9 disulfonates studied.

Chlorosuccinate and dibromomaleate also had interesting fragmentation patterns. In the case of these analytes, the halogen is lost from the anion and remains paired with the trication (or a portion of it). This was seen in our previous study on the linear trications [45]. Figure 6.4a illustrates a proposed fragmentation pattern for dibromomaleate using TTC 1. The distinct isotopic pattern for one bromine atom (Fig. 6.4c) is evidence of the gas phase association of the bromine with a +2 fragment of the trication. The improvement in LOD between SIM and SRM was larger for the halogenated dicarboxylates using the trigonal trications.

Phenylphosphate showed an improvement of 2-3 orders of magnitude by SRM for both linear trications. The SRM LODs for the dicarboxylates ranged from just slightly better than SIM LODS to about 8 times better, with the exception of fumarate and malonate which showed 18-fold (LTC 2) and 20-fold (LTC 1) improvements, respectively. Arsenate (LTC 2), hexachlororhenate (LTC 2, TTC 1), and 1,5-pentanedisulfonate, 1,5-dihydroxy (LTC 1) were the only other analytes with improvements of an order of magnitude or more. In general, the linear trications had lower LODs for SRM than the trigonal cations.

The tricationic reagents can pair with doubly charged anions to form complexes with an overall +1 charge, but can also pair with singly charged anions to form +2 complexes. Five “mono-anions” were evaluated using the four tricationic reagents to determine their limits of detection. The data for SIM and SRM for these anions is shown in Table 6.3. The LOD for benzenedisulfonate both by SIM and SRM is the lowest for the five singly charged anions tested. In comparison to the SIM LOD for the dicationic reagents tested in a previous study [43] the LOD for benzenedisulfonate ranks second using LTC 1 as a pairing reagent. The LODs in this study for perfluoroctanate and monochloroacetate are better than 7-8 (of 23) of the dicationic pairing reagents previously studied [43]. The ability of the tricationic reagents to pair with doubly and singly charged anions shows that the use of a single tricationic pairing reagent could be used to evaluate both monovalent and divalent anions simultaneously.

The LODs in this study compare favorably with those reported for anion analysis by other methods. There are many methods reported for the analysis of biologically relevant organic acids. In our study, the LODs for fumarate and methylsuccinate were 10 and 24 pg, respectively. Lower limits were determined, 0.9 pg fumarate and 0.5 pg methylsuccinate, by an LC method where the analytes were subjected to a long derivatization process to use fluorescence detection [21]. CE analysis with indirect UV detection was used to determine levels of various organic acids. The LODs under the optimized CE conditions for malonic acid, methylsuccinic acid, glutaric acid, and adipic acid reported are 144 pg, 37.3 pg, 34.9 pg, and 72.2 pg respectively. Our SRM tricationic method showed lower LODs for the malonic and methylsuccinic acids (100 pg and 24 pg), similar results for the glutaric acid (37.5 pg), and higher results for adipic acid (120 pg) [24]. A number of the analytes in that study had

very similar migration times and without a more specific detection method, might be indistinguishable in that analysis.

Larger improvements over previous methods were seen with the disulfonates. An LOD of 200 pg for benzenedisulfonate by LC-UV was reported [19]. Using our method and TTC 1, the LOD for the same analyte is 8.75 pg using SIM detection and 500 fg using LTC 1 and SRM detection. Other aromatic sulfonates were determined in concentration ranges of 0.1-1 ng/ml by solid phase extraction-ion pair chromatography using UV detection [11] and 100-400 ng/ml by CE-MS [3]. The LOD for napthalene-1,5-disulfonic acid was determined by ion interaction chromatography both by the direct injection of a large sample volume (100uL) and preconcentration (sample volume of 50 mL) [16]. The LODs were 20 ng for the large sample volume and 30 ng for the sample preconcentration. Using the tricationic pairing method and no preconcentration, the LOD for this analyte is 12.5 pg in SIM mode and 461 fg in SRM.

The analysis of inorganic ions is also important, though not always as facile as the detection of organic acids or disulfonates. A coated-wire membrane sensor electrode was used to determine chromate levels in solution [48]. The LOD for this method was determined in a solution that was 116 ng/mL. In our analysis of chromate, the lowest solution concentration we analyzed was 8 ng/mL in SRM mode using TTC 2, for an absolute detection limit of 40 pg. Molybdate levels in various water samples were determined by coprecipitation and neutron activation analysis, a very labor intensive technique which can necessitate the use of a reactor [49]. The limit of detection for this method was 1 pg/mL using a 100 mL sample, for an absolute detection of 100 pg of molybdate. Using LTC 1, the LOD for molybdate in SRM is 25 pg. Another precipitation method was used to

preconcentrate $ReCl_6^{2-}$ followed by detection using selective excitation of probe ion luminescence [50]. In this study, 150 pg of $ReCl_6$ was needed to see an observable signal. In our study, $ReCl_6^{2-}$ was determined well below 150 pg in both SIM (15 pg) and SRM (2 pg) monitoring modes.

6.4 CONCLUSIONS

Four optimal tricationic pairing reagents were used to determine the limits of detection for 34 divalent anions and 5 monovalent anions. These linear and trigonal tricationic reagents performed about equally as a whole, but the two trications with tripropylphosphonium cationic moieties outperformed trications with imidazolium based charge groups. When evaluating tricationic reagents, our results show that the linear trications provide lower limits of detection for most classes of compounds and should be tested first. The exception to this is the determination of disulfonates, where trigonal trications generally perform better. The use of tandem MS on the trication/di-anion complex helps to improve the sensitivity of detection for most of the dianions studied. Those complexes that dissociate into fragments not common to the trication showed the lowest limits of detection. Tricationic ion-pairing agents can also be used to determine monovalent anions by monitoring the +2 complexes. Therefore, mixtures of monovalent and divalent anions could be studied using a single tricationic reagent. Many of the LODs in this study are better or similar to those that have been previously reported, however this method is advantageous as it does not involve intricate sample preparation nor preconcentration and may be accessible to more laboratories.

6.5 ACKNOWLEDGEMENTS

The authors gratefully acknowledge the Robert A. Welch Foundation for its monetary support.

6.6 REFERENCES

1. Brooks Avery, J., G.; Kieber, R. J.; Witt, M.Willey, J. D. Rainwater monocarboxylic and dicarboxylic acid concentrations in southeastern North Carolina, USA, as a function of air-mass back-trajectory *Atmospheric Environment*, 2006, *40(9)* 1683-1693.

2. Liu, A.; Kushnir, M. M.; Roberts, W. L.Pasquali, M. Solid phase extraction procedure for urinary organic acid analysis by gas chromatography mass spectrometry *Journal of Chromatography B*, **2004**, *806(2)* 283-287.

3. Loos, R.; Riu, J.; Alonso, M.C.; Barceló, D. Analysis of polar hydrophilic aromatic sulfonates in waste water treatment plants by CE/MS and LC/MS *Journal of Mass Spectrometry* **2000**, *35(10)* 1197-1206.

4. Fung, Y.S.; Kap, M.L. Analysis of organic acids and inorganic anions in beverage drinks by capillary electrophoresis *Electrophoresis* **2003**, *24(18)* 3224-3232.

5. Ying-Sing Fung, H. T., Application of capillary electrophoresis for organic acid analysis in herbal studies *Electrophoresis* **2001**, *22(11)* 2242-2250.

6. Blount, B. C.;Valentin-Blasini, L. Analysis of perchlorate, thiocyanate, nitrate and iodide in human amniotic fluid using ion chromatography and electrospray tandem mass spectrometry. *Anal.Chim.Acta* **2006**, *567(1)* 87-93.

7. Dietz, E. A.;Singley, K. F. Determination of fumaric acid, maleic acid, and phthalic acid in groundwater and soil. *J.Liq.Chromatogr.* **1994**, *17(7)* 1637-1651.

8. Kvasnicka, F.;Voldrich, M. Determination of fumaric acid in apple juice by on-line coupled capillary isotachophoresis-capillary zone electrophoresis with UV detection. *Journal of Chromatography, A* **2000**, *891(1)* 175-181.

9. Kitami, H.; Ishihara, Y. Determination of eight organic acids in sake and wine by suppressed ion chromatography with triacontyl groups (C30) as a stationary phase. *Kankyo Kagaku* **2006**, *16(4)* 691-696.

10. Hagen, T.; Korson, M. S.; Sakamoto, M.Evans, J. E. A GC/MS/MS screening method for multiple organic acidemias from urine specimens. *Clinica Chimica Acta* **1999**, *283(1-2)* 77-88.

11. Altenbach, B.;Giger, W. Determination of Benzene- and Naphthalenesulfonates in Wastewater by Solid-Phase Extraction with Graphitized Carbon Black and Ion-Pair Liquid Chromatography with UV Detection *Anal. Chem.* **1995**, *67(14)* 2325-2333.

12. Dudoit, A.;Pergantis, S. A. Ion chromatography in series with conductivity detection and inductively coupled plasma-mass spectrometry for the determination of nine halogen, metalloid and non-metal species in drinking water. *J.Anal.At.Spectrom.* **2001**, *16(6)* 575-580.

13. Urbansky, E. T.; Magnuson, M. L.; Freeman, D.Jelks, C. Quantitation of perchlorate ion by electrospray ionization mass spectrometry (ESI-MS) using stable association complexes

with organic cations and bases to enhance selectivity. *J.Anal.At.Spectrom.* **1999**, *14(12)* 1861-1866.

14. Dyke, J. V.; Kirk, A. B.; Kalyani Martinelango, P.Dasgupta, P. K. Sample processing method for the determination of perchlorate in milk. *Anal.Chim.Acta* **2006**, *567(1)* 73-78.

15. Martinelango, P. K.; Guemues, G.Dasgupta, P. K. Matrix interference free determination of perchlorate in urine by ion association-ion chromatography-mass spectrometry. *Anal.Chim.Acta* **2006**, *567(1)* 79-86.

16. Sarzanini, C.; Bruzzoniti, M. C.; Sacchero, G.Mentasti, E. On-line preconcentration and separation of neutral and charged aromatic compounds by ion interaction chromatography *J. Chrom. A*, **1996**, *739(1-2)* 63-70.

17. Marconi, O.; Floridi, S.Montanari, L. Organic acids profile in tomato juice by HPLC with UV detection. *J.Food Qual.* **2007**, *30(2)* 253-266.

18. Yoshida, H.; Mizukoshi, T.; Hirayama, K.Miyano, H. Comprehensive Analytical Method for the Determination of Hydrophilic Metabolites by High-Performance Liquid Chromatography and Mass Spectrometry *J. Agric. Food Chem.* **2007**, *55(3)* 551-560.

19. Jandera, P.; Fischer, J.Prokeš, B. HPLC determination of chlorobenzenes, benzenesulphonyl chlorides and benzenesulphonic acids in industrial waste water *Chromatographia* **2001**, *54(9/10)* 581-587.

20. Hagberg, J. Analysis of low-molecular-mass organic acids using capillary zone electrophoresis–electrospray ionization mass spectrometry *J. Chrom. A*, **2003**, *988(1)* 127-133.

21. Kubota, K.; Fukushima, T.; Yuji, R.; Miyano, H.; Hirayama, K.; Santa, T; Imai, K. Development of an HPLC-fluorescence determination method for carboxylic acids related to the tricarboxylic acid cycle as a metabolome tool *Biomedical Chromatography* **2005**, *19(10)* 788-795.

22. Al-Dirbashi, O. Y.; Jacob, M.; Al-Amoudi, M.; Al-Kahtani, K.; Al-Odaib, A.; El-Badaoui, F.Rashed, M. S. Quantification of glutaric and 3-hydroxyglutaric acids in urine of glutaric acidemia type I patients by HPLC with intramolecular excimer-forming fluorescence derivatization *Clinica Chimica Acta*, **2005**, *359(1-2)* 179-188.

23. Kuijt, J.; de Rijke, E.; Brinkman, U. A. T.Gooijer, C. Practical implementation of quenched phosphorescence detection in capillary electrophoresis *Analytica Chimica Acta*, **2000**, *417(1)* 15-17.

24. Chen, H.; Xu, Y.; Van Lente, F.Ip, M. P. C. Indirect ultraviolet detection of biologically relevant organic acids by capillary electrophoresis *J. Chrom. B: Biomedical Sciences and Applications*, **1996**, *679(1-2)* 49-59.

25. Schneede, J.; Mortensen, J. H.; Kvalheim, G.Ueland, P. M. Capillary zone electrophoresis with laser-induced fluorescence detection for analysis of methylmalonic acid and other short-chain dicarboxylic acids derivatized with 1-pyrenyldiazomethane *Journal of Chromatography A*, **1994**, *669(1-2)* 185-193.

26. Kappes, T.; Schnierle, P.C. Hauser, P. Potentiometric detection of inorganic anions and cations in capillary electrophoresis with coated-wire ion-selective electrodes. *Anal.Chim.Acta* **1997**, *350(1-2)* 141-147.

27. Isildak, I. Potentiometric detection of monovalent anions separated by ion chromatography using all solid-state contact PVC matrix membrane electrode. *Chromatographia* **1999**, *49(5/6)* 338-342.

28. Isildak, I.;Asan, A. Simultaneous detection of monovalent anions and cations using all solid-state contact PVC membrane anion and cation-selective electrodes as detectors in single column ion chromatography. *Talanta* **1999**, *48(4)* 967-978.

29. Chen, L.; Tian, X.; Tian, L.; Liu, L.; Song, W.Xu, H. Electrochemical reduction and flow detection of iodate on (Bu4N)2Mo6O19 self-assembled monolayer. *Analytical and Bioanalytical Chemistry* **2005**, *382(4)* 1187-1195.

30. Salimi, A.; Mamkhezri, H.Mohebbi, S. Electroless deposition of vanadium-Schiff base complex onto carbon nanotubes modified glassy carbon electrode: Application to the low potential detection of iodate, periodate, bromate and nitrite. *Electrochemistry Communications* **2006**, *8(5)* 688-696.

31. Buchberger, W. W. Detection techniques in ion analysis: what are our choices? *Journal of Chromatography, A* **2000**, *884(1+2)* 3-22.

32. Magnuson, M. L.; Urbansky, E. T.Kelty, C. A. Microscale extraction of perchlorate in drinking water with low level detection by electrospray-mass spectrometry. *Talanta* **2000**, *52(2)* 285-291.

33. Valentin-Blasini, L.; Mauldin, J. P.; Maple, D.Blount, B. C. Analysis of Perchlorate in Human Urine Using Ion Chromatography and Electrospray Tandem Mass Spectrometry. *Anal.Chem.* **2005**, *77(8)* 2475-2481.

34. Cech, N. B.;Enke, C. G. Practical implications of some recent studies in electrospray ionization fundamentals *Mass Spectrom.Rev.* **2001**, *20(6)* 362-387.

35. Kebarle, P.;Ho, Y. In: Electrospray ionization mass spectrometry; Cole, R.B., Ed.; Wiley: New York, **1997,** p14.

36. Cole, R. B.;Harrata, A. K. Charge-state distribution and electric-discharge suppression in negative-ion electrospray mass spectrometry using chlorinated solvents. *Rapid Commun. Mass Spectrom.* **1992**, *6(8)* 536-539.

37. Cole, R. B.;Zhu, J. Chloride anion attachment in negative ion electrospray ionization mass spectrometry. *Rapid Comm. Mass Spectrom.* **1999**, *13(7)* 607-611.

38. Apffel, A.; Chakel, J. A.; Fischer, S.; Lichtenwalter, K.Hancock, W. S. Analysis of Oligonucleotides by HPLC-Electrospray Ionization Mass Spectrometry. *Anal.Chem.* **1997**, *69(7)* 1320-1325.

39. Straub, R. F.;Voyksner, R. D. Negative ion formation in electrospray mass spectrometry. *J.Am.Soc.Mass Spectrom.* **1993**, *4(7)* 578-587.

40. Martinelango, P. K.; Anderson, J. L.; Dasgupta, P. K.; Armstrong, D. W.; Al-Horr, R. S.Slingsby, R. W. Gas-Phase Ion Association Provides Increased Selectivity and Sensitivity for Measuring Perchlorate by Mass Spectrometry. *Anal.Chem.* **2005**, *77(15)* 4829-4835.

41. Martinelango, P. K.; Tian, K.Dasgupta, P. K. Perchlorate in seawater. *Anal.Chim.Acta* **2006**, *567(1)* 100-107.

42. Soukup-Hein, R. J.; Remsburg, J. W.; Dasgupta, P. K.Armstrong, D. W. A General, Positive Ion Mode ESI-MS Approach for the Analysis of Singly Charged Inorganic and Organic Anions Using a Dicationic Reagent. *Anal. Chem.* **2007**, *79(19)* 7346-7352.

43. Remsburg, J. W.; Soukup-Hein, R. J.; Crank, J. A.; Breitbach, Z. S.; Payagala, T.Armstrong, D. W. Evaluation of dicationic reagents for their use in detection of anions using positive ion mode ESI-MS via gas phase ion association. *J.Am.Soc.Mass Spectrom.* **2008**, *19(2)* 261-269.

44. Soukup-Hein, R. J.; Remsburg, J. W.; Breitbach, Z. S.; Sharma, P. S.; Payagala, T.; Wanigasekara, E.; Huang, J.Armstrong, D. W. Evaluating the Use of Tricationic Reagents for the Detection of Doubly Charged Anions in the Positive Mode by ESI-MS. *Anal. Chem.* **2008**, *80(7)* 2612-2616.

45. Breitbach, Z. S.; Warnke, M. M.; Wanigasekara, E.; Zhang, X.Armstrong, D. W. Evaluation of Flexible Linear Tricationic Salts as Gas-Phase Ion-Pairing Reagents for the Detection of Divalent Anions in the Positive Mode ESI-MS. *Analytical Chemistry* **2008,** *in press.*

46. Wanigasekara, E.; Zhang, X.; Nanayakkra, Y.; Moon, H.Armstrong, D. W. Novel Linear Tricationic Room Temperature Ionic Liquids: Synthesis, properties and applications *Submitted to Chem. Mat.* **2008**

47**.** Sharma, P.S.; Payagala, T.; Wanigasekara, E.; Wijeratne, A.B.; Huang, J.; Armstrong, D. W. Trigonal Tricationic Ionic Liquids: Molecular Engineering of Trications to Control Physiochemical Properties. *Chem. Mat.* **2008**, *20(13)*, 4182-4184.

48. Ardakani, M. M.; Dastanpour, A.Salavati-Nisari, M. Novel Coated-Wire Membrane Sensor Based on Bis(Acetylacetonato) Cadmium(II) for the Determination of Chromate Ions *Microchimica Acta* **2005**, *150(1)*, 67-72.

49. Sun, Y.C.; Yang, J.Y; Tzeng, S.R. Rapid determination of molybdate in natural waters by coprecipitation and neutron activation analysis. *Analyst*, **1999**, *124(3)*, 421-424.

50. Haskell, R. J.;Wright, J. C. Determination of rhenium at ultratrace levels by selective laser excitation of precipitates *Anal. Chem.* **1985**, *57(1)*, 332-336.

Table 6.1. Limits of detection for divalent anions using four tricationic pairing reagents in selected ion monitoring (SIM) mode.*

	Linear Trications		Trigonal Trications	
	LTC 1	LTC 2	TTC 1	TTC 2
	LOD (ng)	LOD (ng)	LOD (ng)	LOD (ng)
Disulfonates				
dihydroxynaphthalenedisulfonate	7.50E-02	5.00E-02	**7.50E-03**	1.20E-02
m-benzenedisulfonate	2.50E-02	5.00E-02	**8.75E-03**	1.00E-02
4-formyl-m-benzenedisulfonate	1.25E-01	3.75E-02	**1.00E-02**	1.50E-02
naphthalene-1,5-disulfonate	6.00E-02	**1.25E-02**	2.00E-02	3.00E-02
butanedisulfonate	1.25E-01	5.00E-02	3.00E-02	**2.00E-02**
propanedisulfonate	1.00E-01	2.00E-01	**2.45E-02**	7.50E-02
anthraquinone-2,6-disulfonate	**2.50E-02**	5.00E-02	7.50E-02	5.00E-02
methanedisulfonate	1.00E-01	**3.00E-02**	6.00E-02	**3.00E-02**
ethanedisulfonate	**3.50E-02**	2.25E-01	3.60E-02	4.00E-02
1,4-butanedisulfonate, 1,4-diydroxy	1.25E+01	2.50E+01	**1.25E+00**	5.00E+00
1,5-propanedisulfonate, 1,5-dihydroxy	3.50E+00	2.50E+00	**1.75E+00**	2.50E+00
Dicarboxylates				
dipivolyltartarate	1.75E-02	**1.25E-02**	1.50E-02	1.50E-02
camphorate	**6.00E-02**	1.50E-01	**6.00E-02**	5.00E-01
phenylsuccinate	1.50E-01	7.50E-02	**5.00E-02**	1.00E-01
glutarate	**7.00E-02**	2.00E-01	1.00E+00	5.00E-01
malate	2.60E-01	**5.00E-02**	2.25E-01	5.00E-01
methylsuccinate	2.00E-01	**7.50E-02**	2.50E-01	1.00E-01
fumarate	**1.50E-01**	4.00E-01	1.50E+00	7.50E+00
pimelate	**1.50E-01**	2.00E-01	2.50E+00	7.50E-01
malonate	2.00E+00	1.38E+00	8.75E-01	**3.00E-01**
adipate	**5.00E-01**	8.00E-01	2.25E+00	1.50E+00
dibromomaleate	8.50E-01	1.00E+00	1.00E-01	**1.75E-01**
chlorosuccinate	3.75E+00	1.88E+00	**2.25E-01**	9.00E-01
Metal Containing Compounds				
hexachlororhenate ($ReCl_{6)}$	**1.50E-02**	3.00E-02	1.50E-01	2.00E-02
chromate CrO4	2.50E-01	7.50E-01	6.25E+00	**7.50E-02**
molybdate MoO_4	**1.50E-01**	2.50E+00	3.75E-01	7.50E-01
manganate MnO_4	1.00E+00	---	**3.75E-01**	8.75E-01
arsenate AsO_4	**7.50E-01**	2.25E+00	2.50E+00	1.00E+00
Sulfur-Oxo Compounds				
tetrathionate S_4O_6	**5.00E-04**	2.25E-02	2.50E-02	5.00E-02
peroxidisulfate S_20_8	**1.20E-02**	1.65E-02	7.50E-02	2.00E-01
Miscellaneous compounds				
phenylphosphate	**4.00E-02**	1.00E-01	7.50E-02	5.00E-02
rhodizonate	**1.05E-01**	5.00E-01	3.75E+00	3.75E-01
hydrogen phosphite	**1.50E-01**	5.00E-01	3.75E-01	2.50E-01
selenite	1.25E+00	---	**3.50E-01**	3.75E+00

* Limit of detection determined where the amount of analyte used results in S/N=3. **Bold** typeface indicates the lowest limit of detection for each anion. --- indicates that a dianion/trication complex was not observed.

Table 6.2. Limits of detection for divalent anions using four tricationic pairing reagent in selected reaction monitoring (SRM) mode.*

	Linear Trications		Trigonal Trications	
	LTC 1	**LTC 2**	**TTC 1**	**TTC 2**
	LOD (ng)	LOD (ng)	LOD (ng)	LOD (ng)
Disulfonates				
dihydroxynaphthalenedisulfonate	2.75E-03	5.00E-03	7.50E-03	**1.20E-03**
m-benzenedisulfonate	**5.00E-04**	3.00E-03	6.25E-03	1.25E-03
4-formyl-m-benzenedisulfonate	5.00E-03	1.00E-02	---	**1.50E-03**
naphthalene-1,5-disulfonate	**4.61E-04**	4.38E+00	4.50E-03	3.60E-03
butanedisulfonate	4.50E-03	6.25E-03	**3.50E-03**	4.50E-03
propanedisulfonate	2.00E-02	1.25E-02	7.50E-03	**4.50E-03**
anthraquinone-2,6-disulfonate	1.13E-03	**7.50E-04**	3.60E-03	7.90E-03
methanedisulfonate	3.25E-03	3.15E-03	4.50E-02	**3.00E-03**
ethanedisulfonate	**1.50E-03**	8.75E-03	1.44E-02	9.80E-03
1,4-butanedisulfonate, 1,4-diydroxy	7.50E+00	1.50E+01	**1.50E+00**	5.50E+00
1,5-propanedisulfonate, 1,5-dihydroxy	**5.00E-02**	2.50E+00	8.75E-01	3.00E+00
Dicarboxylates				
dipivolyltartarate	6.25E-03	**3.75E-03**	1.00E-02	5.50E-03
camphorate	4.50E-02	4.50E-02	**3.00E-02**	2.00E-01
phenylsuccinate	1.00E+00	7.50E-02	1.00E-01	**2.50E-02**
glutarate	**3.75E-02**	6.00E-02	7.50E-01	1.50E-01
malate	7.00E-02	**1.50E-02**	---	---
methylsuccinate	**2.40E-02**	3.75E-02	1.05E-01	4.00E-02
fumarate	**1.00E-02**	2.25E-02	1.50E+00	---
pimelate	**3.00E-02**	7.50E-02	3.25E+00	7.50E-01
malonate	**1.00E-01**	1.20E-01	3.00E-01	5.00E-01
adipate	**1.20E-01**	2.25E-01	2.25E+00	1.50E+00
dibromomaleate	7.50E-02	3.00E-02	3.50E-02	**2.50E-03**
chlorosuccinate	1.50E+00	3.75E+00	**4.50E-01**	---
Metal Containing Compounds				
hexachlororhenate (ReCl6)	**2.00E-03**	3.00E-03	1.00E-02	2.00E-02
chromate CrO4	7.50E-02	2.25E-01	3.00E-01	**4.00E-02**
molybdate MoO_4	**2.50E-02**	2.50E+00	5.00E-01	1.58E-01
manganate MnO_4	3.75E-01	---	**1.25E-01**	7.50E-01
arsenate AsO_4	**9.00E-02**	2.00E-01	5.75E-01	2.75E-01
Sulfur-Oxo Compounds				
tetrathionate S_4O_6	**1.00E-05**	4.00E-04	5.00E-04	5.00E-03
peroxidisulfate S_20_8	1.25E-03	**1.15E-03**	6.75E-03	6.00E-03
Miscellaneous compounds				
phenylphosphate	**5.00E-06**	1.00E-03	1.13E-02	1.50E-02
rhodizonate	**1.05E-01**	5.00E-01	3.75E+00	1.25E-01
hydrogen phosphite	**3.25E-02**	2.00E-01	1.00E+00	3.50E-02
selenite	7.50E-02	---	**7.00E-02**	2.63E+00

* Limit of detection determined where the amount of analyte used results in S/N=3. **Bold** typeface indicates the lowest limit of detection for each anion. --- indicates that a dianion/trication complex was not observed.

Table 6.3. LODs in SIM and SRM modes for monovalent anions using four tricationic pairing reagents.*

	Linear Trications		Trigonal Trications	
	LTC 1	**LTC 2**	**TTC 1**	**TTC 2**
SIM Mode	LOD (ng)	LOD (ng)	LOD (ng)	LOD (ng)
benzenesulfonate	**1.50E-03**	9.00E-03	1.50E-02	3.13E-03
perflurooctanoic acid	5.00E-02	2.75E-02	**1.50E-02**	5.00E-02
trifluoromethanesulfonimide	**1.05E-02**	7.50E-02	3.00E-02	1.00E-01
monochloroacetic acid	7.00E+00	1.25E+01	1.00E-01	**2.00E+00**
benzoate	6.25E+01	8.75E+00	3.75E+00	**9.65E-02**
SRM Mode	LOD (ng)	LOD (ng)	LOD (ng)	LOD (ng)
benzenesulfonate	**9.50E-05**	2.70E-03	3.50E-03	1.38E-03
perflurooctanoic acid	**3.00E-04**	4.13E-03	3.00E-03	1.63E-03
trifluoromethanesulfonimide	1.05E-02	6.00E-02	2.50E-02	**3.43E-04**
monochloroacetic acid	---	1.00E+01	**1.00E-02**	7.50E-02
benzoate	---	8.75E+00	3.75E-01	**9.65E-02**

* Limit of detection determined where the amount of analyte used results in S/N=3. **Bold** typeface indicates the lowest limit of detection for each anion. --- indicates that a dianion/trication complex was not observed.

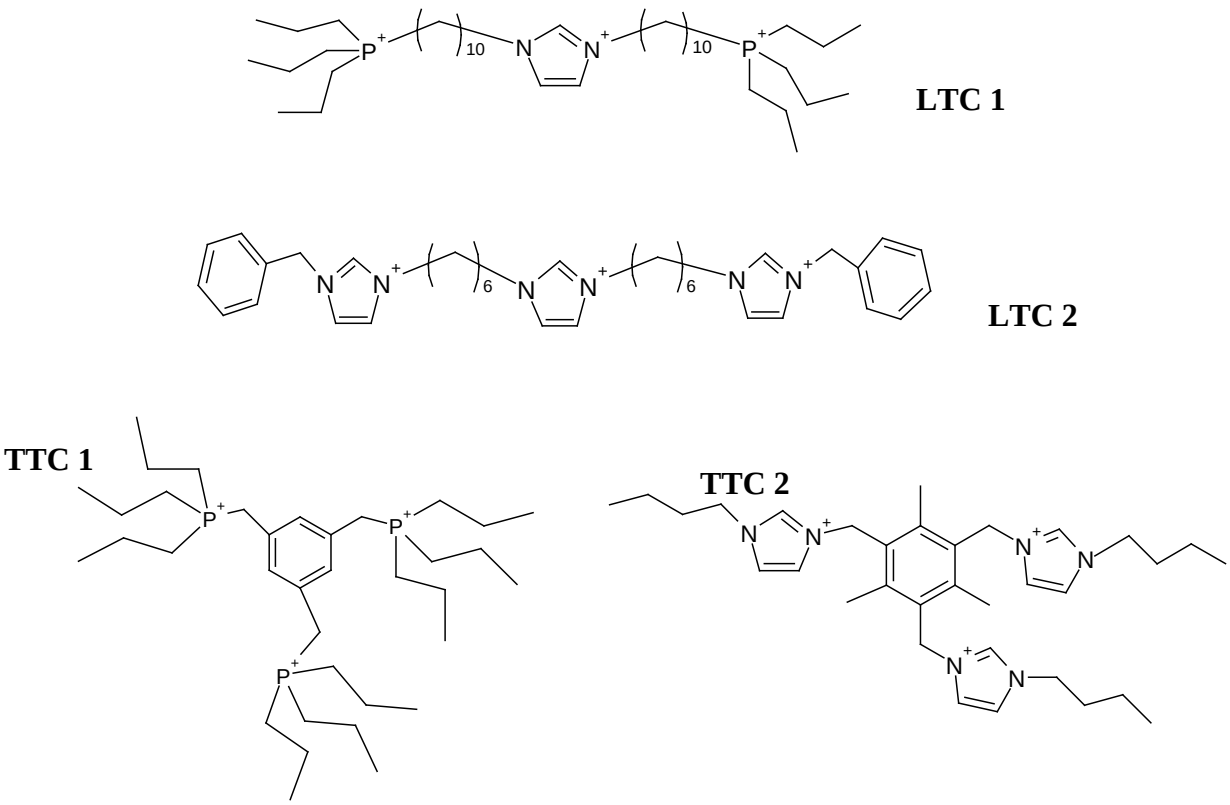

Figure 6.1. The structures of the four tricationic ion-pairing reagents used in this study.

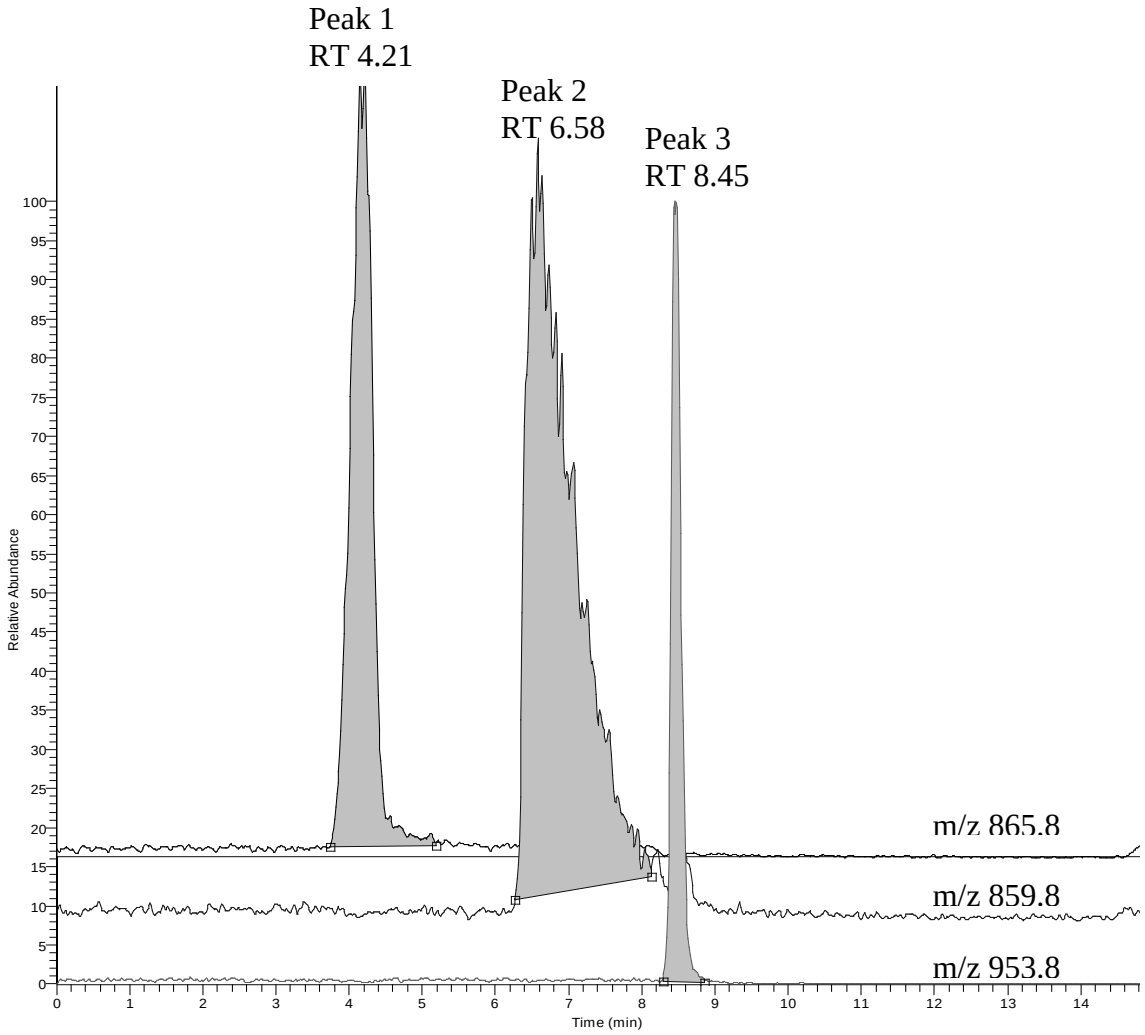

Figure 6.2. An extracted ion chromatogram representing the LC separation of camphorate (peak 1), phenylsuccinate (peak 2), and naphthalene-1,5-disulfonate (peak 3) with the retention times (RT) also listed. This separation was performed on a β-cyclodextrin stationary phase (2.1mm x 25 cm) which was equilibrated with 100% methanol. A step gradient to 100% water was applied at 5 minutes. The flow rate was 300 uL/min and 40 uM LTC 1 was teed into the effluent at a flow rate of 100 uL/min. The three trication-dianion complex masses were monitored in SIM mode.

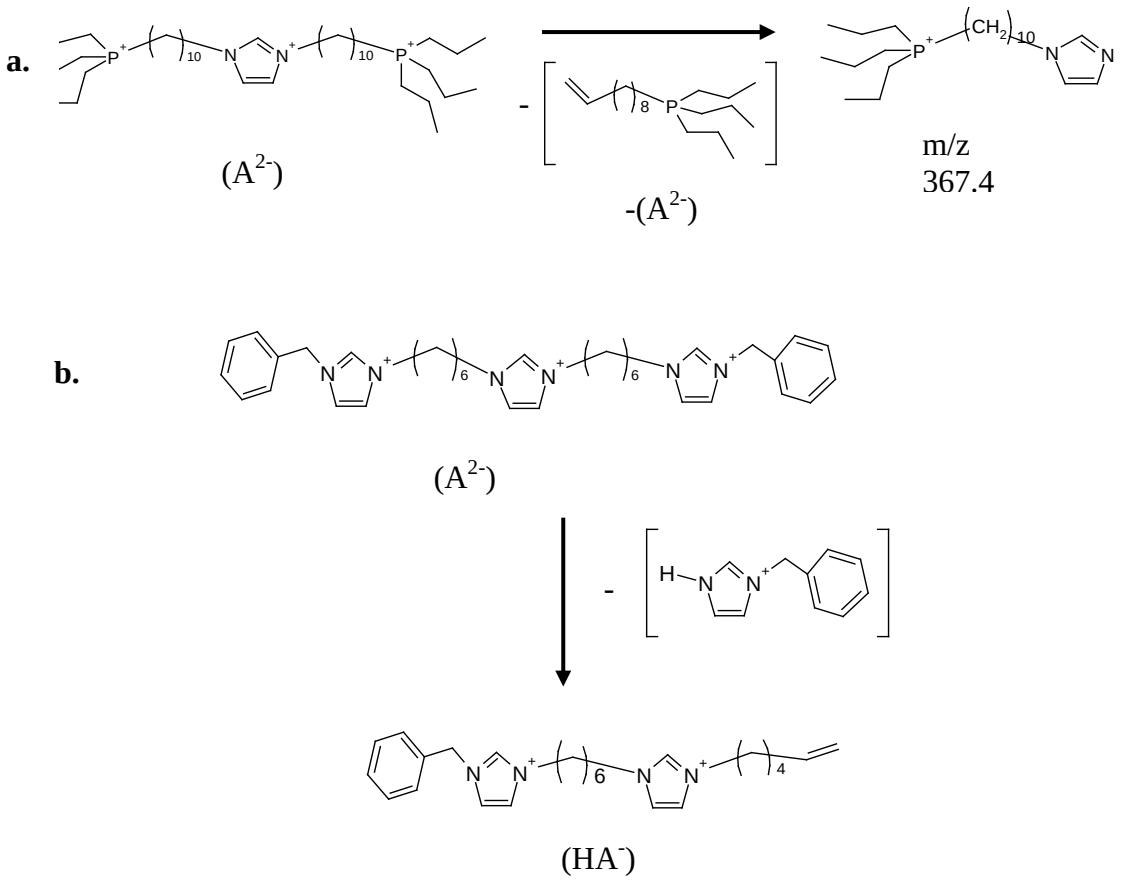

Figure 6.3. Proposed fragmentation pathways for the disulfonates using LTC 1 (a) and LTC 2 (b). A^{2-} represents a general divalent anion and HA^{-} is a singly protonated divalent anion.

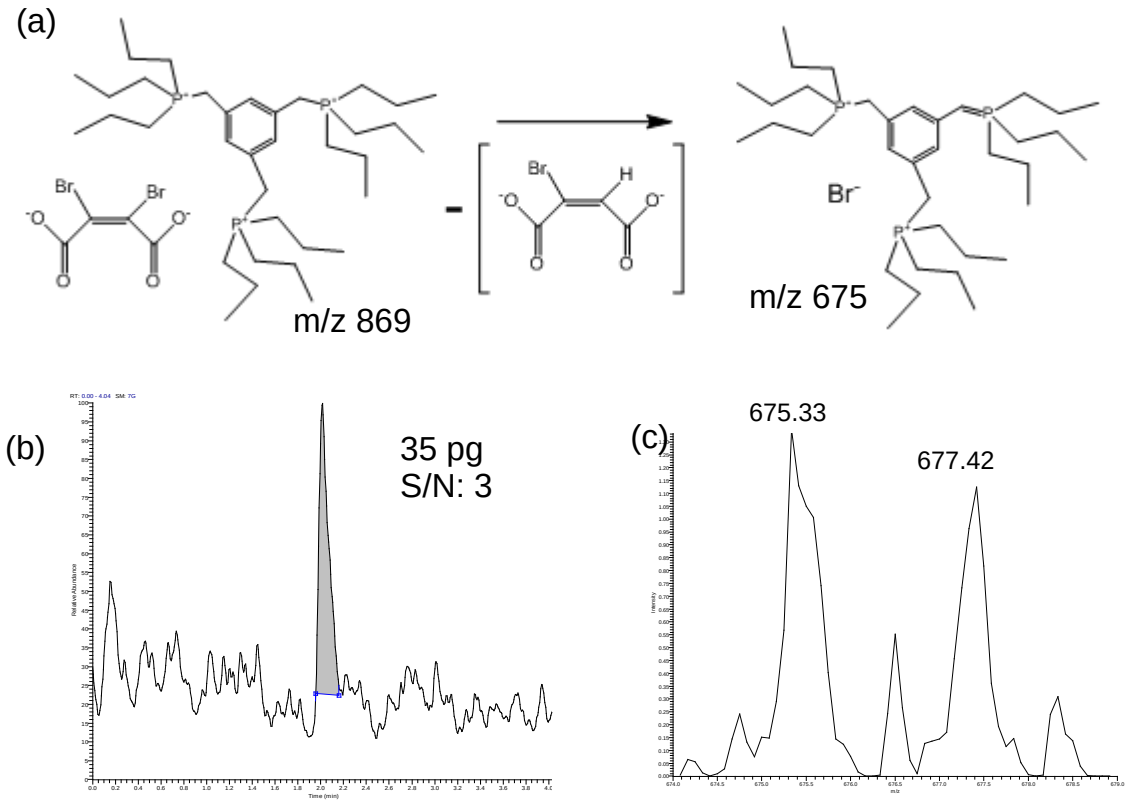

Figure 6.4. Proposed fragmentation pathway of the SRM transition for dibromomaleate(a). Panel (b) shows an injection monitoring the SRM transition from m/z 869→675.33 and 677.42. Panel (c) is the fragment spectrum observed for the peak shown in (b). The main peaks are 2 mass units apart and nearly the same height, indicative of Br.

CHAPTER 7

POSITIVE MODE ELECTROSPRAY IONIZATION MASS SPECTROMETRY OF BISPHOSPHOSPHONATES USING DICATIONIC AND TRICATIONIC ION-PAIRING AGENTS

A paper submitted to *Analytica Chimica Acta*

Molly M. Warnke, Zachary S. Breitbach, Edra Dodbiba, Jeffrey A. Crank, Tharanga Payagala, Pritesh Sharma, Eranda Wanigasekara, Xiaotong Zhang, Daniel W. Armstrong*

ABSTRACT

A general method for detecting bisphosphonate drugs by ESI-MS and LC-ESI-MS as positive ions has been developed. Bisphosphonates can have multiple negative charges in solution. Tricationic ion-pairing reagents were paired with bisphosphonates to form a positively charged complex. It was clear that this facile pairing method worked. However an appreciable presence of -1 bisphosphonate species were observed in positive mode ESI-MS (i.e. as the +2 complex with tricationic reagents). This led to an extended investigation on the use of dicationic pairing agents. The use of dicationic reagents improved the detection sensitivity for all of the bisphosphonates. Tandem mass spectrometry also improved the limits of detection for most of the bisphosphonates using both the tricationic and dicationic pairing reagents. A tricationic reagent also was used as an ion-pairing reagent in chromatography experiments. Thus the addition of a single reagent produced benefits in that it increased chromatographic retention and enhanced the ESI-MS detection of bisphosphonates.

7.1 INTRODUCTION

Bisphosphonates are a class of drug with a P-C-P backbone structure. These drugs are used to treat bone-related diseases, such as osteoporosis and Paget's disease [1, 2]. The detection of bisphosphonates using many traditional separation methods is a challenge because most bisphosphonates either lack or have weak UV chromophores. Bisphosphonates also exist in multiple charge states in solution and are very polar, which can limit chromatographic options. In reverse phase HPLC, bisphosphonates elute at or near the dead volume without the use of ion pairing agents.

Conductivity and indirect UV detection have been used to detect bisphosphonates in capillary electrophoresis (CE) [3] and ion chromatography (IC) experiments [4, 5], respectively. Derivatization methods for fluorescence and spectrophotometric detection have also been reported [6-8]. Evaporative light scattering detection [9] and charged aerosol detection [10] have also been employed for the detection of bisphosphonates. Most separation methods are based on CE, anion-exchange chromatography, or ion-pair chromatography [4, 5, 7, 8].

A few reports on the use of mass spectrometry (MS) for the detection of bisphosphonates have appeared in the literature. Trimethylsilyl-clodronate derivatives were analyzed by GC-MS [11]. Anion-exchange chromatography coupled with ICP-MS detection was used to determine alendronate and etidronate [12]. Electrospray ionization (ESI)-MS was used in negative-ion mode when coupled with CE and also to investigate bisphosphonate charge states and fragmentation [13, 14]. Positive ion-mode IC-ESI-MS-MS was used to detect diazomethane derivatives of the nitrogen containing bisphosphonates risedronate and alendronate [15].

ESI-MS is a logical choice for bisphosphonate detection because the analyte is negatively charged at a wide range of pH values. Negative ion mode ESI-MS is the most common method to detect anions, however standard chromatographic solvents, such as methanol and water can lead to poor spray stability, corona discharge, and arcing. These disadvantages ultimately lead to poor detection limits [16, 17]. Recently, a method was developed to detect singly charged anions using positive mode ESI-MS by pairing the anion with a dicationic reagent to create a positively charged complex [18-21]. The use of tricationic reagents which pair with divalent anions for the detection of a +1 complex also has been reported recently [22-24]. Using positive mode ESI-MS avoids spray stability problems. Beyond this, pairing the anion with the dicationic or tricationic reagent has other benefits. For example, monitoring the anion/cation pair moves the detected species to a higher mass region where there is lower background noise. Also, anions of low mass may be moved well above the low mass cutoff of ion trap instruments.

In this study, tricationic and dicationic pairing agents are examined as a general analytical approach for the ESI-MS and LC-ESI-MS of seven bisphosphonate compounds. Their use in MS-MS and possible dissociation mechanisms also will be discussed. Additionally, these ion-pairing reagents can be used in the mobile phase to enhance the chromatographic retention and separations of bisphosphonates on a C_{18} stationary phase.

7.2 EXPERIMENTAL

HPLC grade water and methanol was obtained from Burdick and Jackson (Morristown, NJ). Reagent grade sodium hydroxide and sodium fluoride were purchased from Fisher Scientific (Pittsburgh, PA). Etidronic acid sodium, alendronate disodium

hydrate, clodronic acid disodium salt, and neridronate were purchased from Sigma-Aldrich (Milwaukee, WI). Risedronate sodium and ibandronate were purchased from AkSci (Mountain View, CA) and zoledronic acid was purchased from Waterstone Technology (Carmel, IN). Stock solutions (1 mg mL^{-1}) were made weekly and diluted serially for analysis.

The tricationic and dicationic reagents used in this study were synthesized according to previous reports [19, 22, 23, 25-27]. Before analysis, each cationic reagent was anion exchanged to the fluoride form as previously reported [18, 22].

For direct injection analysis, a 40 μM dication-fluoride or trication-fluoride solution was pumped into a Y-type mixing tee at 0.1 mL min^{-1} using a Shimadzu LC-6A pump (Shimadzu, Columbia, MD). A 67:33 methanol:water mixture was also directed into the mixing tee at a flow rate of 0.3 mL min^{-1} using the Surveyor MS pump (Thermo Fisher Scientific, San Jose, CA). The resulting flow into the mass spectrometer is 50:50 methanol:water with a cationic pairing reagent concentration of 10 μM and a total flow rate of 0.4 mL min^{-1}. The six-port injection valve on the mass spectrometer (5 uL loop) was used for sample introduction.

A Finnigan LXQ (Thermo Fisher Scientific, San Jose, CA) ESI-MS was used for the analysis of anions in this study. The ESI-MS conditions used were: spray voltage 3 kV; sheath gas flow, 37 arbitrary units (AU); auxiliary gas flow rate, 6 AU; capillary voltage, 11 V; capillary temperature, 350° C; tube lens voltage, 105 V. The trication-anion complex was monitored in SIM mode with a width of 5 m/z units. For SRM experiments, the isolation width was 1-5 units with a normalized collision energy of 30 and an activation time of 30 ms. These conditions were used for all compounds for comparison purposes, but the optimization

of parameters for a given complex often leads to an improvement in sensitivity. Data were analyzed using the Xcalibur and Tune Plus software. The limits of detection were determined when multiple injections of a given concentration resulted in a signal-to-noise ratio of three.

For the chromatography experiments, the mobile phase was pumped isocratically using a Shimadzu LC-6A pump. Sample introduction was made by a six-port injection valve (Rheodyne, Cotati, CA). The stationary phase used was a Supelco Ascentis C_{18} (25 cm x 2.1 mm, 5 µm particle). The mobile phase was 80:20 50 µM tricationic reagent:methanol with a flow rate of 0.3 mL min^{-1}. Methanol (0.1 mL min^{-1}) was teed into the flow post-column. The MS was operated in SIM mode, monitoring the mass of each bisphosphonate/trication complex throughout the chromatographic run.

7.3 RESULTS AND DISCUSSION

The first facet of this study was an investigation on the use of tricationic pairing reagents with bisphosphonate analytes. In aqueous solution at pH 6, the predominant bisphosphonate species has a -2 charge, so paired with the tricationic reagent, a +1 overall complex will be observed by MS. The tricationic reagents used in this study were chosen to represent the best performing trigonal and linear trications identified in previous studies [22-24]. These four tricationic reagents (Fig. 7.1) offer a variety of functional groups as well as differences in rigidity. The linear trications (TriA and TriB) contain an imidazolium core with different chain lengths and terminal charged groups. TriA (Fig. 7.1) has C_{10} linkages between the central imidazolium and tripropylphosphonium (TPP) terminal charged groups. TriB has benzylimidazolium terminal charge groups and C_6 linkage chains. TriC and TriD (Fig. 7.1) are trigonal trications, which have a more rigid structure. TriC consists of a

mesitylene core with three n-butylimidazolium groups in the 2,4,6 positions. TriD has a benzene core with three TPP charged groups.

The seven bisphosphonates used in this study are illustrated in Figure 7.2. Table 7.1 shows the LOD results for each of the bisphosphonates using the four tricationic reagents. In the SIM mode, ibandronate had the lowest limit of detection (1.3 ng, TriA) of all of the bisphosphonates. In general, ibandronate and the other nitrogen-containing bisphosphonates (alendronate, risedronate, neridronate, zoledronate) had lower LODs than etidronate and clodronate. The LODs for some of the analytes varied significantly with the use of different tricationic reagents. For example, the lowest LOD for zoledronate was found with reagent TriC (2.5 ng) while the use of TriD resulted in an LOD which was 20 times higher (50 ng). Also, the same tricationic reagent often showed varying LODs for the analysis of different bisphosphonates. The LOD for neridronate (1.5 ng) using reagent TriA was 23 times better than the LOD for etidronate (35 ng) when using the same pairing agent. Overall, TriC and TriA were found to be the best tricationic pairing reagents for the bisphosphonates in this study. TriD performed poorly for all of the analytes.

Selected reaction monitoring (SRM) improved the limits of detection to varying degrees for all of the bisphosphonates analyzed when using tricationic reagents (Table 7.1). Some advantages of SRM are to improve specificity in analysis, to lower background noise in the region being analyzed, and/or to eliminate interference by a background ion in the mass spectrometer. In SRM, the bisphosphonates-trication complex is trapped, excited, and the transition to a resultant fragment is monitored.

For the linear trications, TriA and TriB, most SRM transitions involved the loss of a portion of the bisphosphonate while the remainder stayed complexed with the tricationic

pairing reagent. This is illustrated in Figure 7.3. For neridronate, MS-MS of the neridronate-TriB complex results in a fragment which is 82 Da lighter. This loss corresponds to H_2PO_3. MS-MS of the remaining fragment results in $[TriB\text{-}2H]^+$ at m/z 549.5. The trigonal trication complexes primarily fragmented to a portion of the trication. For TriC the monitored fragment corresponds to the loss of the butylimidazolium group from the overall complex, while for TriD, the monitored fragment corresponds to $[TriD\text{-}2H]^+$.

In terms of overall sensitivity, the linear trications, TriA and TriB, are the best tricationic agents for use in SRM mode. Using reagent TriA, the LODs for all of the bisphosphonates are 500 pg or less. All LODs were also sub-ng in the SRM mode using reagent TriB. Improvements in sensitivity between SIM and SRM mode ranged from a 1.25 fold improvement for zoledronate using TriC, to a 70 fold improvement for etidronate using reagent TriA. Some of the largest improvements were seen with TriA (5-70 fold). For alendronate, the lowest LOD in SIM mode is 2.75 ng using TriC. In SRM mode, its LOD is improved by a factor of about 2 using TriC (1.5 ng) and by a factor of 7 to an overall lower limit of detection (375 pg) using reagent TriA. This illustrates that the best reagent for a particular analyte in SIM mode might not always show the highest sensitivity in SRM mode. The linear trications had lower LODs in SRM than the trigonal trications, possibly due to the difference in fragmentation trends or their more flexible nature. It should also be noted that in SRM mode, the LODs for etidronate and clodronate are more similar to those of the nitrogen containing bisphosphonates in SRM mode.

Though trication-bisphosphonate complexes were observed, the LODs were higher than expected based on previously reported LODs using these reagents and other types of divalent anions [23, 24]. It turns out that when using a +3 reagent, the signal intensity for +2

complexes was higher than for +1 complexes. The +2 signals corresponded to the complexation of -1 charged bisphosphonates (BP), either $[BP^{-2}+H]^-$ or $[BP^{-2}+Na]^-$ with the tricationic agents. Attempts to further control the charge state of the bisphosphonates in solution by increasing the pH to ensure deprotonation did not increase the amount of +1 complex observed. It is more likely that the bisphosphonates are protonated during the electrospray process. This is consistent with previous ESI studies of bisphosphonates. In negative mode ESI-MS, the predominant bisphosphonate species was found to be -1, even at solution pHs that would indicate nearly complete dissociation to the -2 species [13,14]. It was apparent that the dominant bisphosphonate species is -1 in positive mode ESI. Therefore, it would be more advantageous to use dicationic pairing agents which should provide even greater sensitivity.

Four of the most useful dicationic reagents (Fig. 7.4) with a variety of structures and charged groups were chosen to evaluate LODs for bisphosphonates. These four dicationic reagents were found to be the best of 23 ion-pairing reagents evaluated for a variety of singly charged anions [19]. DiA consists of 2 benzylimidazolium groups with a C_5 alkyl linkage chain. DiB has a C_3 linkage chain with 2 tripropylphosphonium charged groups. DiC is a C_9 alkyl chain linking 2 methylimidazolium charge groups and DiD has pyrolidinium charged groups with a C_5 linkage chain and N-butyl groups.

The bisphosphonates were evaluated with the dicationic reagents in the same manner as were the tricationic reagents. The results are shown in Table 7.2. In the SIM mode, ibandronate had the lowest LOD of all the bisphosphonates using DiA (300 pg) and DiC (325 pg). Sub-ng LODs for alendronate (400 pg) and zoledronate (750 pg) were also found with reagents DiA and DiB, respectively. As with the tricationic reagents, the nitrogen containing

bisphosphonates generally had lower LODs than clodronate and etidronate in the SIM mode. Large differences can be seen in the LODs for a single bisphosphonate using various dicationic reagents. The LOD for neridronate using DiD is 21.3 ng, while the LOD using DiA is 1.3 ng which is about 20 times better. There was also a wide range of LODs when using one dicationic reagent and different bisphosphonates. The LODs for all bisphosphonates using DiA fall into a range of over an order of magnitude, from 0.3-4.5 ng. For DiD, the lowest LOD is for zoledronate (2.5 ng) while the highest is for clodronate (75 ng), which is a 30 fold difference. Clearly, it is important to test more than one cationic reagent to find the best sensitivity for a given bisphosphonate analyte. Overall, DiA and DiB were the best dicationic reagents for detecting bisphosphonates (lower LODs).

The limits of detection when using dicationic reagents were lowered for all of the bisphosphonates when operating in the SRM mode (Table 7.2). The lowest LOD in SRM mode is 170 pg for ibandronate using reagent DiC. Every SRM LOD for DiA is 500 pg or less making it the best dicationic reagent for use in SRM. While the LODs were not necessarily the lowest for a given analyte, larger improvements in sensitivity between the SIM and the SRM mode were seen for DiC and DiD. For neridronate the LOD decreased about 85 times between SIM and SRM mode (21.3 ng vs. 0.25 ng) using reagent DiD. DiC showed a 20 fold improvement between SIM and SRM for clodronate (50 ng vs. 2.5 ng). The SRM fragmentation for DiC and DiD was similar to that of the linear tricationic reagents, where a portion of the bisphosphonate molecule is lost and the resultant complex is monitored. A previous study using MS-MS with dication-anion complexes found that phosphonium and pyrrolidinium based dicationic reagents did not work well in SRM mode because they do not fragment significantly [19]. In our study, DiB and DiD can be used in

SRM monitoring and show improvements in sensitivity for bisphosphonates, even with their phosphonium and pyrrolidinium charge groups, because the dicationic reagent remains intact.

For SIM mode, the best LOD using tricationic reagents for each bisphosphonate was improved upon by using dicationic pairing reagents. Zoledronate, ibandronate, and alendronate showed the largest improvements (3, 4, and 7 fold, respectively) between the best tricationic and the best dicationic reagent. The LODs using dicationic reagents in SRM mode were also lower than the best tricationic reagent SRM LODs. The LOD for ibandronate was 3 times lower using SRM mode with DiA than for TriC, which is the greatest improvement seen when comparing SRM mode LODs. The lowest LOD for 5 of the 7 bisphosphonates (ibandronate, neridronate, risedronate, etidronate, clodronate) was found in the SRM mode using dicationic reagents. For alendronate and zoledronate, the best LOD was found in SRM mode with one or more of the tricationic reagents. For these bisphosphonates, if MS-MS capabilities are present, the best tricationic reagent (TriA) should be used, but for SIM analysis, the dicationic reagents are superior.

Previous reports on the use of dicationic or tricationic pairing reagents have shown that they can be used with LC by post-column addition to a reverse phase mode eluent for use in ESI-MS detection [18, 19, 24]. Bisphosphonates do not retain in typical reverse phase conditions, so this was not possible for this study. Since many chromatographic methods for bisphosphonates rely on ion-pair formation, it was thought that the dicationic or tricationic pairing reagents could be used as a mobile phase additives to both increase chromatographic retention and enhance MS detection. Tricationic reagent B was used successfully to increase retention and separate clodronate, etidronate, and neridronate as shown in Figure 7.5. The overall concentration of tricationic pairing reagent in the mobile phase is 40μM. Typical ion-

pair experiments using amine pairing reagents or monocationic pairing reagents (e.g. ionic liquids) typically use much higher concentrations, from 1-50 mM. Ion pair chromatography with negative mode ESI-MS is often used to analyze oligonucleotides. In these experiments, the ion pairing reagent is used solely for chromatographic retention and the negatively charged, unpaired oligonucleotide is determined by MS [28,29]. Tricationic reagent B was used successfully to increase retention and separate clodronate, etidronate, and neridronate and the ion pairing agent complexes with the bisphosphonates for MS detection as shown in Figure 5. The overall concentration of tricationic pairing reagent in the mobile phase is 40 μM. To the best of our knowledge, this is the first report of a tricationic reagent as an LC mobile phase additive.To the best of our knowledge, this is the first report of a tricationic reagent as an LC mobile phase additive. Furthermore it is both interesting and essential that these multifunctional ion pairing agents work at much lower concentration in LC, since higher concentrations can negate the advantage of positive ion ESI-MS detection of anions [21].

7.4 CONCLUSIONS

Trigonal and linear tricationic ion-pairing reagents were used to determine the limits of detection of seven bisphosphonate drugs both in using SIM and SRM modes. SRM mode lowered the LOD for all of the bisphosphonates. It was clear that this pairing method works, however the presence of -1 bisphosphonate species in positive mode ESI-MS led to the investigation of dicationic pairing reagents. The LODs for all of the bisphosphonates in SIM mode showed improvement with the use of dicationic reagents versus tricationic reagents. Using dicationic reagents in SRM mode, the LODs for bisphosphonates were lowered

compared to SIM mode and compared to the SRM mode when using tricationic pairing reagents. Tricationic reagent TriB can also be used as an ion-pairing reagent in reversed phase chromatography experiments to increase retention and subsequently pair with the bisphosphonate for ESI-MS detection.

7.5 REFERENCES

[1] E. Robert, Oncologist, 9 (2004) 14.

[2] P.P. Major, R. Cook, Am. J. Clin. Oncol., 25 (2002) 10.

[3] D. Bexheti, E.I. Anderson, A.J. Hutt, M. Hanna-Brown, J. Chrom. A, 1130 (2006) 137.

[4] C. Fernandes, R.S. Leite, F.M. Lancas, J. Chromatogr. Sci., 45 (2007) 236.

[5] E.W. Tsai, S.D. Chamberlin, R.J. Forsyth, C. Bell, D.P. Ip, M.A. Brooks, J. Pharm. Biomed. Anal., 12 (1994) 983.

[6] W.F. Kline, B.K. Matuszewski, J. Chrom., Biomed. App., 583 (1992) 183.

[7] M.J. Lovdahl, D.J. Pietrzyk, J. Chrom. A, 850 (1999) 143.

[8] S.X. Peng, S.M. Dansereau, J. Chrom. A, 914 (2001) 105.

[9] Z. Xie, Y. Jiang, D. Zhang, J. Chrom. A, 1104 (2006) 173.

[10] X. Liu, J.B. Fang, N. Cauchon, P. Zhou, J. Pharm. Biomed. Anal., 46 (2008) 639.

[11] S. Auriola, R. Kostiainen, M. Ylinen, J. Mönkkönen, P. Ylitalo, J. Pharm. Biomed. Anal., 7 (1989) 1623.

[12] M. Kovacevic, A. Gartner, M. Novic, J. Chrom. A, 1039 (2004) 77.

[13] K. Huikko, R. Kostiainen, J. Chrom. A, 872 (2000) 289.

[14] K. Huikko, T. Katiaho, J. Yli-Kauhaluoma, R. Kostiainen, J. Mass Spectrom, 37 (2002) 197.

[15] Lee S. Zhu, Veniamin N. Lapko, Jean W. Lee, Yousef J. Basir, Chris Kafonek, Richard Olsen,Chad Briscoe, Rapid Comm. Mass Spectrom., 20 (2006) 3421.

[16] N.B. Cech, C.G. Enke, Mass Spectrom. Rev., 20 (2001) 362.

[17] R.B. Cole, A.K. Harrata, Rapid Comm. Mass Spectrom, 6 (1992) 536.

[18] R.J. Soukup-Hein, J.W. Remsburg, P.K. Dasgupta, D.W. Armstrong, Anal. Chem., 79 (2007) 7346.

[19] J.W. Remsburg, R.J. Soukup-Hein, J.A. Crank, Z.S. Breitbach, T. Payagala, D.W. Armstrong, J. Am. Soc. Mass Spectrom., 19 (2008) 261.

[20] P.K. Martinelango, K. Tian, P.K. Dasgupta, Anal. Chim. Acta, 567 (2006) 100.

[21] P.K. Martinelango, J.L. Anderson, P.K. Dasgupta, D.W. Armstrong, R.S. Al-Horr, R.W. Slingsby, Anal. Chem., 77 (2005) 4829.

[22] R.J. Soukup-Hein, J.W. Remsburg, Z.S. Breitbach, P.S. Sharma, T. Payagala, E. Wanigasekara, J. Huang, D.W. Armstrong, Anal. Chem., 80 (2008) 2612.

[23] Z.S. Breitbach, M.M. Warnke, E. Wanigasekara, X. Zhang, D.W. Armstrong, Anal. Chem., (2008), *in press*

[24] M.M. Warnke, Z.S. Breitbach, E. Dodbiba, E. Wanigasekara, X. Zhang, P. Sharma, D.W. Armstrong, J Amer Soc Mass Spectrom (2008) .

[25] P.S. Sharma, T. Payagala, E. Wanigasekara, A.B. Wijeratne, J. Huang, D.W. Armstrong, Chem. Mat., 20 (2008) 4182.

[26] T. Payagala, J. Huang, Z.S. Breitbach, P.S. Sharma, D.W. Armstrong, Chem. Mat., 19 (2007) 5848.

[27] E. Wanigasekara, X. Zhang, Y. Nanayakkra, H. Moon, D.W. Armstrong, Chem. Mat. (2008) *submitted*

[28] R.H. Griffey, M.J. Greig, H.J. Gaus, K. Liu, D. Monteith, M. Winniman, L.L. Cummins, J. Mass Spectrom., 32 (1997) 305.

[29] G. Dai, X. Wei, Z. Liu, S. Liu, G. Marcucci, K.K. Chan, J. Chromatogr. B, 825 (2005) 201.

Table 7.1. Limits of detection for the tricationic pairing reagents and bisphosphonates in SIM and SRM mode[a].

		SIM ng injected	SRM ng injected	SRM fragment monitored
ibandronate				
	TriC	1.3E+00	1.0E+00	724.4
	TriA	2.0E+00	5.0E-01	801.7
	TriB	2.5E+00	5.0E-01	685.5
	TriD	8.0E+00	1.8E+00	595.5
neridronate				
	TriA	1.5E+00	2.8E-01	842.7
	TriC	2.0E+00	1.5E+00	682.3
	TriB	5.5E+00	5.0E-01	744.5
	TriD	8.0E+01	4.8E+00	595.5
risedronate				
	TriC	1.9E+00	5.8E-01	688.2
	TriB	4.5E+00	4.5E-01	750.5
	TriA	1.2E+01	4.0E-01	866.7
	TriD	1.5E+01	3.0E+00	796.5
zoledronate				
	TriC	2.5E+00	2.0E+00	677.4
	TriA	6.0E+00	3.8E-01	745.6
	TriB	7.5E+00	7.5E-01	739.6
	TriD	5.0E+01	5.0E+00	785.5
alendronate				
	TriC	2.8E+00	1.5E+00	654.2
	TriA	3.8E+00	3.8E-01	814.6
	TriB	4.0E+00	6.0E-01	698.5
	TriD	5.0E+01	2.0E+01	595.5
etidronate				
	TriC	3.0E+00	2.1E+00	611.3
	TriB	3.9E+00	4.3E-01	673.5
	TriD	2.0E+01	4.8E+00	595.5
	TriA	3.5E+01	5.0E-01	789.7
clodronate				
	TriA	1.0E+01	5.0E-01	809.6
	TriB	2.0E+01	5.6E-01	693.4
	TriC	2.0E+01	5.0E-01	649.3
	TriD	5.0E+01	7.5E+00	595.5

[a] Limit of detection determined where the amount of analyte used results in S/N=3.

Table 7.2. Limits of detection for bisphosphonates using dicationic reagents.[a]

		SIM ng injected	SRM ng injected	SRM fragment monitored
ibandronate				
	DiA	3.0E-01	3.0E-01	686.4
	DiC	3.3E-01	1.6E-01	590.5
	DiB	1.5E+00	1.1E+00	662.4
	DiD	2.8E+00	1.5E+00	560.2
neridronate				
	DiA	1.3E+00	5.0E-01	562.2
	DiB	2.0E+00	1.1E+00	620.4
	DiC	5.8E+00	5.0E-01	466.3
	DiD	2.1E+01	2.5E-01	500.4
risedronate				
	DiB	1.1E+00	1.7E-01	562.3
	DiC	2.8E+00	5.6E-01	490.3
	DiA	3.5E+00	2.3E-01	586.3
	DiD	1.0E+01	4.2E-01	524.3
zoledronate				
	DiB	7.5E-01	7.5E-01	551.3
	DiA	1.5E+00	5.0E-01	575.3
	DiC	2.5E+00	7.5E-01	479.3
	DiD	2.5E+00	1.0E+00	513.4
alendronate				
	DiA	4.0E-01	4.0E-01	616.2
	DiB	2.5E+00	6.3E-01	592.3
	DiC	2.5E+00	1.3E+00	520.3
	DiD	5.0E+00	7.5E-01	554.4
etidronate				
	DiA	2.0E+00	3.0E-01	509.1
	DiB	8.5E+00	1.9E+00	485.3
	DiC	1.8E+01	1.8E+00	413.3
	DiD	5.0E+01	6.0E+00	447.4
clodronate				
	DiA	4.5E+00	2.5E-01	465.3
	DiB	5.0E+00	---[b]	---[b]
	DiC	5.0E+01	2.5E+00	369.2
	DiD	7.5E+01	2.0E+00	403.3

[a] Limits of detection determined where the amount of analyte used results in S/N=3.
[b] Indicates a SRM transition could not be monitored.

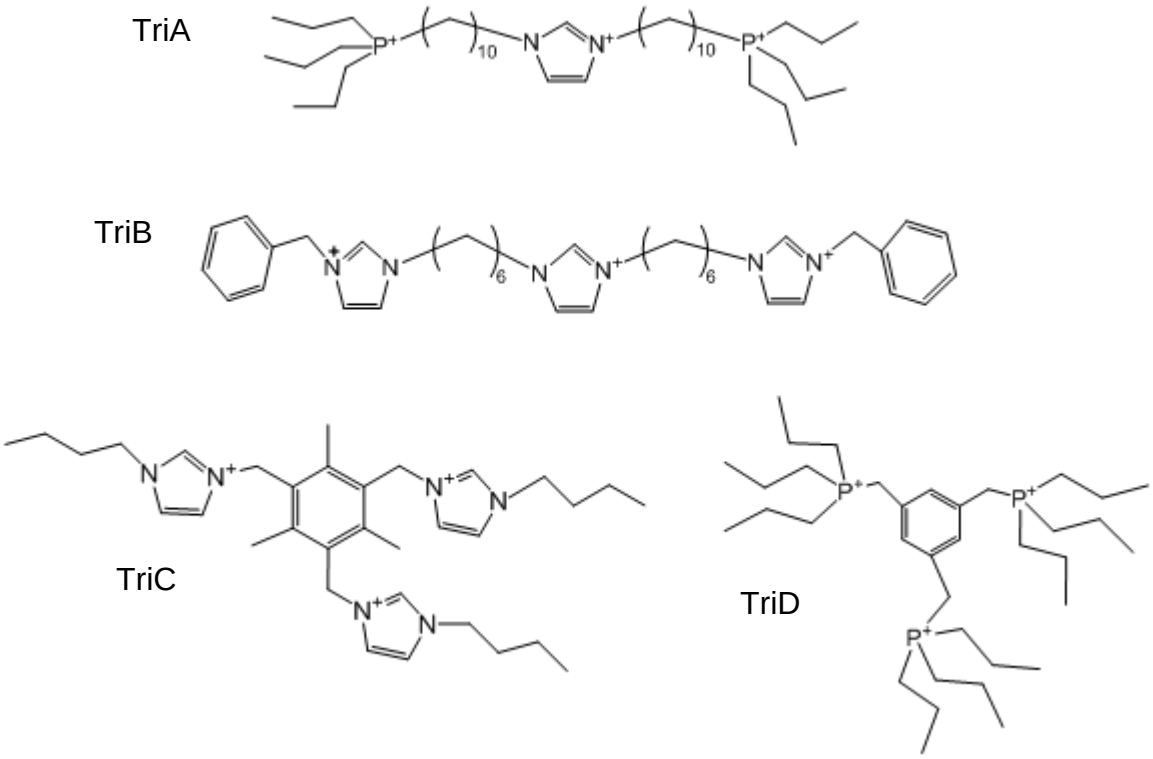

Figure 7.1. Structures of the tricationic ion-pairing reagents used in this study. Each reagent is labeled with an abbreviation used throughout the text.

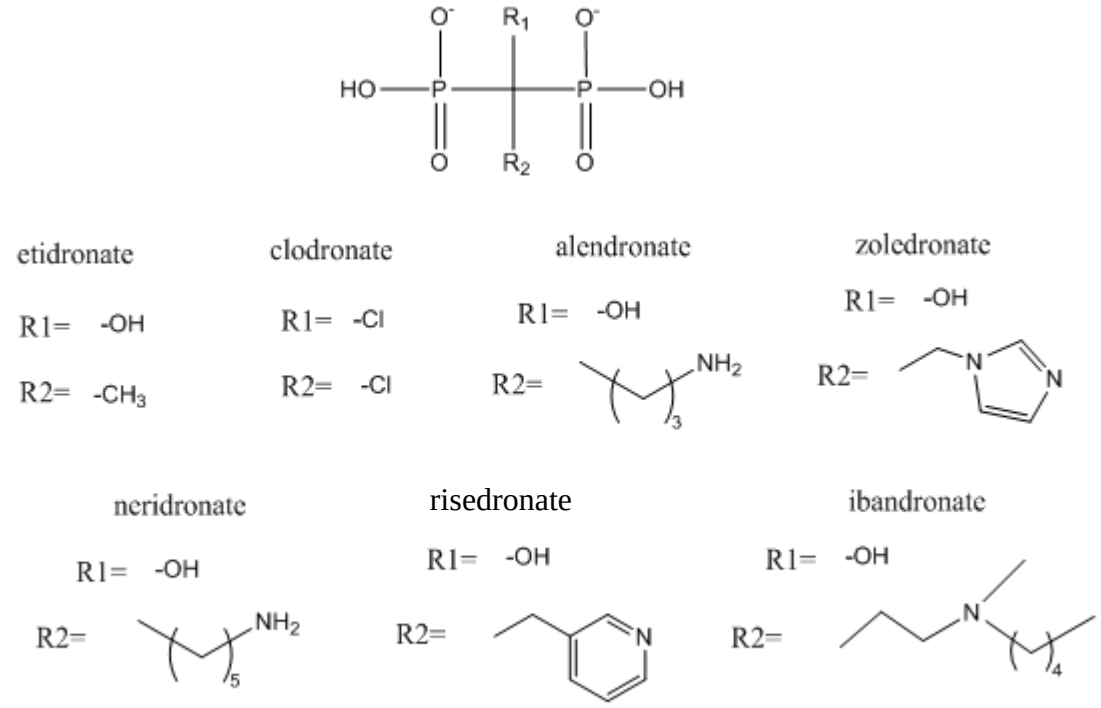

Figure 7.2. Structures of the bisphosphonate compounds studied.

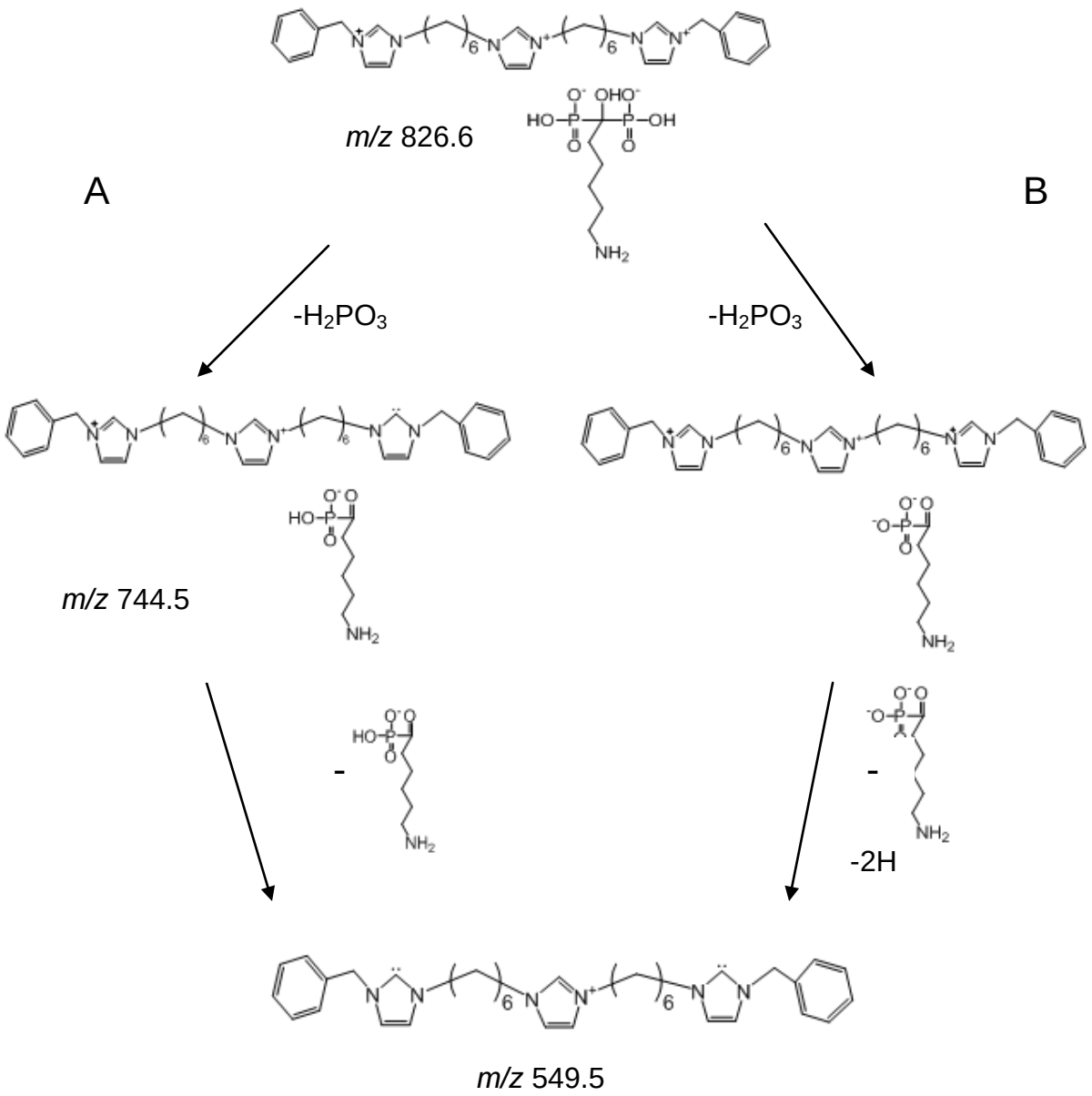

Figure 7.3. Tandem MS and proposed fragmentation of the neridronate-TriB complex. In proposed mechanism A, the first transition (*m/z* 826.6→744.5) is a loss of 82 mass units which corresponds with H_2PO_3, which results in a complex between a +2 trication fragment and a -1 neridronate fragment. In proposed mechanism B, the *m/z* 744.5 complex is between an unfragmented trication and a -2 form of the neridronate fragment. The second transition for both mechanisms shown (MS^3) is a loss of 195 mass units. The final fragment shown (*m/z* 549.5) represents $[TriB-2H]^+$.

DiA

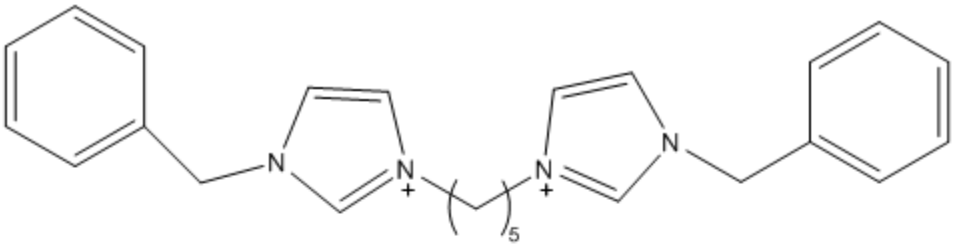

DiB

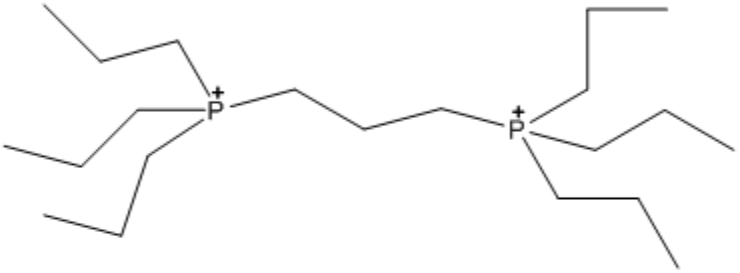

DiC

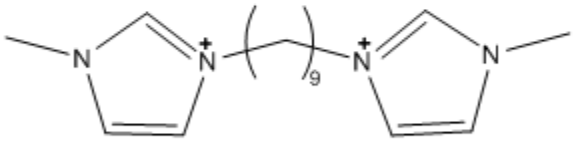

DiD

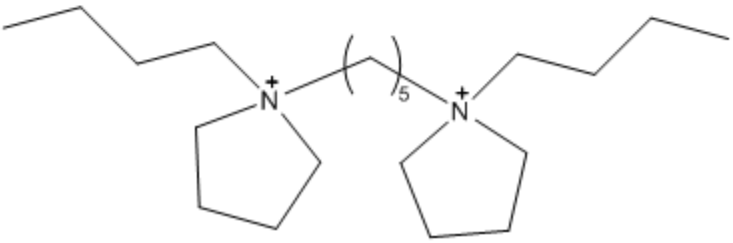

Figure 7.4. Structures of the dicationic reagents used in this studied. They are labeled with the abbreviations used throughout the text.

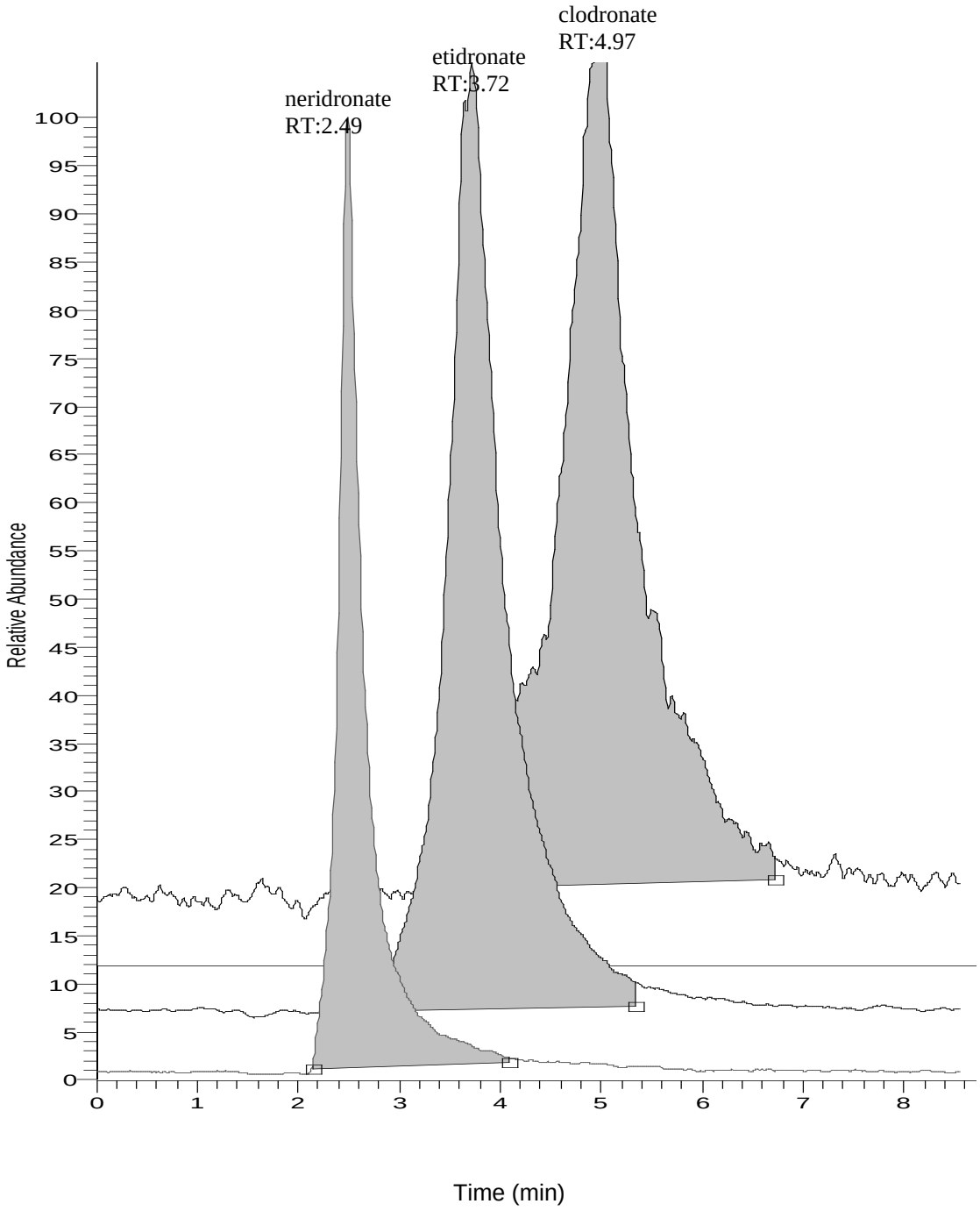

Figure 7.5. An extracted ion chromatogram representing the LC separation of neridronate, etidronate, and clodronate using tricationic reagent TriB as a mobile phase ion-pair additive. This separation was performed on a C_{18} stationary phase with a mobile phase of 80:20 Water:MeOH with 40μM TriB concentration. The flow rate was 0.3 mL min^{-1} and methanol was teed into the effluent at a flow rate of 0.2 mL min^{-1}. The three trication-bisphosphonate complex masses were monitored simultaneously in SIM mode.

CHAPTER 8

GENERAL CONCLUSIONS

Chiral stationary phases based on cyclodextrins and macrocyclic glycopeptides proved to be very useful for the separation of enantiomeric pterocarpans. Enantioselectivity for all five compounds was found using b and gamma native cyclodextrin CSPs (Cyclobond I and II, respectively) in the reverse phase mode. The Cyclobond I 2000 RSP and Cyclobond I 2000 AC columns were more effective, however, and between the two of them baseline separations for all compounds were achieved in the reverse phase mode. Of the macrocyclic glycopeptides CSPs, the Chirobiotic R column separated the most compounds in the reverse phase mode and had the best resolution and enantioselectivities (Rs=7.07, a=1.65, compound 3) found in this study. In the normal phase mode of operation, the three benzofuran substituted pterocarpan complexes could be separated. The DMP derivatized B-cyclodextrin CSP was the only cyclodextrin based CSP to show enantioselectivity in the normal phase mode. Also in normal phase mode, these benzofuran substituted compounds were partially separated on the Chirobiotic R and Chirobiotic V CSPs. The nitro-substituted pterocarpan was baseline resolved on the Cyclobond I 2000 DMP, Chirobiotic T, and Chirobiotic TAG stationary phases.

The macrocyclic glycopeptide stationary phase based on vancomycin successfully separated five EMAC complexes with varying ligands and metals with partial or baseline resolutions. Upon HPLC injection of EMAC complexes in the reverse phase mode, chromatographic peaks corresponding to the dipyridylamine ligand were observed. Due to the instability of the complexes in water, the polar organic mode or the normal phase mode of chromatography was utilized. In addition, mobile phase additives were determined to be

necessary for enantioseparations in the polar organic mode. These additives enhanced enantioselectivity but also improved resolution by increasing efficiency. Polarimetry experiments confirmed the enantiomeric separation of $Ni_3(dpa)_4Cl_2$ and also determined that the nickel complex enantiomers have very high specific rotation values (on the order of 5000 deg·cm/g·dm). The resolution of $Ni_3(dpa)_4Cl_2$ enantiomers led to absolute configuration assignment using vibrational circular dichroism, electronic circular dichroism, optical rotatory dispersion, and density functional theory calculations. The first eluted enantiomer was assigned *P*-helical chirality.

The second part of this dissertation demonstrated the application of tricationic ion-pairing reagents for the detection of doubly charged anions using positive ion mode ESI-MS. A variety of newly synthesized linear tricationic ion-pairing agents were evaluated for structural elements important for the detection of divalent anions. The optimum alkyl chain lengths coupling the cationic moieties should be between six and ten carbons in length. Tripropylphosphonium and benzylimidazolium charge moieties were found to provide lower LODs for the anions in the study. In comparison to previously reported rigid tricationic ion-pairing agents, the flexible linear trications evaluated generally showed more sensitivity than rigid (trigonal) tricationic reagents. However successful the linear tricationic reagents may be, it was found that the trigonal trication with a benzene core and tripropylphosphonium charge groups is still very useful as it was often complimentary to the linear trications. Lastly, tandem mass spectrometry (SRM) was used to lower LODs.

The application of the four optimal tricationic pairing reagents, two linear and two trigonal were used to determine the limits of detection for 34 divalent anions, such as dicarboxylates and disulfonates, and 5 monovalent anions. Taking into account the wide

array of analytes studied, the linear class and trigonal classes of tricationic reagents performed about equally as a whole. The two trications with tripropylphosphonium cationic moieties (linear and trigonal) outperformed trications with imidazolium based charge groups. When evaluating tricationic reagents, linear tricationic reagents provide lower limits of detection for most classes of compounds and should be tested first. The exception to this is the determination of disulfonates and halogenated dicarboxylates, where trigonal trications generally perform better. The use of tandem MS on the trication/di-anion complex helps to improve the sensitivity of detection for most of the dianions studied. Those complexes that dissociate into fragments not common to the trication showed the lowest limits of detection. Tricationic ion-pairing agents can also be used to determine monovalent anions by monitoring the +2 complexes. Therefore, mixtures of monovalent and divalent anions could be studied using a single tricationic reagent. Many of the LODs in this study are better or similar to those that have been previously reported, however this method is advantageous as it does not involve intricate sample preparation nor preconcentration and may be accessible to more laboratories.

The same trigonal and linear tricationic ion-pairing reagents used in chapter 6 were evaluated in chapter 7 to determine the limits of detection of seven bisphosphonate drugs using both SIM and SRM modes. SRM mode lowered the LOD for all of the bisphosphonates. Evidence of -1 bisphosphonate species in positive mode ESI-MS led to the investigation of dicationic pairing reagents. The LODs for all of the bisphosphonates in SIM mode showed improvement with the use of dicationic reagents in comparison to tricationic reagents. Dicationic reagents can also be used in SRM mode and the LODs for the bisphosphonates were improved upon. SRM improvement was noted for two of the

dicationic reagents which had previously not shown detection sensitivity enhancement in MS-MS. An overall sensitivity improvement from 5-40 fold was observed between the best tricationic reagent in the SIM mode to the best dicationic reagent in SRM mode. One of the tricationic reagents was also used as an ion-pairing reagent in reversed phase chromatography experiments to increase retention and subsequently pair with the bisphosphonate for ESI-MS detection.

ACKNOWLEDGEMENTS

If I were go back ten years, I would have never pictured myself with a doctoral degree in chemistry. This path in life has been the culmination of the guidance, advice, and inspiration by many people.

First, I would like to thank Dr. Armstrong for his mentorship during my time in graduate school. He is an excellent researcher and teacher and has helped me immensely with my laboratory and communication skills. I appreciate his patience and assistance in helping me become the scientist that I am today. I would also like to acknowledge past and present Armstrong group members and associated scientists who helped me through the years.

My interest in chemistry was piqued in high school when I was fortunate to have a wonderful chemistry teacher, Mr. Vic Johnson. In his class, I realized that I wasn't just "good" at chemistry, but that I really liked it too. This led me to pursue a chemistry degree at Hamline University where I was inspired by the faculty and thrived in a small student-oriented department. My undergraduate advisors, Dr. Gene Smith and Dr. John Matachek played pivotal roles in my application and entrance into graduate school.

Last but certainly not least, I must thank my family. I truly appreciate my parents and sister's undying support and encouragement and any sacrifices they have made to help me further my education.

APPENDIX A

APPENDIX ACCOMPANYING CHAPTER 4

SUPPLEMENTAL INFORMATION

Table A.1: Vibrational frequencies and vibrational descriptions for $Ni_3(dpa)_4Cl_2$

Band Number[a]	Experimental frequency (cm^{-1})	Calculated frequency[b] (cm^{-1})	Vibrational description[c]
1a,1b	1142	1157	scissoring vibrational mode among H-C-C-H groups of rings
2	1153	1157	
3	1284	1289	bond stretching between N3-C15, N5-C31, N6-C33, N8-C49, N9-C69, N11-C85, N12-C51, N14-C67
4a,4b	1315	1308	symmetric stretching of C23-N4-C24, C41-N7-C42, C77-N10-C78, C59-N13-C60 with bond stretching between N3-C15, N5-C31, N6-C33, N8-C49, N9-C69, N11-C85, N12-C51, N14-C67, as well as some rocking of H-C-C-H groups of rings
5a,5b	1358	1344	pronounced asymmetric stretching of C23-N4-C24, C41-N7-C42, C77-N10-C78, C59-N13-C60 with some ring breathing modes and rocking of H-C-C-H groups of rings
6	1369	1362	asymmetric stretching of C23-N4-C24, C41-N7-C42, C77-N10-C78, C59-N13-C60 with ring breathing modes and some rocking of H-C-C-H groups of rings
7a,7b	1423	1402	asymmetric stretching of C23-N4-C24, C41-N7-C42, C77-N10-C78, C59-N13-C60 with bond stretching between N3-C15, N5-C31, N6-C33, N8-C49, N9-C69, N11-C85, N12-C51, N14-C67, as well as some rocking vibrational mode among H-C-C-H groups of rings
8	1435	1416	asymmetric stretching of C23-N4-C24, C41-N7-C42, C77-N10-C78, C59-N13-C60 with some rocking vibrational mode among H-C-C-H groups of rings
9a,9b	1462	1448	asymmetric stretching of C23-N4-C24, C41-N7-C42, C77-N10-C78, C59-N13-C60 with stretching of N3-C23, N5-C24, N6-C41, N8-C42, N9-C77, N11-C78, N12-C59, N14-C60 as well as wagging of H-C-C-H groups of rings
10	1473	1473	asymmetric stretching of C23-N4-C24, C41-N7-C42, C77-N10-C78, C59-N13-C60 with some ring breathing modes
11	1551	1527	asymmetric stretching of C15-C17=C19-C21, C25-C27=C29-C31, C33-C35=C37-C39, C43-C45=C47-C49, C51-C53=C55-C57, C61-C63=C65-C67, C69-C71=C73-C75, C79-C81=C83-C85.
12a,12b	1605	1578	asymmetric stretching, within rings, between N3=C15-C17, N5=C31-C29, N6=C33-C35, N8=C49-C47, N9=C69-C71, N11=C85-C83, N12=C51-C53, N14=C67-C65 and also stretching between C19=C21-C23, C24-C25=C27, C37=C39-C41, C42-C43=C45, C55=C57-C59, C60-C61=C63, C73=C75C-C77, C78-C79=C81.
13	1605	1578	asymmetric stretching, within rings, between N3=C15-C17, N5=C31-C29, N6=C33-C35, N8=C49-C47, N9=C69-C71, N11=C85-C83, N12=C51-C53, N14=C67-C65 and also stretching between C19=C21, C25=C27, C37=C39, C43=C45, C55=C57, C61=C63, C73=C75C, C79=C81.

[a]see Figure 3 for band numbers
[b]scaled by 0.9612
[c]The atom numbers for **1** are given in Figure S1.

Table A.2. Cartesian coordinates for optimized geometry of *P*- $Ni_3(dpa)_4Cl_2$.

Atoms	X	Y	Z
Cl	0	0	5.383953
Cl	0	0	-5.383953
N	-0.647899	1.847126	2.267992
N	0	1.914565	0
N	0.647899	1.847126	-2.267992
N	0.647899	-1.847126	2.267992
N	0	-1.914565	0
N	-0.647899	-1.847126	-2.267992
N	-1.847126	-0.647899	2.267992
N	-1.914565	0	0
N	-1.847126	0.647899	-2.267992
N	1.847126	0.647899	2.267992
N	1.914565	0	0
N	1.847126	-0.647899	-2.267992
C	-1.240264	2.39475	3.368484
H	-1.223796	1.769501	4.257818
C	-1.790871	3.676964	3.361661
H	-2.239136	4.075237	4.265006
C	-1.75403	4.41151	2.155976
H	-2.205264	5.399062	2.096333
C	-1.152422	3.857276	1.026488
H	-1.158815	4.390643	0.083636
C	-0.570429	2.555239	1.083495
C	0.570429	2.555239	-1.083495
C	1.152422	3.857276	-1.026488
H	1.158815	4.390643	-0.083636
C	1.75403	4.41151	-2.155976
H	2.205264	5.399062	-2.096333
C	1.790871	3.676964	-3.361661
H	2.239136	4.075237	-4.265006
C	1.240264	2.39475	-3.368484
H	1.223796	1.769501	-4.257818
C	1.240264	-2.39475	3.368484
H	1.223796	-1.769501	4.257818
C	1.790871	-3.676964	3.361661
H	2.239136	-4.075237	4.265006
C	1.75403	-4.41151	2.155976
H	2.205264	-5.399062	2.096333

Table A.2. (continued)

Atoms	X	Y	Z
C	1.152422	-3.857276	1.026488
H	1.158815	-4.390643	0.083636
C	0.570429	-2.555239	1.083495
C	-0.570429	-2.555239	-1.083495
C	-1.152422	-3.857276	-1.026488
H	-1.158815	-4.390643	-0.083636
C	-1.75403	-4.41151	-2.155976
H	-2.205264	-5.399062	-2.096333
C	-1.790871	-3.676964	-3.361661
H	-2.239136	-4.075237	-4.265006
C	-1.240264	-2.39475	-3.368484
H	-1.223796	-1.769501	-4.257818
C	2.39475	1.240264	3.368484
H	1.769501	1.223796	4.257818
C	3.676964	1.790871	3.361661
H	4.075237	2.239136	4.265006
C	4.41151	1.75403	2.155976
H	5.399062	2.205264	2.096333
C	3.857276	1.152422	1.026488
H	4.390643	1.158815	0.083636
C	2.555239	0.570429	1.083495
C	2.555239	-0.570429	-1.083495
C	3.857276	-1.152422	-1.026488
H	4.390643	-1.158815	-0.083636
C	4.41151	-1.75403	-2.155976
H	5.399062	-2.205264	-2.096333
C	3.676964	-1.790871	-3.361661
H	4.075237	-2.239136	-4.265006
C	2.39475	-1.240264	-3.368484
H	1.769501	-1.223796	-4.257818
C	-2.39475	-1.240264	3.368484
H	-1.769501	-1.223796	4.257818
C	-3.676964	-1.790871	3.361661
H	-4.075237	-2.239136	4.265006
C	-4.41151	-1.75403	2.155976
H	-5.399062	-2.205264	2.096333
C	-3.857276	-1.152422	1.026488
H	-4.390643	-1.158815	0.083636
C	-2.555239	-0.570429	1.083495
C	-2.555239	0.570429	-1.083495
C	-3.857276	1.152422	-1.026488
H	-4.390643	1.158815	-0.083636
C	-4.41151	1.75403	-2.155976
H	-5.399062	2.205264	-2.096333
C	-3.676964	1.790871	-3.361661

Table A.2. (continued)

Atoms	X	Y	Z
H	-4.075237	2.239136	-4.265006
C	-2.39475	1.240264	-3.368484
H	-1.769501	1.223796	-4.257818
Ni	0	0	2.405801
Ni	0	0	0
Ni	0	0	-2.405801

Table A.3: Vibrational frequencies (unscaled), infrared absorption intensities and rotational strengths obtained with B3LYP/LANL2DZ for *P*-$Ni_3(dpa)_4Cl_2$

Frequency (cm^{-1})	IR intensities (Km/mol)	Rotational strengths (10^{-44} esu^2cm^2)
1138.7423	11.4043	0.7494
1138.7478	9.2745	0.6696
1139.72	0.1845	0.0012
1141.1743	0.4167	-5.8388
1141.1751	0.2641	-4.5302
1142.3654	0.0135	0.0001
1143.2552	0.1783	-0.0013
1147.0597	1.0024	-7.1176
1202.3929	0.0415	-0.0087
1202.5908	12.3849	-233.509
1202.5912	10.7057	-217.2415
1204.8709	134.0096	100.2787
1209.2924	0.0281	-0.001
1209.4842	2.1763	-16.0606
1209.4847	1.6234	-13.7375
1210.3222	0.0178	0.0002
1287.6273	0.3457	0.6325
1287.6407	1.7348	-159.3462
1287.6424	2.5226	-182.5075
1289.0193	58.6656	198.4972
1293.2949	0.802	-0.0027
1293.9678	2.4869	15.3377
1293.9737	0.0753	3.4889
1306.4039	0.1972	-0.0031
1310.471	32.1692	-283.5366
1310.4715	38.2829	-304.0475
1312.1539	0.8294	-0.0087
1315.0668	1.3604	-0.0046
1335.7796	0.0218	-0.0004
1335.9633	18.1853	469.9014
1335.9634	16.9864	453.826
1342.0235	92.3698	-125.0386
1357.8199	0.0006	0

Figure A.3. (continued)

Frequency (cm^{-1})	IR intensities (Km/mol)	Rotational Strengths 10^{-44} esu^2 cm^2
1360.5412	111.1895	-285.9843
1360.5417	111.7443	-286.7345
1366.5245	0.0008	0.0009
1399.7667	133.7472	-1097.1061
1399.77	108.929	-989.5989
1404.0734	0.6315	0.0148
1417.1753	130.9879	19.1763
1457.2031	0.2733	-0.4626
1457.3026	149.2384	-2352.5365
1457.304	135.662	-2243.5633
1462.1507	0.0631	0.0015
1463.1787	5.7185	106.5131
1463.1794	4.6193	96.3907
1471.1176	0.1653	0.1583
1472.3118	749.997	1189.4255
1504.2256	0.4045	-0.0106
1506.4906	259.6489	-2516.6163
1506.4914	235.2126	-2396.0811
1518.73	56.9314	76.1808
1518.7316	66.6298	82.5816
1518.9227	0.366	0.0145
1526.2357	0.5853	0.3856
1531.5466	2153.2996	3614.4504
1584.0771	0.0174	-0.0023
1584.1968	0.0274	14.4264
1584.1969	0.1213	35.6376
1588.3871	274.5246	532.8852
1594.1771	0.2137	-0.0411
1594.2722	28.4624	-172.8409
1594.2731	23.3544	-155.8937
1599.551	0.2391	0.0034
1636.4982	0.0088	0
1636.9786	87.0652	-227.7672
1636.9787	86.8877	-227.5455
1640.759	475.0854	531.4397
1645.8258	0.0544	0.0001
1647.5504	168.5512	-61.9276
1647.5509	174.7432	-63.0295
1654.8228	0.0981	0.0002

Table A.4: Electronic transition wavelengths and rotational strengths for the first 50 transitions of *P*-Ni3(dpa)4Cl2 obtained with BHLYP/LANL2DZ.

State	Wavelength (nm)	Rotational strength (velocity) (10^{-44} esu^{2}cm^2)
1	1287.04	0
2	1268.04	0
3	715.35	0
4	704.86	-29.2924
5	704.86	-29.3218
6	704.2	40.9534
7	704.2	40.9444
8	624.61	-31.7233
9	623.82	0
10	574.78	-82.2667
11	536.79	-9.5224
12	536.79	-9.5227
13	314.93	0
14	307.42	-595.6237
15	307.42	-595.6385
16	285.32	925.8074
17	278.88	0
18	276.81	-104.383
19	276.81	-104.3827
20	272	0
21	271.81	0
22	267.57	80.8031
23	267.57	80.7419
24	264.56	-74.7892
25	263.87	153.2272
26	263.87	153.2275

Table A.4. (continued)

State	Wavelength (nm)	Rotational strength (velocity) (10^{-44} esu^2cm^2)
27	263.42	0
28	261.73	-2.5056
29	255.91	0
30	254.74	-21.1878
31	254.74	-21.1878
32	253.75	0
33	248.19	0
34	244.64	0
35	244.1	-0.5716
36	243.37	1.1142
37	243.37	1.1123
38	243.17	0
39	242.19	1.4319
40	242.19	1.4314
41	241.65	9.5723
42	241.65	9.5755
43	240.24	0
44	239.83	0.6436
45	239.83	0.6419
46	238.54	4.0169
47	238.54	4.0232
48	237.98	0
49	237.45	-7.6501
50	237.45	-7.673

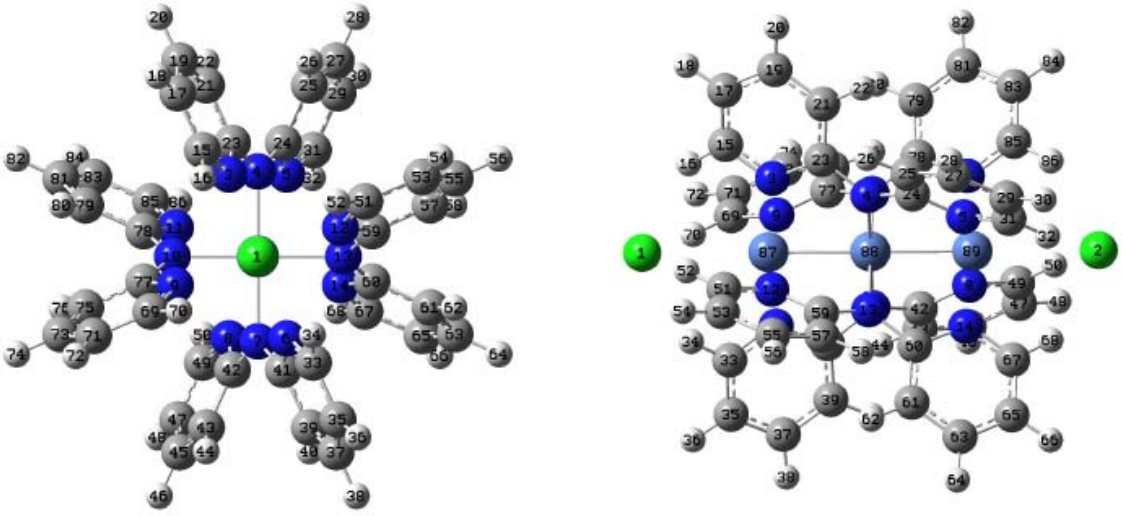

Figure A.1. Structure of $Ni_3(dpa)_4Cl_2$ showing atom numbering used in Table A.1.

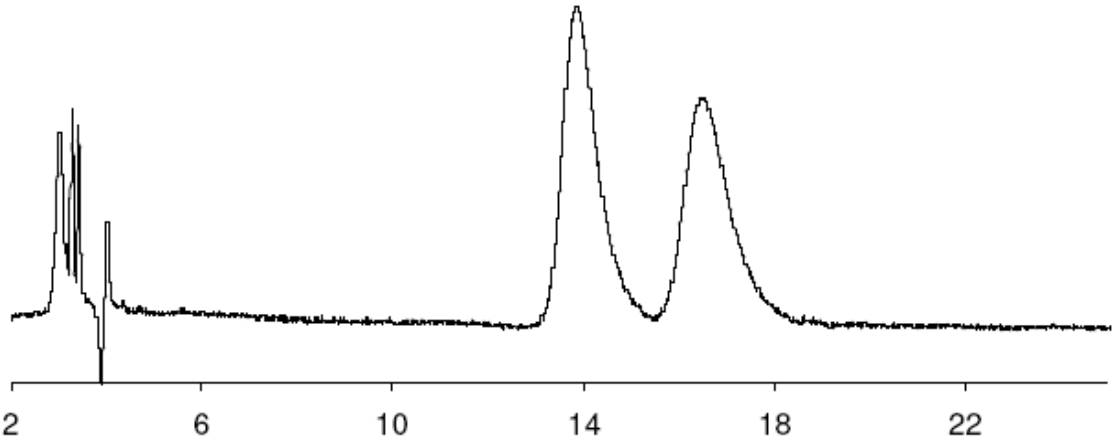

Figure A.2. Chromatogram of the enantioseparation of $Ni_3(dpa)_4Cl_2$. The complex was separated on the vancomycin-based chiral stationary phase (Chirobiotic V, Astec, Whippany, NJ) with a mobile phase containing 95/5 acetonitrile/methanol with 0.15% w/v ammonium trifluoroacetate and 0.05% w/v ammonium nitrate. The wavelength of detection was 270 nm.

Full citation for Ref.9:
Gaussian 03, M. J. Frisch, G. W. Trucks, H. B. Schlegel, G. E. Scuseria, M. A. Robb, J. R. Cheeseman, J. A. Montgomery, Jr., T. Vreven, K. N. Kudin, J. C. Burant, J. M. Millam, S. S. Iyengar, J. Tomasi, V. Barone, B. Mennucci, M. Cossi, G. Scalmani, N. Rega, G. A. Petersson, H. Nakatsuji, M. Hada, M. Ehara, K. Toyota, R. Fukuda, J. Hasegawa, M. Ishida, T. Nakajima, Y. Honda, O. Kitao, H. Nakai, M. Klene, X. Li, J. E. Knox, H. P. Hratchian, J. B. Cross, C. Adamo, J. Jaramillo, R. Gomperts, R. E. Stratmann, O. Yazyev, A. J. Austin, R. Cammi, C. Pomelli, J. W. Ochterski, P. Y. Ayala, K. Morokuma, G. A. Voth, P. Salvador, J. J. Dannenberg, V. G. Zakrzewski, S. Dapprich, A. D. Daniels, M. C. Strain, O. Farkas, D. K. Malick, A. D. Rabuck, K. Raghavachari, J. B. Foresman, J. V. Ortiz, Q. Cui, A. G. Baboul, S. Clifford, J. Cioslowski, B. B. Stefanov, G. Liu, A. Liashenko, P. Piskorz, I. Komaromi, R. L. Martin, D. J. Fox, T. Keith, M. A. Al-Laham, C. Y. Peng, A. Nanayakkara, M. Challacombe, P. M. W. Gill, B. Johnson, W. Chen, M. W. Wong, C. Gonzalez, and J. A. Pople, Gaussian, Inc., Pittsburgh PA, 2003.

APPENDIX B

APPENDIX ACCOMPANYING CHAPTER 5

SUPPLEMENTAL EXPERIMENTAL INFORMATION

.

B.1 MATERIALS

Figure 1 gives the structures of all the linear tricationic ion-pairing reagents used in this study. The reagents required for synthesis included sodium imidazole, 1,3-dibromoproapne, 1,6-dibromohexane, 1,10-dibromodecane, 1,12-dibromododecane, methylimidazole, butylimidazole, benzylimidazole, and tripropylphosphine which were purchased from Sigma-Aldrich (Milwaukee, WI, USA). All synthetic reagents were of reagent grade and were used without further purification. The anions that were tested for LOD (listed in Table 1) were ordered as either the lithium, sodium, or potassium salt or as the disassociative free acid. They were also obtained from Sigma-Aldrich and were used as the reagent grade without further purification. HPLC grade water and methanol were purchased from Burdick and Jackson (Honeywell Burdick and Jackson, Morristown, NJ, USA).

B.2 SYNTHESIS

Linear trications A1-4, B1-4, C1-4, and D1-4 were synthesized in an analogous manner, which included two steps. The first step was to produce a 1,3-(dialkylbromide)imidazolium bromide salt core. In short, this was done by first slowly adding a solution of sodium imidazole (1 molar eq.) in anhydrous DMF with a syringe pump to the corresponding dibromoalkane (5 molar eq.) under a vigorous stream of nitrogen. The reaction mixture was stirred for 12h at room temperature, then heated to 70°C and allowed to react for an additional 12h. Next, DMF was removed by roto-evaporation and the excess dibromoalkane was extracted with hexane. The resulting viscous liquid was purified by column chromatography (SiO_2, methanol:dichloromethane (1:9)) to obtain the pure 1,3-

(dialkylbromide)imidazolium bromide salt core in 65% yield. The next step is to react a solution of the preceding (1 molar eq.) in anhydrous THF (100mL) with the corresponding imidazole or phosphine (2.5 molar eq.) under reflux for 24h. Then the solvent was removed by roto-evaporation and the resulting tricationic bromide salt was dissolved in DI water (10-20 mL) and washed with ethyl acetate (5 x 50 mL) to remove the excess imidazole or phosphine. Lastly, water was removed by roto-evaporation and the product was dried under vacuum over phosphorous pentoxide resulting in the pure tricationic ionic liquid in 90% yield. A full report of the synthesis of these unique tricationic ionic liquids, including the NMR, MS, and other physiochemical data will be reported in due course. The bromide salt then had to be exchanged to the fluoride form for use as the ion-paring agent in ESI-MS. We have previously reported the procedure for this anion exchange.[37,39]

B.3 ESI-MS

The ESI-MS conditions used here were the same as those previously used and optimized for the detection of perchlorate with a dicationic reagent, and were as follows: spray voltage, 3kV; sheath gas flow, 37 arbitrary units (AU); auxiliary gas flow rate, 6 AU; capillary voltage, 11 V; capillary temperature, 350°C; tube lens voltage, 105 V. When detecting the trication/dianion complex in the positive SIM mode, the SIM width was 5. When performing the SRM experiments, the isolation widths were between 1 and 5, the normalized collision energy was 30, and the activation time was 30 ms. All data analysis was performed using the Xcalibur and Tune Plus software.